2013-04-23

Pole shift control based adaptive power system stabilizer for a superconducting generator

Vincent De Paul, Felix

THE UNIVERSITY OF CALGARY

"Pole Shift Control Based Adaptive Power System Stabilizer for a Superconducting Generator"

By

Felix Vincent De Paul

A THESIS

SUBMITTED TO THE FACULTY OF GRADUATE STUDIES

IN PARTIAL FULFILMENT OF THE REQUIREMENTS FOR THE

DEGREE OF MASTER OF SCIENCE

DEPARTMENT OF ELECTRICAL AND COMPUTER ENGINEERING

CALGARY, ALBERTA

APRIL, 2013

Abstract

Over the past few decades, an international effort has been undertaken to develop electric generators using rotors with super-conducting windings. The main differences between superconducting generators (SCGs) and the conventional generators are that (i) the SCG has a double rotor screen and (ii) the SCG's field windings on the rotor are made up of super-conductors that have zero resistance at cryogenic temperature and, therefore, completely eliminate resistive losses from the rotor.

In order to enhance power system stability, a conventional power system stabilizer (CPSS) is commonly applied to the conventional generator excitation system to damp oscillations. In an SCG, due to the long field time-constant and the shielding effect of the double rotor screen, it is not effective to control through the generator excitation system. A possibility, considered here, is to control the SCG through an electro-hydraulic governor as its time-constant is much less than that of the field winding. The objective of this research is to test the performance of an adaptive power system stabilizer for a SCG based on the pole-shift linear feedback control algorithm and acting through the SCG electro-hydraulic governor.

The system considered is a single SCG – infinite-bus power system driven by a three stage turbine that includes a re-heater. The turbine is controlled by an electro-hydraulic governor. A third order autoregressive moving average (ARMA) model is used to represent the plant that can be controlled by an adaptive pole-shift controller through the electro-hydraulic governor

Acknowledgements

First of all, I would like to express my sincere gratitude to my supervisor Dr. O.P. Malik for giving me the wonderful opportunity to work under him. I would also like to greatly acknowledge his continuous support, invaluable guidance, and constructive criticism throughout the period of my master's studies. The technical contribution to adaptive control of power systems was established by him remains a source of inspiration to me. Also, I would like to appreciate and thank him for the careful reading of this thesis.

I would also like to extend my appreciation to my examination committee members Dr. Chris Macnab, Dr. Brent Maundy from the Department of Electrical and Computer engineering, and Dr. Anil Mehrotra from the Department of Chemical and Petroleum engineering.

Special thanks to Dr. Swarn Kalsi, Ex. Director of American Superconductors, and Rebecca Nold, senior design engineer, GE Energy, USA for their technical inputs during this research. Also, I would like to thank my senior colleague Anas Albakkar for his unconditional support.

My deepest thanks to my uncles Christopher and his family, Jesu raja and his family, also I would like to extend my thanks to my friends Bharath, Bharani, Dr. Karthikeyan, Deepak Mahadevan, Karthik, Mitchel and his wife Anna, Rahul, Sridhar and Shivarajan for their kindness and unconditional support.

Finally, I would like to thank my family especially my dad Vincent De Paul regardless his health who has crossed so many hurdles to bring me up in the society, my mum Sofana Mary, my sister Ophelia, my brother in law Kennedy, my lovely nieces Lerisha, and Lanisha, my grandpa and grandma for their prayers and continuous help.

Table of Contents

List of Figures

List of Tables

List of Abbreviations

AC	Alternating Current
APSS	Adaptive Power System Stabilizer
ARMA	Auto Regressive Moving Average
ARMAX	Auto Regressive Moving Average Exogenous
AMSC	American Superconductor
AVR	Automatic Voltage Regulator
CPSS	Conventional Power System Stabilizer
CSG	Conventional Synchronous Generator
DC	Direct Current

FACTS	Flexible AC Transmission System
GE	General Electric Company
HP	High Pressure
HTSC	High Temperature Superconductor
HVDC	High Voltage Direct Current
IEEE	The Institute of Electrical and Electronic Engineers Inc
IP	Intermediate Pressure
ISO	Independent System Operator
kWh	Kilowatt -hour
LP	Low Pressure
LTSC	Low Temperature Superconductor
LQR	Linear Quadratic Regulator
MRAC	Model Reference Adaptive Control
MV	Minimum Variance
MVA	Mega Volt Ampere
MW	Mega Watt
NMP	Non – Minimum Phase
NO PSS	System without any supplementary control
P	Active Power (W)
PA	Pole Assignment
pf	Power Factor
PS	Pole Shifting
PSS	Power System Stabilizer

p.u	Per Unit representation of electrical variables
PZA	Pole Zero Assignment
Q	Reactive Power (VAr)
RLS	Recursive Least Squares
SCG	Superconducting Generator
SSSC	Static Synchronous Series Compensator
STATCOM	Static Synchronous Compensator
STC	Self Tuning Adaptive Control
SVC	Static VAr Compensator
TCSC	Thyristor Controlled Series Capacitor
UPFC	Unified Power Flow Controller

List of Symbols (chapter wise)

Chapter 1

u(t)	Controller output
y(t)	System output
ω_O	Synchronous speed of the generator (rad/sec)
$\Delta\omega$	Speed deviation of the generator with respect to synchronous speed (rad/sec)
ω	Also speed deviation (rad/sec)
T_{ref}	Initial torque reference signal (N-m)

y_p	Controlled coordinates of the system
y_r	Model reference of the system

Chapter 2

R	Resistance (Ω)
L	Inductance (H)
NbTi	Niobium titanium
Nb3Sn	Niobium tin
YBCO	Yttrium barium copper oxide
BSCCO	Bismuth strontium calcium copper oxide
K	Kelvin
T	Temperature (^{0}C or K)
T_c	Critical temperature (^{0}C or K)
ρ_i	Intrinsic electrical resistivity (Ω-m)
$\rho_{defects}$	Resistivity due to the lattice defects (Ω-m)
B_c	Critical magnetic field (T)
$P_{max(SCG)}$	Power transferred from the SCG (W)
$P_{min\ (CSG)}$	Power transferred from the CSG (W)
P_{out}	Power output from any rotating machine (W)

N	Speed of any rotating machine (rpm)
V	Active volume of the machine (m^3)
J_{max}	Electrical loading on the stator (A/m)
B_{max}	Air gap magnetic flux density (T)
V_{FL}	Terminal voltage at full load (V)
V_{NL}	Terminal voltage at no load (V)
δ	Rotor angle (rad)
Vt	Terminal voltage (V)
V_{ref}	Terminal reference voltage (V)
U_{MAX}	Upper control limit of the controller
U_{MIN}	Lower control limit of the controller.
ψ_d	Generator d-axis flux linkage of SCG (Wb)
ψ_f	Generator field flux linkage of SCG (Wb)
ψ_{D1}	Generator d-axis outer screen flux linkage of SCG (Wb)
ψ_{D2}	Generator q-axis inner screen flux linkage of SCG (Wb)
ψ_q	Generator q-axis flux linkage of SCG (Wb)
ψ_{q1}	Generator q-axis outer screen flux linkage of SCG (Wb)
ψ_{q2}	Generator d-axis inner screen flux linkage of SCG (Wb)
U_g	Governor reference signal
V_d	Generator d-axis voltage (V)
V_f	Generator field voltage (V)

V_q	Generator q-axis voltage (V)
I_d	Generator d-axis current of SCG (A)
I_f	Generator field current of SCG (A)
I_q	Generator q-axis current of SCG (A)
I_{D1}	Generator d-axis outer screen current of SCG (A)
I_{D2}	Generator d-axis inner screen current of SCG (A)
I_{Q1}	Generator q-axis outer screen current of SCG (A)
I_{Q2}	Generator q-axis inner screen current of SCG (A)
R_a	Generator armature resistance of SCG (Ω)
R_e	Transmission line resistance of SCG (Ω)
R_f	Generator field winding resistance of SCG (Ω)
R_{D1}	Generator d-axis outer screen resistance of SCG (Ω)
R_{D2}	Generator d-axis inner screen resistance of SCG (Ω)
R_{Q1}	Generator q-axis outer screen resistance of SCG (Ω)
R_{Q2}	Generator q-axis inner screen resistance of SCG (Ω)
G_M	Main valve position
G_I	Intermediate valve position
ρ_{max}	Maximum movement constraints of the valve
ρ_{min}	Minimum movement constraints of the valve
L_{fd}	Mutual inductance between armature and field winding (H)
L_{fd1}	Mutual inductance between outer screen on d –axis and field winding (H)

L_{fd2}	Mutual inductance between inner screen on d –axis and field winding (H)
L_{dD1}	Mutual inductance between armature and outer screen on d axis stator winding (H)
L_{dD2}	Mutual inductance between armature and inner screen on d axis stator winding (H)
L_{D1D2}	Mutual inductance between inner and outer screen on d axis stator winding (H)
L_{qQ1}	Mutual inductance between armature and outer screen on q axis stator winding (H)
L_{qQ2}	Mutual inductance between armature and inner screen on q axis stator winding (H)
L_{Q1Q2}	Mutual inductance between outer and inner screen on q axis stator winding (H)
L_f	Self-inductance of the field winding (H)
L_d	Self-inductance of the d –axis stator winding (H)
L_{D1}	Self-inductance of d-axis outer screen (H)
L_{D2}	Self-inductance of d-axis inner screen (H)
L_q	Self-inductance of the q –axis stator winding (H)
L_{Q1}	Self-inductance of q-axis outer screen (H)
L_{Q2}	Self-inductance of q-axis inner screen (H)
λ_d	Generator d-axis flux linkage of CSG (Wb)

λ_f	Generator field flux linkage of CSG (Wb)
λ_{kd}	Generator d-axis damper winding of CSG (Wb)
λ_q	Generator q-axis flux linkage of CSG (Wb)
λ_{kq}	Generator q-axis damper winding of CSG (Wb)
i_d	Generator d-axis current of CSG (A)
i_q	Generator q-axis current of CSG (A)
i_f	Generator field current of CSG (A)
i_{kd}	Damper winding d-axis current of CSG (A)
i_{kq}	Damper winding q-axis current of CSG (A)
e_d	Generator d-axis voltage of CSG (V)
e_f	Generator field voltage CSG (V)
e_q	Generator q-axis voltage of CSG (V)
r_a	Generator armature resistance of CSG (Ω)
r_f	Generator field winding resistance of CSG (Ω)
r_{kd}	Damper winding d-axis field resistance of CSG (Ω)
r_{kq}	Damper winding q-axis field resistance of CSG (Ω)
K_d	Generator damping coefficient
a, b	Governor gain constant
T_g	Governor time constant
T_m	Generator mechanical torque output of SCG or CSG (N-m)

T_e	Generator electric torque output SCG or CSG (N-m)
F_{HP}	Fractional contribution of high pressure stage of the turbine (p.u)
F_{IP}	Fractional contribution of intermediate pressure stage of the turbine (p.u)
F_{LP}	Fractional contribution of low pressure stage of the turbine (p.u)
Y_{HP}	Output from the high pressure of the turbine (p.u)
Y_{IP}	Output from the intermediate pressure of the turbine (p.u)
Y_{LP}	Output from the low pressure of the turbine (p.u)
X_s	Synchronous reactance (p.u)
H	Generator inertia (kWs/kVA)
τ_{GM}	Time constant of main governor (s)
τ_{GI}	Time constant of intermediate governor (s)
τ_{HP}	Time constant of high pressure stage of the turbine (s)
τ_{RH}	Time constant of reheat pressure stage of the turbine (s)
τ_{IP}	Time constant of intermediate pressure stage of the turbine (s)
τ_{LP}	Time constant of low pressure stage of the turbine (s)
τ_f	Time constant of field winding of SCG

Chapter 3, 4

$\hat{\theta}(t)$	Parameter vector estimate
λ	Forgetting factor

Σ	Constant for forgetting factor calculation
$\theta(t)$	Identified system parameter vector
$\phi(t)$	Measurement vector
$\xi(t)$	White noise
$A(z^{-1})$	System polynomial in the backward shift operator z^{-1}
a_i	Elements of the polynomial $A(z^{-1})$.
$B(z^{-1})$	System polynomial in the backward shift operator z^{-1}
b_i	Elements of the polynomial $B(z^{-1})$
$C(z^{-1})$	System noise polynomial
C_i	Elements of the noise polynomial $C(z^{-1})$
e(t)	Identification error
K(t)	Modifying gain vector for parameter identification
P(t)	Covariance matrix for parameter identification
y(t)	System output at time t
$\hat{y}(t)$	Predicted system output
α	Pole-shift factor
σ	Security coefficient
λ_c	Absolute value of the largest characteristic root of $A(z^{-1})$
β	Identified system parameter vector
α_{opt}	Optimal value of the pole-shifting factor α
$F(z^{-1})$	Denominator polynomial in the backward shift operator z^{-1} corresponding to the feed-back loop

f_i	Elements of the system polynomial $F(z^{-1})$
$G(z^{-1})$	Numerator polynomial in the backward shift operator z^{-1} corresponding to the feed-back loop
g_i	Elements of the system polynomial $G(z^{-1})$
J	Performance index
n_a, n_b	Orders of the system polynomials $A(z^{-1})$, $B(z^{-1})$
n_f, n_g	Orders of the system control polynomials $F(z^{-1})$, G(z-1)
P_i	i^{th} term of the row vector $X_c^T(t)M^{-1}$
S_i	i^{th} order sensitivity constant
u(t)	Controller output
U_{ref}	System input reference
X_c	Measurement variable vector
y(t)	System output
$\hat{y}(t+1)$	Predicted system output

Appendix

SCG

$E_{f\,max}$	Maximum limit voltage of an exciter (V)
$E_{f\,min}$	Minimum limit voltage of an exciter (V)
K_e	AVR gain
T_1, T_2	Time constant of CPSS or Phase advance network (s)
τ_e	Time constant of an exciter (s)

CSG

L_d	Self-inductance of the d –axis stator winding (H)
L_q	Self-inductance of the q –axis stator winding (H)
L_f	Self-inductance of the field winding (H)
L_{kd}	Self-inductance of the d –axis damper winding (H)
L_{kq}	Self-inductance of the q –axis damper winding (H)
L_{md}	Mutual inductance on d axis (H)
L_{mq}	Mutual inductance on q axis (H)
A1, A2	CPSS filter constants
K_A, K_C, K_F	AVR gains
K_{LF} ,I_{LF}	AVR gains
K_s	CPSS gain
T1 to T6	Time constants of CPSS
T_A, T_R,T_F	AVR time constants
T_B, T_C	AVR time constants
T_{B1}, T_{C1}	AVR time constants
V_{OEL}	AVR over excitation limit
V_{UEL}	AVR under excitation limit
V_{PSS}	Output of CPSS
V_{STMAX}	Upper limit of CPSS
V_{STMIN}	Lower limit of CPSS

Chapter One: Introduction

1.1 Research motivation

Energy is a vital part of modern life and the world net electricity generation is predicted to increase from 19.1 trillion kWh in 2008 to 25.5 trillion kWh in 2020 and 35.2 trillion kWh in 2035. As energy needs keep on growing, interest in energy efficiency and energy saving practices is gaining more importance throughout the world [1]. As energy demand keeps on growing, more power plants will be built in the future. In electric power systems throughout the world, many research initiatives are being undertaken in the exploration of generating electric power through alternative methods, and in restructuring the existing power grids to make them efficient and to meet the present energy needs. Some of them are smart grid, virtual power plant, and hybrid systems. All these new technologies are emerging and being implemented in many countries [2].

Some statistics and problems with the present technology about losses from generation to transmission and consumption are listed here. According to the USA Department of Energy, motors account for 70% of the energy consumption by manufacturing sector and this sector uses over 55% of the total electricity generated in the USA. Rotating machines like motors and generators employ conventional copper windings on stator and rotor. When the current flows through these windings, it generates resistive losses. Any significant improvement in this will result in the improvement of energy efficiency [3]. When electricity is transmitted from the power plant, a loss of about 8% occurs in Canada and USA before reaching the consumers [4].

Also, independent power producers are engaging in power business in the deregulated electric market and it is a must for them to look for higher efficiency and higher stability in the power systems [5].

1.2 Power generation

Presently, synchronous generators are used to meet the energy demand. Rating of the generators has been increasing since its inception, having reached as high as 1300 MW. Correspondingly, increase in the rating increases the size of the machine because a lot of iron and copper has to be used in the machine. Due to the present growth of energy demand, there is a continuous need for increase in the rating of the generator even beyond 1300 MW. However, with the present technology of the conventional design, the magnetic loading is limited to 1 Tesla. Also, there is a limit on electrical loading. It is restricted by slot area and thermal-cooling considerations. Due to all these restrictions, with the present technology the rating of the conventional generators is limited to 2000 MVA [6].

Problems mentioned above can be addressed with the generators constructed using super-conducting materials. The invention of super-conductors, such as Low Temperature Superconductor (LTSC) and High Temperature Superconductor (HTSC), has paved the way to the new era by replacing the Conventional Synchronous Generator (CSG) for power generation in the base power plants with the improved stability, reduced losses and hence higher efficiency.

1.3 Cryogenic power generation

For more than a decade, researchers throughout the world are actively engaged in the application of cryogenic technology in power systems. As a result, the field winding of the CSG is replaced with super-conductors. These are generally called as Superconducting Synchronous Generators (SCGs). The SCG offers lots of potential advantages to replace the existing CSG machine [7, 8]. Some of the potential impacts of SCG in comparison with CSG are given below:

- Smaller in size
- Lighter in weight
- No iron core on the armature winding
- Very low synchronous reactance hence improved steady state stability
- 0.5 % increase in efficiency so less emission per kWh
- No resistive losses in the excitation field despite high magnetic loading
- Rating beyond the conventional machine with smaller size is possible.

Considering all these potential advantages, it can be used for power generation in the base power plants by replacing the CSG. However, SCG's are characterised by low inertia, low inherent damping which affects the stability of the machine and the system when it is connected to the power system. Also, due to the very long time constant of the field winding and shielding effects of two screens it is very tough to control through the field excitation [8]. However, operation of any synchronous machine requires some sort of damping of power swings, and damping is necessary to maintain the stability of the machine in parallel with the power systems and for the stability of the machine [9]. The following is an overview of power system stability and control strategies from the literature.

1.3.1 Power system stability

Power systems are spread over wide geographic areas. They are operated as an interconnected system and are subject to many kinds of disturbances and abnormalities. As SCGs have stability issues when connected to the grid, regardless of many advantages, the stability issue has to be resolved. If it is not resolved, the stability problem arises and it can result in blackout. It is a must to keep the system stable during disturbances.

Power system stability is defined as *"the property of a power system that enables it to remain in a state of operating equilibrium under normal operating conditions and to regain an acceptable state of equilibrium after being subject to a disturbance"* [10, 11].

During the past few decades extensive research has been conducted in regards to the stability issues with the synchronous generator connected to the grid. So the main concern in this dissertation is the control of SCG when it is connected to the grid. The following is an overview of some control strategies applicable to SCG when it encounters low frequency oscillations due to power swing.

1.3.2 Power systems damping control strategies

Oscillations in power systems due to power swing are classified as local and inter-area oscillations. When a single generator oscillates against the large system in the frequency range of 0.9 to $2.0\,Hz$, it is called local area oscillations. If a group of generators oscillates against another group of generators in the range of 0.2 to $0.8\,Hz$, it is called an inter-area oscillation [12]. If the oscillations are not damped, it could lead to loss of synchronism.

In order to enhance the dynamic performance of the power system and to prevent oscillations, controllers like Power System Stabilizer (PSS) are used in practice. They help to decay the oscillations. In the recent past, many damping methodologies have been proposed in the literature. Generally, two types of strategies are followed to improve the stability of the power systems:

- Damping in the transmission path
- Damping at the site of the generator

1.3.3 Damping in the transmission path

Damping in the transmission path can be carried out by two methods as follows:

- High Voltage Direct Current Transmission System (HVDC)
- Flexible A.C Transmission System (FACTS)

1.3.3.1 High Voltage Direct Current Transmission System (HVDC)

The very fast flow of energy through HVDC link helps in damping oscillations as it can change the power flow between the respective AC systems. However, HVDC is very costly because of special requirement of equipment, like rectifiers and inverters. It also introduces harmonics to the AC systems [13, 14].

1.3.3.2 Flexible Alternating Current Transmission System (FACTS)

FACTS devices are well known in power systems for their very high controllability. Different types of FACTS devices are available. Each has its own functionality and it helps in improving the power system stability and power flow control. Some of the FACTS devices are:

- Static VAr Compensator (SVC)
- Static Synchronous Compensator (STATCOM)
- Thyristor Controlled Static Compensator (TCSC)
- Unified Power Flow Controller (UPFC)

These FACTS devices help in either absorbing or supplying the reactive power and controlling the real power depending on the device selected. However, FACTS devices are also very costly [15, 16, 17].

1.3.4 Damping at the site of the generator

In the literature, CSG damping at the location of the generator can be controlled by excitation control, governor control, and some other miscellaneous types of control [18, 19, 20, 21, 22, 23]. Of these, the excitation control is widely used. The following is an overview of control strategies of SCG through excitation, governor and other methods available in the literature.

1.3.4.1 Excitation control and field forcing of SCG

The main role of the exciter in the generator is to control the system voltage and reactive power. It also helps to provide positive damping by adding supplementary signal to it. The small

loop time constant of the exciter system helps to obtain the fast response and to damp the oscillations quicker than the mechanical systems in the CSGs, as shown in Fig. 1.1. The supplementary signal that helps to damp the oscillations through the exciter is called the PSS. Either one of speed deviation, frequency deviation, rotor angle deviation or active power deviation or a combination of more than one can be used as the input feedback signal to the PSS [23, 24]. However, the exciter loop of the SCG has very long field winding time constant of about 750 s and the shielding effect of the two rotor screens rules out the option of controlling through the exciter by adding the supplementary signal to damp the oscillations [25]. Some investigators have gone through the field by forcing it, but it has some implications such as quenching that may lead to a loss of super-conducting state of the field winding [26, 27, 28, 29, and 30].

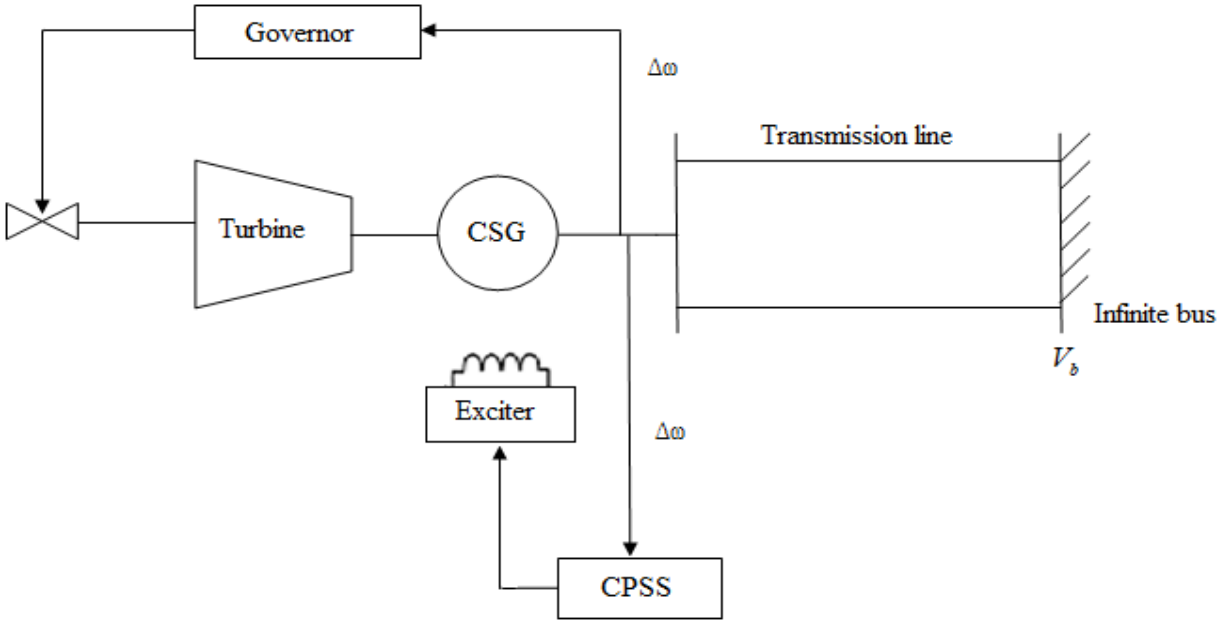

Fig. 1.1 Excitation control of the conventional synchronous generator

1.3.4.2 Miscellaneous types of control of SCG

In the literature, apart from the conventional method of controlling through the field excitation, some other methods are mentioned that are all covered under this topic.

1.3.4.2.1 Armature motion damping

In this method, the armature is allowed to rotate against a spring [31]. Damping the motion is accomplished by mounting a spring and a torsional dashpot connected in parallel with it. The rotation of the armature is constrained by the spring. It carries the steady state torque while the dashpot carries the rapid transient torques and dissipates the swing energy with the result that damping is achieved. However, as the parameters of the spring, and the spring and dash pot's sizes are pre-calculated, dashpot size can't change and adapt according to the time, operational temperature or in case of excessive torques. Also, there are chances for unilateral displacement of the stator winding, and vibrations between the stator and the rotor due to the weak suspension.

1.3.4.2.2 Shielding

The combination of thermal and magnetic shield is called as an electromagnetic shield. The main function of the electromagnetic shield is to protect the rotor from time varying magnetic field which penetrates into the cold rotor. Also, it serves as a damper winding by improving the machine and system damping. In this method, the time constant of the electromagnetic shield has to be of the order of electro-mechanical oscillations [32].

1.3.4.2.3 Double screening

The single screen cannot provide adequate damping. So the required damping can be achieved by adding double screen. In this method, the inner screen has a longer time constant, low temperature and the outer screen has a shorter time constant that acts with short circuit forces to damp oscillations [25, 33]. Regardless of the armature motion damping, shielding, and double screening, low frequency oscillations exist. So an alternative control has to be followed to fix it.

1.3.4.3 Electro-hydraulic governor control of SCG

The primary function of the governor is to control the mechanical power, but it can also be used to damp the oscillations by adding a phase advance network or PSS to the governor. The mechanical loop of the CSG is characterized by a relatively long time constant, so exciter is preferred to apply the PSS signals. The mechanical loop of the SCG has a much shorter time constant because, due to the smaller size of the machine, inertia is much smaller than that of the CSG. Fast turbine valving is possible with the help of an electro-hydraulic governor. The effectiveness of PSS through the governor can be found in the literature [34, 35, 36, 37, 38, 39, 40, 41].

1.4 Power system stabilizer

The generators were initially equipped with an Automatic Voltage Regulator (AVR). The main purpose of the AVR is to regulate the terminal voltage of the generator and to control the

reactive power [42]. Though the AVR helps to improve the steady state and transient stability, low frequency small magnitude oscillations often exist in the network which results in the loss of synchronism. The PSS became the prime solution and various techniques regarding PSSs have been developed.

1.4.1 Phase advance network

The supplementary controller that is commonly added to the exciter or governor is called the conventional power system stabilizer (CPSS) or phase advance network. It acts on the generator through the governor in SCG to damp the oscillations. The role of governor control is discussed in [34, 35, 37, 38]. It improves the performance of the system. It is a fixed parameter device that provides lead-lag compensation and the design is based on classical control theory using a fixed transfer function for all operating conditions. Because of its fixed type, when applied to the non-linear power system operating over wide range of operating conditions, it has the following drawbacks:

- The transfer function chosen for the CPSS is a compromise for different operating conditions
- It cannot track the variations for different operating conditions
- It is designed for a specific operating condition, so it cannot be used for different operating conditions without tuning its parameters manually.

Considering the above drawbacks, it is better to implement an adaptive controller by replacing the CPSS with an adaptive PSS [40, 43].

1.4.2 Adaptive Power Systems Stabilizer (APSS)

Adaptive control is a specific type of control where the process is controlled in closed loop and the knowledge about the system is obtained online when the system is operating. The Adaptive Power System Stabilizer (APSS) can be defined as a controller that adapts to the changes in the environment by self adjusting its transfer function to the different operating conditions of the power system [23, 44]

The adaptive controller based on adaptive control theory is classified into two categories such as [45, 46, 47]:

- Model Reference Adaptive Control (MRAC)
- Self-Tuning Adaptive Control (STC)

1.4.2.1 Model Reference Adaptive Control

The role of MRAC is to adjust the parameters of the controller so that the output of the controlled system matches, agrees with the reference model. The difference between the model and controlled coordinates of the system is used as an adjustment. The performance of the controller solely depends on the determination of suitable reference model and the learning mechanism as shown in the Fig. 1.2. This type of control is also called direct adaptive control.

1.4.2.2 Self-Tuning Adaptive Control

The self-tuning control is one of the most successful and well established techniques. Substantial amount of experiment and research has been done with this strategy to improve the power system stability. It has gained popularity because of its flexibility. The role of STC is to

compute the control signal based on the identified system parameters. It has two loops, one is the controlled process with a linear feedback controller and another one that the online parameter identification as shown in Fig. 1.3 This type of control is also called as an indirect adaptive control.

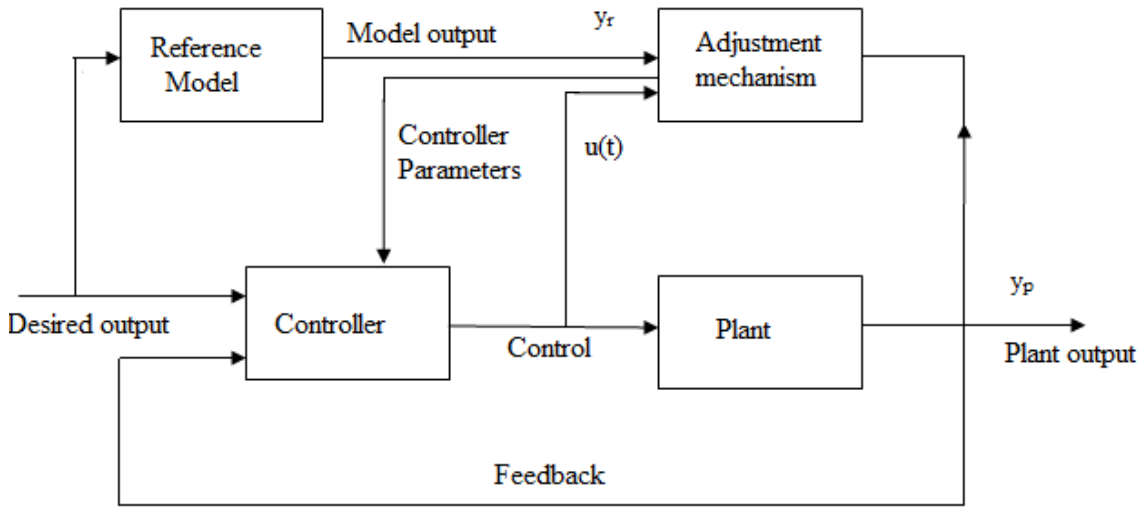

Fig. 1.2 Model reference adaptive scheme

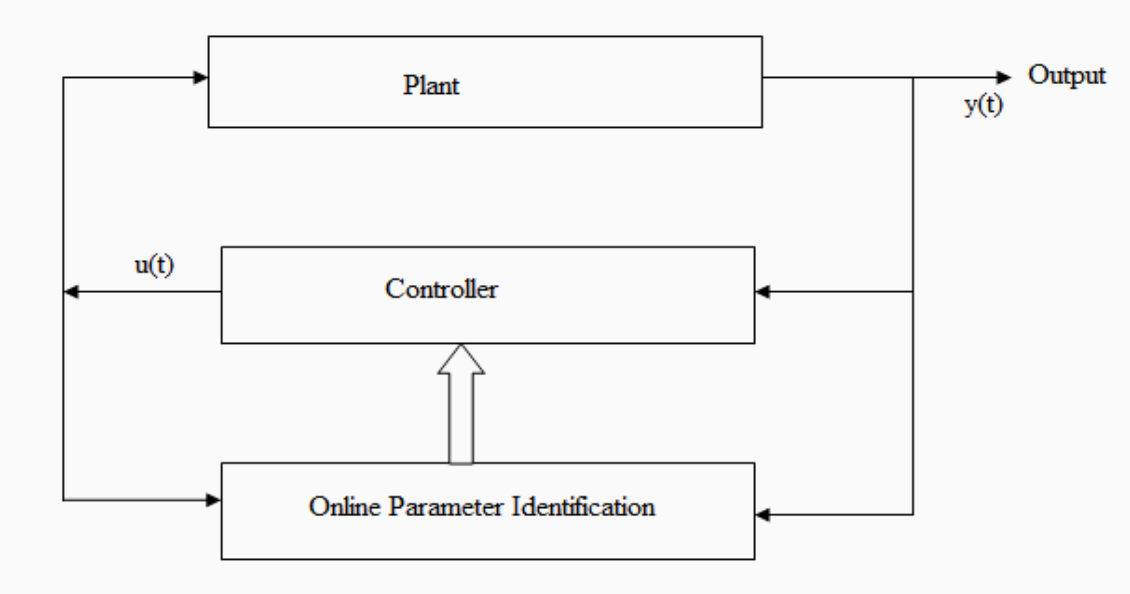

Fig.1.3 Self-tuning adaptive control scheme

1.5 Strategies for online identification and control

The behaviour of the power system changes from time to time. So it is necessary that the identification schemes track the changes each sampling period as closely as possible. Performance of the APSS improves as the identified model closely fits the actual system. After the parameters are identified online, the appropriate control signal is obtained. In order to develop the control strategy, it is assumed that the identified model reflects the actual system. Also, the controller has to have good tolerance to errors in the identified model. Thus, when the identified model closely matches the actual system and when the controller has the error tolerance to the identified model, better performance can be achieved.

In control strategies, the identified model may be minimum or non-minimum phase (NMP). In case of NMP, there are some restrictions imposed on strategies for the controller. Discussion about the widely used controllers is given below.

In the Minimum Variance (MV) control the goal of the controller is to minimize the variance. After predicting the output error for the next sampling instant, the controller helps in reducing the predicted error to zero. This controller has good features when the sampled system is NMP. However, it cannot establish or ensure stability as it requires exact cancellation of the zeros of the sampled system inside the unit circle in the z–domain and it could lead to excessive oscillations [48].

The Generalized minimum variance controller is a simple controller and an extension of MV control. Although it is simple, the stability of the closed loop is not taken into consideration [49]. To address these issues, a Linear Quadratic Regulator (LQR) Controller is used [43] and the performance index is chosen so that the error between the system input and output is minimized. When the identified parameters are correct it helps in improving the closed loop stability. As LQR requires the solution of the matrix Ricatti equation, it imposes computational burden and also it requires the state space form. So, there is a need to convert the system parameters to the canonical form [47].

Pole Zero Assignment (PZA) control can be used. In this strategy unlike the MV, both the open-loop poles and zeros are shifted to the left in the s-domain. The designer has to pre-specify the poles and zeros so it can overcome the problems like NMP that are associated with MV controller. However, better performance can be obtained only if the designer has very good knowledge of the system characteristics. Also, it is very hard to choose the poles and zeros for the non- deterministic systems and it may lead to an unstable system if the poles and zeros are not chosen properly. If the poles alone are shifted, then it is Pole Assignment (PA) Controller

that has also the same issues as PZA. So the proper controller has to be used to overcome all these issues [50, 51].

Pole Shifting (PS) control strategy is the modern version of the PA control. In this the closed loop poles are obtained by shifting the identified open loop poles radially towards the center of the unit circle in the z-domain. Shifting the poles has the direct impact in increased damping. The factor by which the poles are shifted is called as pole shifting factor. This PS controller offers more stability than any other algorithm. Also, the performance of this controller depends solely on the pole-shifting factor. From the past studies and experiments, in fact many controllers need manual tuning and are practically very difficult to apply. As pole-shifting controller is practically very easy to implement and it has lots of advantages, attention is given to PS in this thesis [47].

1.6 Adaptive governor scheme based on self-tuning adaptive control

As discussed earlier, it is very hard to control the SCG through the exciter similar to the CSG. Due to the smaller time constant of the governor loop, fast acting electro-hydraulic governor with fast turbine response and smaller size of the machine with less inertia constant than the CSG of the same rating offers very good fast acting damping performance through the governor.

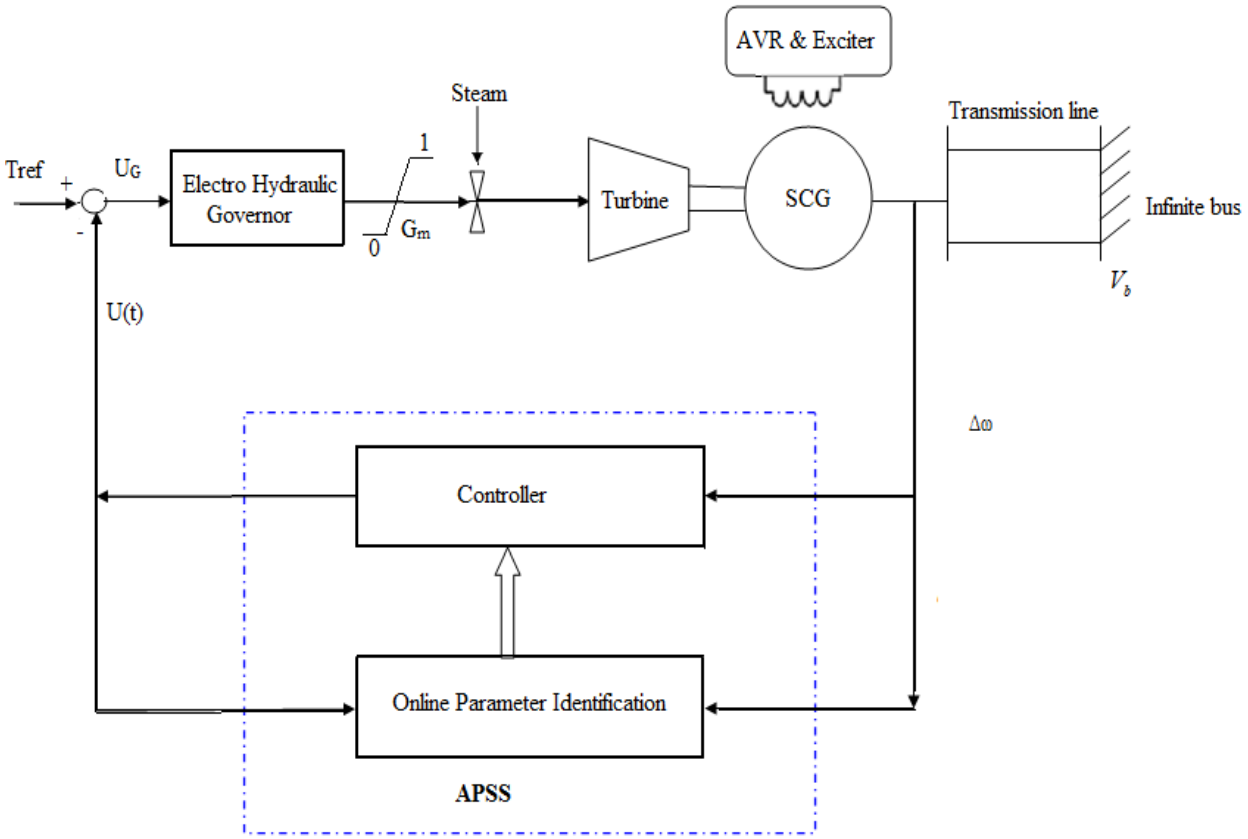

Fig.1.4 Governor control scheme of SCG with the APSS

Considering the advantages of controlling through the governor, the scheme as shown in Fig. 1.4 is followed in this investigation. Earlier investigators kept the AVR and exciter constant during the transients. However, in this research it is not kept constant and it is allowed to react freely during the transients. Also the literature survey showed RLS and Kalman identifiers applications to a SCG through the electro-hydraulic governor to improve damping. It did not reveal any applications of the pole-shift control based APSS.

1.7 Research objectives

The primary goal of this research is to design and develop an adaptive power system stabilizer based on a pole-shift linear feedback control algorithm for the super-conducting generator powered by fossil fuels (thermal power plant) and connected to an infinite bus

A third order discrete auto regressive moving average (ARMA) model is used to represent the power system that includes the superconducting generator connected to an infinite bus through a three stage turbine with a single reheater and equipped by an electro-hydraulic governor.

The Recursive Least Squares (RLS) and Kalman Filter (KF) identification techniques are applied to track the dynamics of the system during the steady state and transients so that it can update the controller for different operating conditions.

The closed loop poles are determined by shifting online the open loop poles, obtained from the identified parameters, with the help of PS control. Poles are shifted radially towards the center of the unit circle in the z-plane and the desired control signal is calculated.

The APSS with the PS controller is applied successfully to the electro- hydraulic governor under a single machine infinite bus environment.

1.8 Thesis organization

This thesis consists of 7 chapters including the introductory part as chapter 1.

Chapter 2 reviews the laws, properties of superconductivity, types of superconductors, development, construction, advantages of high temperature and low temperature

superconducting based generators, mathematical modeling of generators and applications of superconductors in power systems.

Chapter 3 starts with a discussion about the stochastic modeling like ARMA, ARMAX, and followed by discussions about the system identification techniques like RLS, Kalman Filter.

Chapter 4 describes the detailed concepts of PS control strategy. Then, a discussion about how to self-optimize the Pole-Shifting factor for the PS strategy is discussed.

Results of the system identification techniques such as; RLS with a variable forgetting factor, Kalman filter, with the third order ARMA model are presented in Chapter 5 for different types of disturbances and operating conditions.

Chapter 6 presents the simulation studies of the APSS based on pole shift controller employed with RLS algorithm with a variable forgetting factor under a single machine infinite bus environment. Comparative studies of the performance without PSS, and with CPSS and APSS are presented for different types of disturbances and operating conditions. Finally, conclusions and comments about future research are given in Chapter 7.

Chapter Two: Superconductivity and Superconducting generator

2.1 Background

The opposition of a circuit to the flow of electric current is called as electrical resistance. Ohm's law can be described as current I through a circuit is proportional to the potential difference V and a constant of proportionality, called the resistance R. Dutch physicist "H.K Onnes" discovered in 1911 that the resistivity of mercury dropped to zero at a temperature of 4.2^0 K. Later on this phenomenon was called as superconductivity and the mercury below 4.2^0 K was called as "superconductor" which has zero resistance unlike the conventional conductors. After that many other superconductors were also discovered. The major breakthrough was after the discovery of high temperature superconductor (HTSC) by J.Georg Bednorz and K.Alex Muller in 1986. They found the HTSC in the oxides of lanthanum, barium, and copper. Before that, the liquid helium which is relatively a rare chemical and very expensive was used to cool the low temperature superconductors (LTSCs). The potential advantages of using superconductors are:

- Superconductors can transmit D.C without any loss and no dissipation of energy due to resistive heating.
- Superconductors can transmit much larger amounts of electricity than the conventional conductors, like copper, aluminum of the same size.
- Superconductors actively exclude magnetic fields. When a magnet is placed above a superconductor, it results in magnetic levitation.

Many potential advantages of superconductors over conventional conductors led to the development of new equipment in different fields like energy, medical, and transportation [52, 53, 54]

2.2 Properties of superconductors

Applications of superconductors in power systems take advantage of their electrical and magnetic properties. The following is a brief overview of the properties of superconductors, types of superconductors, materials and applications of superconductors in power systems.

2.2.1 Critical temperature

The specific temperature at which the electrical resistance of a superconductor drops to zero is called as critical temperature T_C. The value of T_C depends upon the type of superconductor. The highest known critical temperature is 135^0 K that is observed in mercury thallium barium calcium copper oxide [55].

2.2.2 Zero resistance

In normal metals due to the collision between the scattered electrons and thermal vibrations of ions in the metal lattice, the resistance of the metal to the flow of D.C increases. On the other hand, the resistance of metal decreases when it is cooled down to absolute zero because of much lesser vibrations in the lattice, but it does not reach zero due to the impurities, $\rho_{defects}$, in the lattice. It is defined by the equation (2.1):

$$\rho(T) = \rho_i + \rho_{defects} \qquad (2.1)$$

where

ρ_i is the intrinsic electrical resistivity measured in Ω·m

$\rho_{defects}$ is the resistivity due to the lattice defects measured in Ω·m

In superconducting materials, the resistance falls to zero once it reaches T_c. Variation of resistivity between the normal and superconducting material according to the temperature is shown in Fig. 2.1. The electrical resistance disappears with D.C, but there are finite losses with A.C due to the hysteresis and eddy current effects [55].

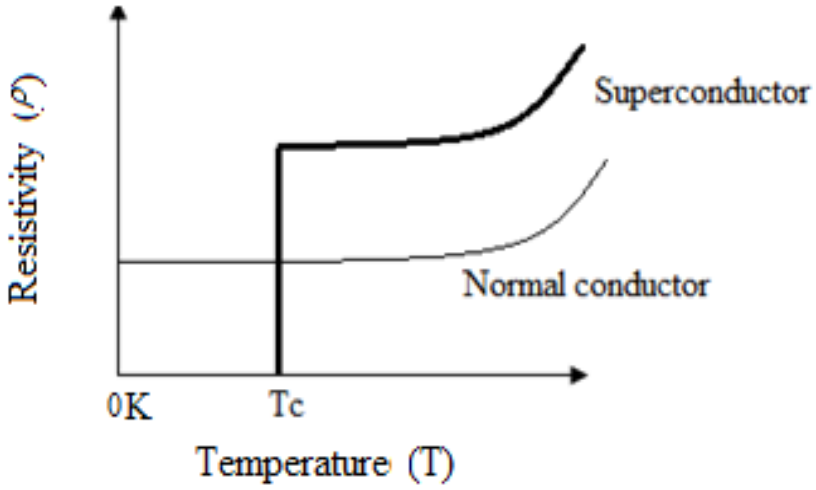

Fig.2.1 Variation of resistivity for a normal and a super conductor with temperature [56]

2.2.3 Meissner effect

The phenomenon of expulsion of magnetic flux during the transition from normal conductor to a superconductor is called as the Meissner effect. As shown in Fig. 2.2 when

$T > T_C$ the magnetic flux penetrates through the conductor, but when $T < T_C$ it expels it. This phenomenon usually occurs in the Type I superconductor [55]

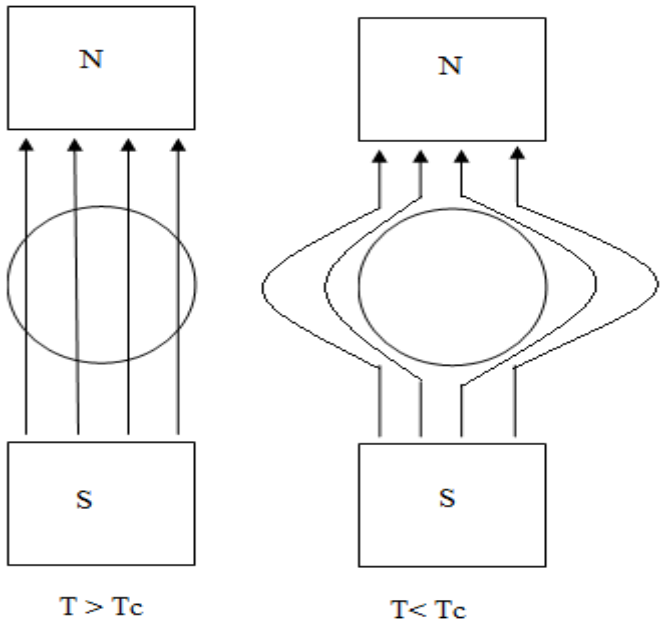

Fig.2.2 Exclusion of magnetic flux explained by Meissner effect [56]

2.3 Types of superconductors

2.3.1 Type I superconductors

Usually pure metals like mercury, and lead, are classified as Type I superconductors and they possess zero resistance below critical temperature. When the magnetic field exceeds the critical magnetic field (B_c) then the superconducting state cannot exist in the presence of magnetic field greater than its critical value and it reverts back to normal conductor as shown in Fig. 2.3 (a).

So the maximum current that can be carried through Type I superconductors is limited by its critical field. It has very low B_c, 0.2 Tesla. So it cannot be used in any application. The value

of B_c depends on the critical temperature for the Type I superconductor [56]. As B_c depends upon the temperature, critical temperature, and material it is defined by:

$$B_C(T) = B_C[0]\left[1-\left(\frac{T}{T_c}\right)^2\right] \qquad (2.2)$$

where, $B_c[0]$ is the critical magnetic field when $T = 0$.

2.3.2 Type II Superconductors

Compounds like Niobium Titanium, and Liquid nitrogen are classified as Type II superconductors. These materials are characterized by two critical magnetic fields such as B_{c1}, B_{c2} as shown in Fig 2.3 (b). When the magnetic field is less than B_{c1} at T_C then it reaches superconducting state without any flux penetration on it. However, when the magnetic field exceeds B_{c2} it reverts back to the normal state as in Type I superconductors. In between B_{c1}, B_{c2} the material has mixed state, called as "Vortex state", with partial penetration of flux. The critical magnetic field of Type II superconductors is much larger than the Type I superconductors. So Type II superconductors are well suited for the superconducting magnets to obtain high densities of flux [56].

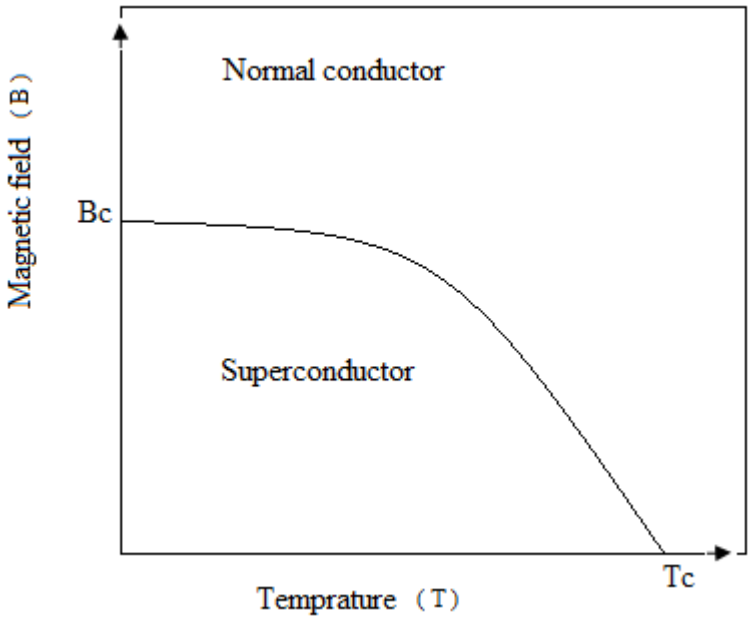

(a) Type I superconductors

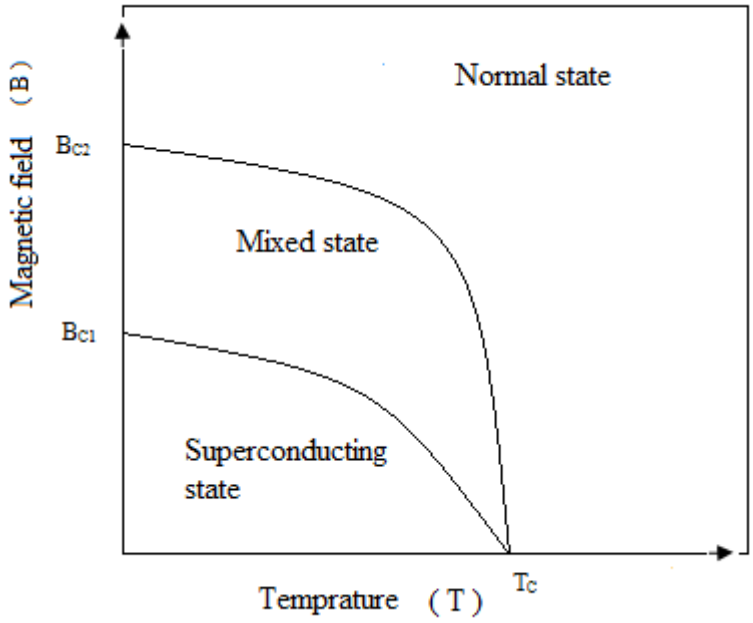

(b) Type II superconductors

Fig. 2.3 Phase diagrams of superconductors [56]

2.4 Classification of type II superconductors

Type II Superconductors are classified in to two types such as LTSC and HTSC.

- LTSC such as NbTi, Nb3Sn. This type of superconductor has critical temperature less than or equal to 23^0 K and it typically needs expensive liquid helium as a coolant.
- HTSC such as YBCO, BSCCO. This type of superconductor has critical temperature up to 135^0 K and it needs inexpensive liquid nitrogen as a coolant. So HTSC is widely preferred [55].

2.5 Applications of Superconductivity in power systems

The phenomenon of superconductivity offers many advantages over the conventional conductors and it has been applied in power systems in many devices such as [56]:

- Superconducting fault current limiters
- Superconducting magnetic storage [SMES]
- Superconducting power transmission cables
- Superconducting transformers
- Superconducting motors and generators.

2.6 Overview of the development of SCG

Since early 1960s superconductivity has been a hope and vision for power generation. Due to the development of nuclear power the generator ratings increased and the SCG has been considered as the solution to increase the power densities and ratings. Since then several programs have been started worldwide on SCGs. The following is a brief overview of the development of SCG

A prototype model of SCG was initially developed around 1960s. An SCG rated 50 kW, in which both the armature winding and the field winding are superconducting, was developed by Dynatech for US Air Force in 1967 with the use of LTSC technology. Although it was not successful, testing revealed that there were some AC losses in the superconducting armature winding [57]. Later, several small synchronous SCGs were developed with the conventional armature windings and the superconducting field winding. These early efforts from MIT include 45 kVA and 2 MVA machines. The NbTi was used on the rotor winding at 4.2^0 K operation and they found that there is a need for thermal and electromagnetic shields to avoid the problem of heating [58]

The second wave for LTSC was started between the late 1970s and 1990s. Westinghouse achieved high speed rotation with the use of superconducting field winding and also the capability of handling large centrifugal loads. In 1975, EPRI in collaboration with Westinghouse and General Electric performed design studies for the 300 MVA and 1200 MVA SCG [59]. After that, the first SCG in Japan was built in 1977. Mitsubishi Electric and Fuji Electric together developed a 6.25 MVA SCG with the field coils made up of monolithic NbTi, 2 poles, 60 Hz, 3600 rpm. Around 1982, Hitachi constructed a 50 MVA machine followed by 1000 MVA machine as well [60]. The development of SCG also started in France, China, and Germany in between 1970s – 1980s. A 320 kVA SCG was built with rotating armature and its dynamic performance was investigated at the University of Munich. General Electric built another 20 MVA SCG in which the field winding was made up of NbTi with the plan to add Nb_3Sn wire [61]. However, the LTSC based SCG‘s development was halted with the discovery of HTSC in 1986.

2.6.1 LTSC vs. HTSC based SCG

The main advantage of using the LTSC in the field winding is to avoid resistive losses. Apart from that, high field current densities and higher ratings can also be achieved. However, the operating cost of LTSC in order to maintain the refrigeration unit (4^0 K) is higher than HTSC (20^0 -77^0 K). So maintaining the winding at such ultra-low temperature and the complexity of cooling equipment raised questions about the economic feasibility of LTSC generators. On the other hand, with the use of HTSC, the operating temperature of HTSC conductors like BSCCO (20^0 - 35^0 K), YBCO (60^0 – 77^0 K), MgB2 (20^0 -30^0 K), eliminates the need for continuous supply of liquid cryogens to it. Also, on HTSC conductor with the use of cryogenic refrigerator the cooling can be done with much less complications. All the above advantages of HTSC like simple cooling system, higher thermal margin over LTSC, paved the way to the new era of using the HTSC in the field winding of the SCG and called as high temperature superconducting generators. In the mid 1990s companies like AMSC, Westinghouse and General Electric (GE) had shown interest in developing the HTSC based SCGs with the use of BSCCO in the field winding and liquid nitrogen as a coolant. Some notable models are 50 MW, 3600 rpm developed by AMSC, 850 kW, 1800 rpm developed by Westinghouse and a 1.5 MVA developed by GE [30].

In 2010, a company named converter team (a part of GE) installed a 1.7 MW, 214 rpm HTSC based generator in Germany for a small hydro power plant and it resulted in 30 % more power output than the existing unit [62].

2.7 Topologies of SCG

Many topologies of SCGs are mentioned in the literature. However, in practise predominately the rotating field winding, stationary armature topology is followed for both HTSC and LTSC generators.

2.7.1.1 Stator

Similar to the CSG the stator has water cooled three phase copper winding, but the armature teeth of SCG have been removed from the stator that results in a large air gap. An environmental shield covers the stator in order to limit the strong magnetic field within the generator [63, 64, 65].

2.7.1.2 Rotor

The rotor of SCG is not monolithic and its subdivisions are as follows; the inner rotor, superconducting field winding, inner cold shield, outer damper shield, refrigeration system, as shown in Fig. 2.4. The superconducting field windings are placed in the slots of the inner rotor and depending upon the type of superconductor, HTSC or LTSC, the appropriate temperature is maintained. Correspondingly, the coolant liquid nitrogen or liquid helium is used. The inner rotor is made up of non-magnetic steel and the ends are supported by torque tubes. It helps to transmit the peak torque during the faults. Damper shields are used in order to prevent the quenching of superconducting field winding. It has two concentric electromagnetic shields, called as inner and outer damper shields. The outer damper shield acts as a damper and it damps the oscillations during the faults. It also prevents the magnetic flux with high frequencies, and it helps to shield

the entire cryogenic zone. On the other hand, the inner damper shield helps in shielding the superconducting field winding from time varying magnetic field [25, 66].

2.7.1.3 Refrigerator

The important aspect of the SCG is to keep the field winding at low temperature that is enhanced by the refrigerator. The refrigeration unit has four parts such as cryostat, cryogenic pump, heat exchanger, and liquid coupling junction. Depending on the type of superconductors (HTSC, LTSC), liquid cryogen like helium or nitrogen is chosen and the most used cryocooler is Gifford – McMahon cryocooler. At present all known superconductors have to be operated at cryogenic temperature between 4^0 and 80^0 K [3, 56].

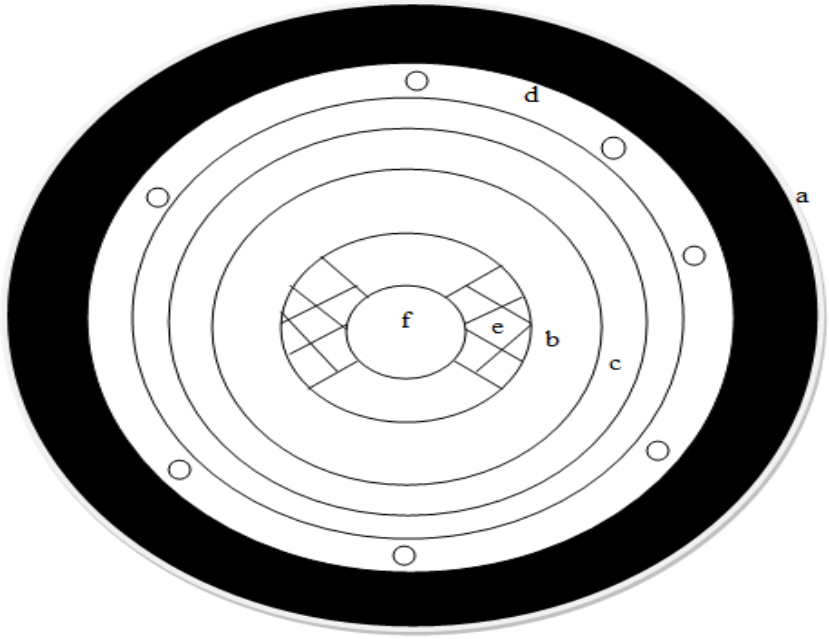

Fig.2.4 Cross view of superconducting generator [25]

a) Environmental shield b) Cold inner shield c) Warmer cold shield d) Armature

e) Superconducting field winding f) Inner rotor

2.8 Characteristics of SCG vs CSG

2.8.1 Improved steady state stability

SCGs are characterised by low synchronous reactance that helps to enhance the power transfer capacity of a transmission line. The SCG is represented as a voltage source connected to the infinite bus through the reactance *Xe* as shown in Fig. 2.5

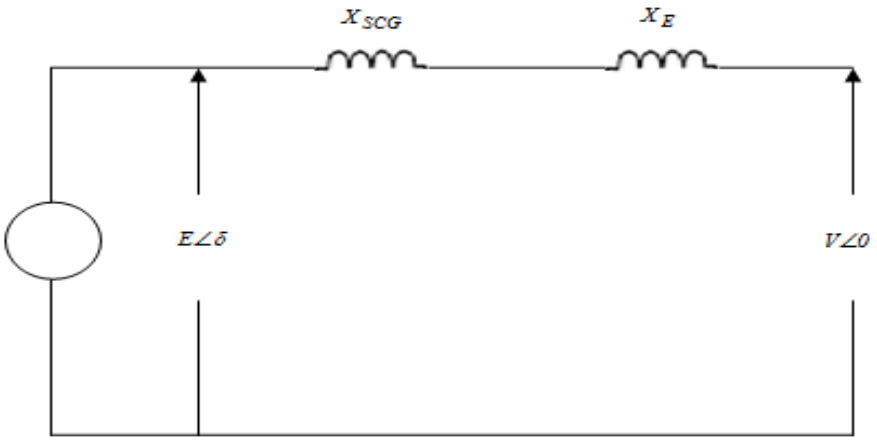

Fig.2.5 Single machine connected to an infinite bus

The maximum power transmitted from SCG is given by:

$$P_{\max(SCG)} = \frac{E.V}{X_{SCG} + X_E} \qquad (2.3)$$

where

X_{SCG} is the per unit synchronous reactance of SCG. It is $\frac{1}{3}$rd to $\frac{1}{4}$th of the synchronous reactance of a CSG of similar rating. This results in increased steady state stability of SCG by the

factor of 3 to 4 times. On the other hand, if the SCG is replaced by CSG then the maximum power transmitted to the infinite bus is given by:

$$P_{\max(CSG)} = \frac{E.V}{X_{CSG} + X_E} \qquad (2.4)$$

where X_{CSG}, the synchronous reactance of CSG is usually 3 to 4 times higher than the synchronous reactance of SCG of similar rating.

From equations (2.3) and (2.4), equation (2.5) is written as:

$$P\,max(SCG) > P\,max(CSG) \qquad (2.5)$$

It is clear from equation (2.5) that the power transfer capacity of SCG is larger than CSG as shown in Fig.2.6.

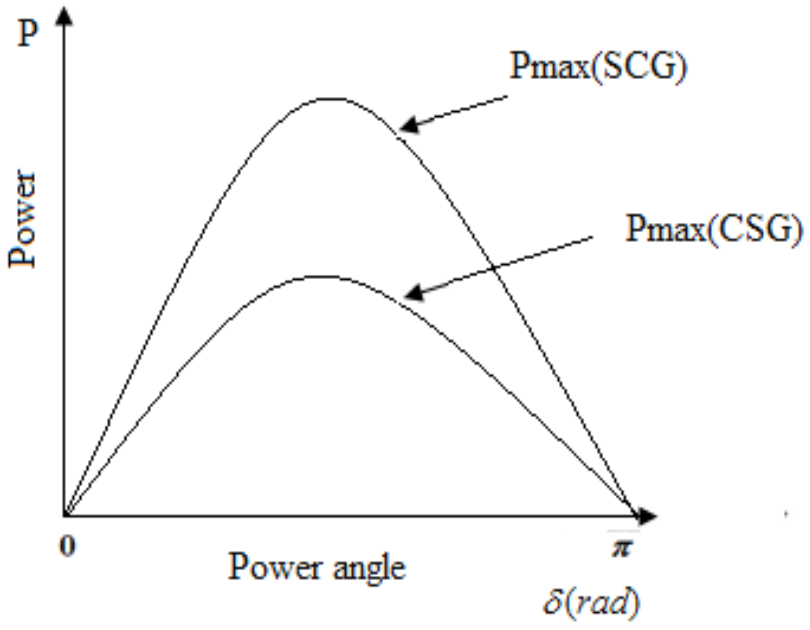

Fig.2.6 Power angle characteristics of SCG vs CSG

2.8.2 High current density

In any DC or AC conventional rotating machine, exceptionally large amount of iron is used to achieve the high permeability paths that also help in obtaining the largest possible air gap magnetic flux density for a given amount of excitation [3, 67]. The power output of any rotating machine can be expressed as

$$P_{out} = K.N.V.B_{max}.J_{max} \tag{2.6}$$

where

K is proportionality constant

N is the speed measured in rpm

V is the active volume of the machine, is directly proportional to the square of the internal stator diameter and active length of the machine (m^3)

J_{max} is the electrical loading on the stator measured in (A/m)

B_{max} is the air gap magnetic flux density in SCG due to the superconducting field winding, is much higher than in the CSG so that the armature of SCG does not need any iron. Also, the size of the SCG is much smaller than the CSG.

2.8.3 Improved voltage regulation

The field current of SCG between no load and full load is much smaller than the CSG. It is clear from this that the SCG can be operated at any power factor within its MVA rating. Also,

the short circuit ratio (SCR) of SCG is much higher than the CSG due to the low synchronous impedance [68].

$$SCR_{(SCG)} > SCR_{(CSG)} \quad (2.7)$$

where $SCR = \frac{1}{X_S}$ (2.8)

Due to the high value of SCR of SCG it has superior voltage regulation and it provides stable operation for any type of load.

$$\text{Voltage regulation of SCG} = \frac{V_{NL} - V_{FL}}{V_{FL}} * 100 \quad (2.9)$$

where V_{NL} is the no load terminal voltage (V)

V_{FL} is the full load terminal voltage (V)

2.9 System description

The system considered for simulation using MATLAB is a two pole single machine (SCG) connected to an infinite bus through two parallel transmission lines. The SCG has superconducting field winding on the rotor surrounded by outer and inner screens. The outer screen (D1: d – axis representation of outer screen, Q1: q-axis representation of outer screen) has shorter time constant than the inner screen, and it serves as a damper. The inner screen (D2: d – axis representation of inner screen, Q2: q-axis representation of inner screen), having longer time constant than the outer screen, helps to shield the superconducting field windings from the time varying magnetic fields. The SCG is driven by a three stage steam turbine with a re-heater between the high and intermediate pressure stages. Fossil fuel, coal or oil, fired boiler is used to

produce the steam as shown in Fig.2.7. In the literature the input to the steam turbine is assumed to be constant as 1.2 p.u. The fast acting electro hydraulic governor is used to obtain the fast turbine response and the turbine is controlled by the main and interceptor governor valves, both working together from the speed deviation signal of the SCG. A simple exciter is considered in the system that helps to excite the field winding through the signal received by AVR [66].

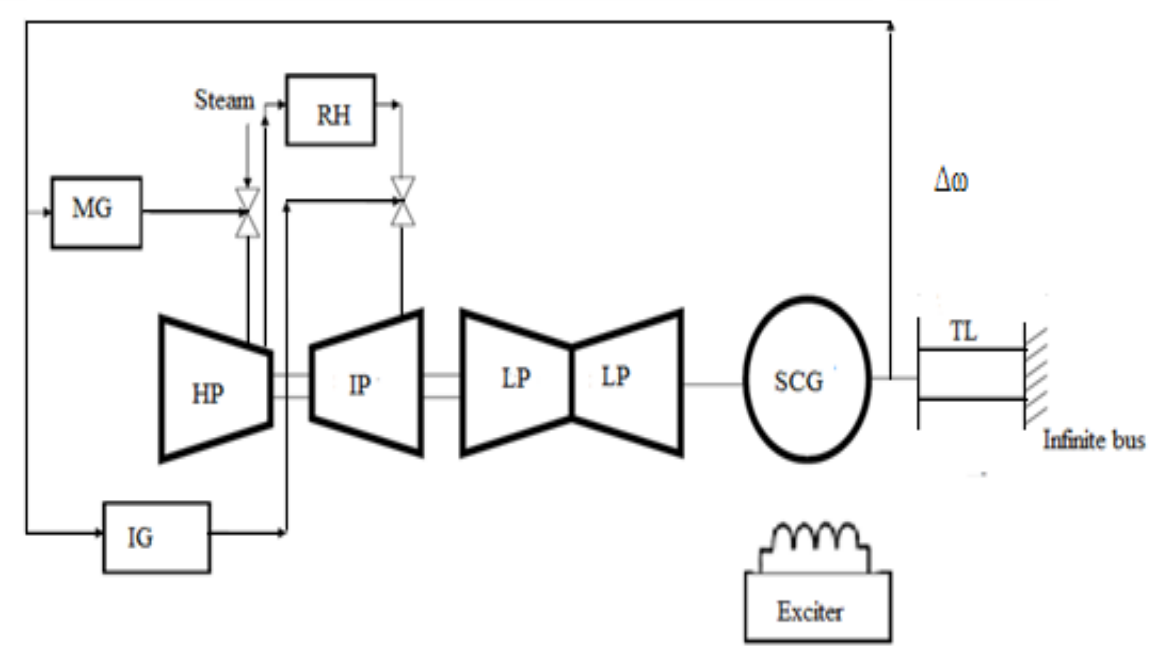

HP - High pressure stage, IP - Intermediate pressure stage, LP - low pressure stage

TL - Transmission line, IG - Intercept governor, MG - Main governor, RH – Reheater

Fig.2.7 Detailed model of a superconducting generator with a three stage turbine connected to an infinite bus through a transmission line

2.9.1 Mathematical modeling of SCG

Park's d–q axis representation is widely used in the literature to represent the synchronous generators and is used to represent the SCG as well. A ninth order model, with the non-linear differential equation from 2.10 to 2.18, is used to represent the SCG. The two axis representation of SCG is shown in Fig. 2.8 and the flux linkage model is also mentioned in the form of matrices (2.19) and (2.20).

$$p\psi_f = (V_f - i_f.R_f) \quad (2.10)$$

$$p\psi_d = \omega_O(V_d + i_d R_a + \psi_q) + \psi_q.\omega \quad (2.11)$$

$$p\psi_{D1} = -\omega_O i_{D1} R_{D1} \quad (2.12)$$

$$p\psi_{D2} = -\omega_O i_{D2} R_{D_2} \quad (2.13)$$

$$p\psi_Q = \omega_O(V_q + i_q.R_a - \psi_d) - \psi_d.\omega \quad (2.14)$$

$$p\psi_{Q1} = -\omega_O i_{Q_1} R_{Q1} \quad (2.15)$$

$$p\psi_{Q2} = -\omega_O i_{Q_2} R_{Q2} \quad (2.16)$$

$$p\delta = \omega \quad (2.17)$$

$$p\omega = \frac{\omega_O}{2H}(T_m - T_e) \quad (2.18)$$

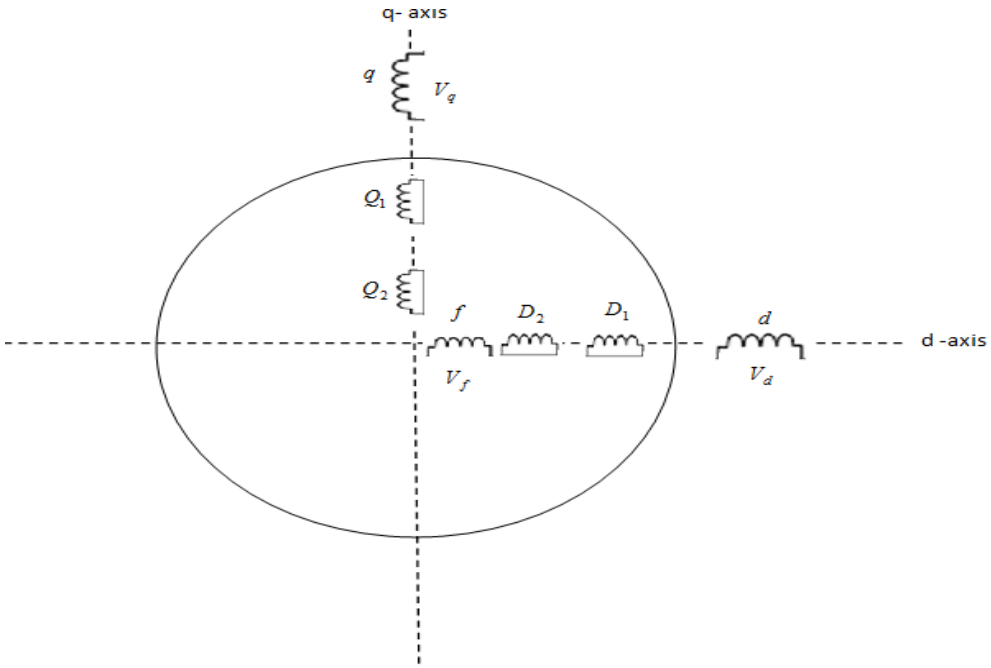

Fig.2.8 d-q axis representation of SCG [67]

f: d –axis representation of field winding , d : d –axis representation of stator winding ,

q: q – axis representation of stator winding

$$\begin{bmatrix} i_f \\ i_d \\ i_{D1} \\ i_{D2} \end{bmatrix} = \begin{bmatrix} Lf & -L_{fd} & L_{f\,D1} & L_{fD2} \\ L_{fd} & -L_d & L_{dD1} & L_{dD2} \\ L_{fD1} & -L_{dD1} & L_{d1} & L_{D1D2} \\ L_{fD2} & -L_{dD2} & L_{D1D2} & L_{D2} \end{bmatrix}^{-1} \begin{bmatrix} \psi_f \\ \psi_D \\ \psi_{D1} \\ \psi_{D2} \end{bmatrix} \qquad (2.19)$$

$$\begin{bmatrix} i_q \\ i_{q_1} \\ i_{q2} \end{bmatrix} = \begin{bmatrix} -L_q & L_{qQ_1} & L_{qQ2} \\ -L_{qQ_1} & L_{Q1} & L_{Q1Q2} \\ -L_{qQ2} & L_{Q1Q2} & L_{Q2} \end{bmatrix}^{-1} \begin{bmatrix} \psi_q \\ \psi_{q1} \\ \psi_{q2} \end{bmatrix} \qquad (2.20)$$

The typical values of the variables in the matrix are mentioned in Appendix A3.

2.9.2 Modeling of steam turbine

The tandem compound steam turbine is simulated with a single reheat stage as shown in Fig.2.9 [69]. Dynamics of the turbine are represented by four first order differential equations as shown from equations (2.21) to (2.27). The typical values of time constant in the equations from (2.21) to (2.27) are mentioned in Appendix A3.

$$pY_{HP} = \frac{(G_M P_0 - Y_{HP})}{\tau_{HP}} \tag{2.21}$$

$$pY_{RH} = \frac{(Y_{HP} - Y_{RH})}{\tau_{RH}} \tag{2.22}$$

$$pY_{I\,P} = \frac{(G_I Y_{RH} - Y_{IP})}{\tau_{IP}} \tag{2.23}$$

$$pY_{LP} = \frac{(Y_{IP} - Y_{LP})}{\tau_{LP}} \tag{2.24}$$

$$T_m = F_{HP}.Y_{HP} + F_{IP}.Y_{IP} + F_{LP}..Y_{LP} \tag{2.25}$$

$$p_{GM} = \frac{(Ug - G_M)}{\tau G_M} \tag{2.26}$$

$$p_{GI} = \frac{(Ug - G_I)}{\tau G_I} \tag{2.27}$$

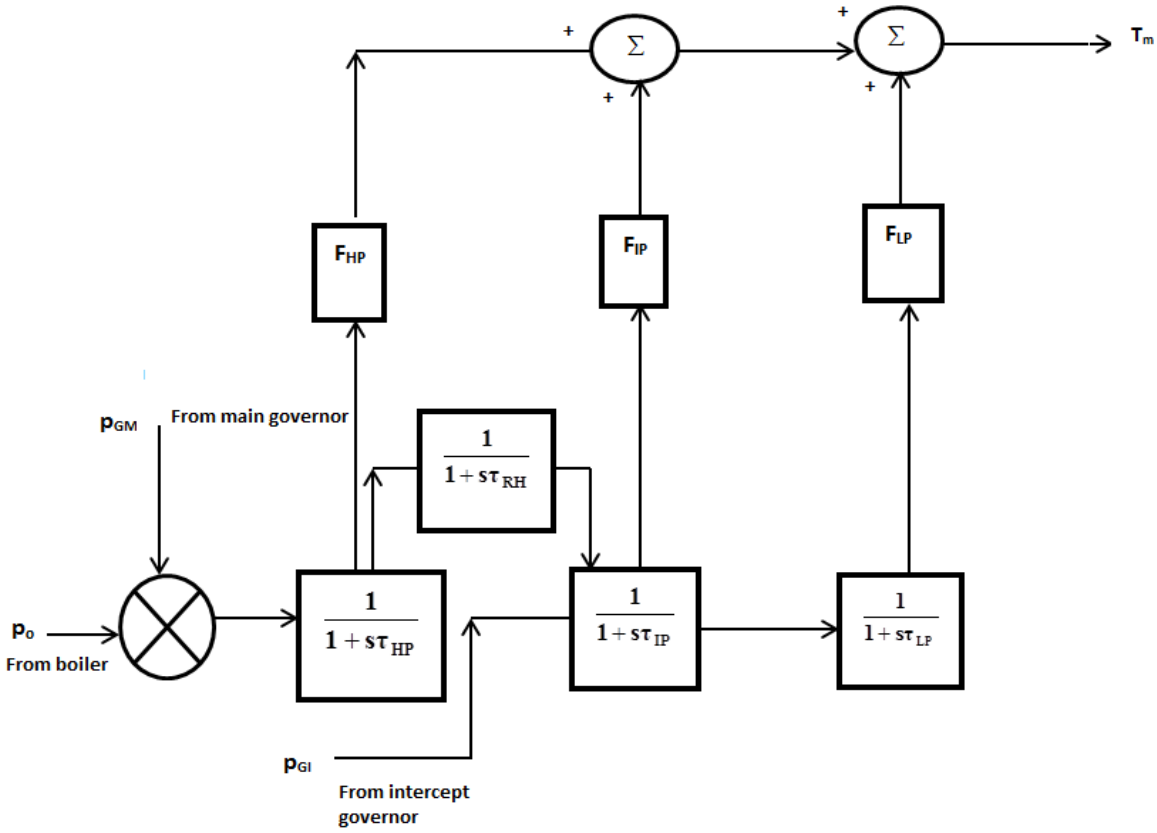

Fig.2.9 Model of steam turbine with a re-heater

2.9.3 Configuration of the controller

The generator shaft speed deviation signal is used as an input to the PSS and its output is limited with limiters $U_{\max}$, $U_{\min}$ to prevent an excessive signal from the controller. The output of the controller (phase advance network) is then fed to a fast response electro-hydraulic governor. The position, movement of the valves of electro hydraulic governor, is also limited by the limiters with the constraints ($G_{\max}$, $G_{\min}$) & ($\rho_{\max}$, $\rho_{\min}$). A 1% droop is also considered

for stable operation. Dynamics of the electro-hydraulic governor are represented by two differential equations for the main and interceptor governor as shown in the equation (2.26) and (2.27) [69] and the governor is simulated as shown in Fig. 2.10.

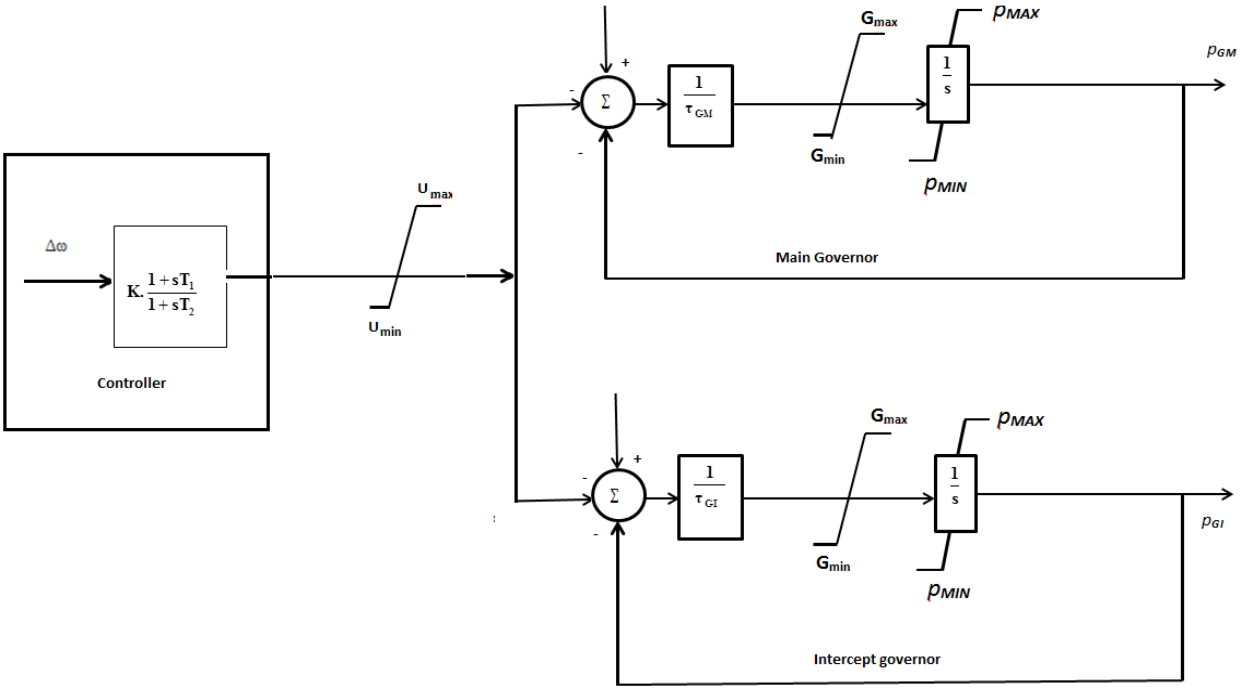

Fig.2.10 Electro-hydraulic governor with the conventional controller

2.10 Modeling of synchronous generator

A seventh order model, with the non-linear differential equation from 2.28 to 2.34, is used to represent the CSG. The simple governor is used to govern the speed of CSG and it is shown in the equation 2.35. The detailed model of exciter and the CPSS for SCG are shown in the Appendix 4, 5 and the typical parameters for the CSG are given in Appendix 6.

$$p\lambda_f = (e_f - i_f.r_f) \quad (2.28)$$

$$p\lambda_d = e_d + r_a.i_d + \omega_O(\omega+1).\lambda_q \quad (2.29)$$

$$p\lambda_{kd} = -i_{kd}.r_{kd} \quad (2.30)$$

$$p\lambda_Q = e_q + r_a.i_q - \omega_O(\omega+1).\lambda_d \quad (2.31)$$

$$p\lambda_{kq} = -i_{kd}.r_{kq} \quad (2.32)$$

$$p\delta = \omega \quad (2.33)$$

$$p\omega = \frac{\omega_O}{2H}(T_m + g + K_d.\delta - T_e) \quad (2.34)$$

$$g(s) = \left[a + \frac{b}{1+sT_g} \right] \dot{\delta} \quad (2.35)$$

Chapter Three: System Identification

3.1 Introduction

Modeling of any dynamic system can be done either by analytical or experimental approach. In the analytical approach, the dynamics of the system are modeled using the laws of physics, like Newton laws, balance equations, etc., whereas in the experimental approach some experiments are conducted on the system. Based on the laws of physics or experimental data a mathematical model is developed to describe the system behaviour. It is called 'system identification' and it is widely used in many fields, such as power systems, process control, biomedical engineering, etc. [70].

In 1795, K.F Gauss developed and applied the concept of least squares for astronautic computations [71]. The basic idea of least squares is to obtain a mathematical model from the observed data by minimizing the sum of the squares of the difference between the observed and the estimated data. However, it is not accurate when there is some noise in the observed data and it results in an inaccurate mathematical model. Various types of identification methods have been proposed in the literature [72]. Under proper conditions, any of these methods can be applied to identify the parameters of the model of a system to be controlled. In system identification, although it includes the identification of the model and the parameters, only the parameters of a pre-defined system model are identified in the self-tuning control. The parameter identification

algorithm can be either online or offline. The offline techniques are more accurate than the online techniques. However, the online or real time identification is followed here because the power systems are highly non-linear and the actual parameters have to be identified in real time so that the APSS can compute the control signal based on the actual parameters for the instantaneous operating conditions. Also, as the performance of the APSS depends solely on the identified parameters, the identified values have to be close enough to reflect the actual system [73].

3.2 Modeling of the System

The system is defined as a physical object that generates an observed output signal $y(t)$ at time t, where $u_i(t)$ is the measurable input signal, and the model is defined as the knowledge of system properties. In a stochastic system as shown in Fig 3.1 input, output or both input and output can be corrupted by white noise.

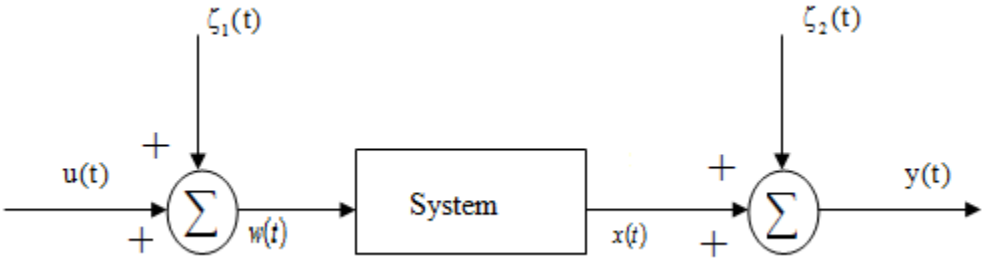

Fig.3.1. Stochastic model

The single input and single output system is considered in this thesis. In power systems and control research, the model is necessary to develop the controller. From a practical point of view, most of the systems are non-linear. However, it is common to use a linear model. In this

thesis, the mathematical model considered is a linear model with time varying parameters. It is in the discrete form because it is really convenient to solve with the digital computers. Two discrete models, namely; Auto Regressive Moving Average Model (ARMA) and Auto Regressive Moving Average Exogenous Model (ARMAX), are frequently used in the adaptive control systems. The following is an overview of these models.

3.2.1 ARMA Model

Time series in a linear combination of past observations and white noise is called an ARMA Model [74] and the block diagram of the ARMA model is shown in Fig.3.2. The discrete ARMA model takes the form:

$$A(z^{-1}).y(t) = z^{-1}B(z^{-1}).u_i(t) + \xi(t) \qquad (3.1)$$

where,

$A(z^{-1}), B(z^{-1})$ are polynomials with the delay operator z^{-1} in which

$$A(z^{-1}) = 1 + a_1 z^{-1} + a_2 z^{-2} + ... + an_a z^{-n_a} \qquad (3.2)$$

$$B(z^{-1}) = b_1 z^{-1} + b_2 z^{-2} + ... + b_n z^{-n_b} \qquad (3.3)$$

$n_a > n_b$

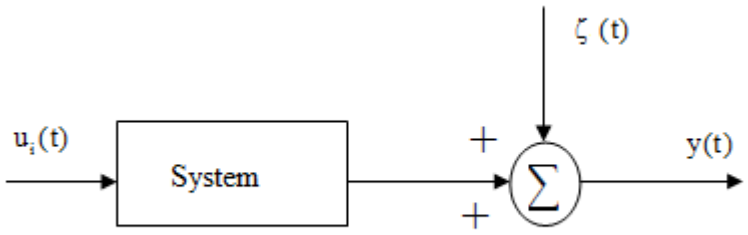

Fig.3.2. ARMA Model

3.2.2 ARMAX Model

ARMAX model can be explained from Fig.3.2. The output and input are corrupted by white noise signals. Now, the system takes the form [75]:

$$w(t) = u(t) + \zeta_1(t) \tag{3.4}$$

$$x(t) = y(t) - \zeta_2(t) \tag{3.5}$$

and the system is modeled by the equation:

$$A(z^{-1}).x(t) = z^{-1} B(z^{-1}).w(t) \tag{3.6}$$

On substituting equations (3.4) and (3.5) in equation (3.6) and after rearranging, it takes the form:

$$A(z^{-1}).x(t) = z^{-1} B(z^{-1}).u(t) + C(z^{-1}).\zeta(t) \tag{3.7}$$

in which

$$C(z^{-1}) = 1 + c_1 z^{-1} + c_2 z^{-2} + \ldots + c_{n_c} z^{-n_c} \tag{3.8}$$

and

C_i , $(i = 1,\ldots..n_C)$ is a function of $a_j, (j = 1,\ldots.n_b), b_k, (k = 1,\ldots.n_b)$

Equation (3.7) is called as auto regressive moving average exogenous model.

3.3 Schemes for system identification

Practically, power systems are never in true steady state as there are always changes happening in the operating condition due to some types of disturbances. The APSS has to act very quickly as well as it has to adapt to the changes. Thus, the tracking property is very important to achieve the desired performance. When designing an APSS some compromise has to be made between the quality and the computation time, because some sophisticated algorithms are better in tracking but require longer computation time. Because of the computation time constraints, the parameters are identified using recursive techniques. Two identification techniques, i.e. recursive least squares (RLS) and Kalman filter, have been used in this thesis to track the parameters and their performance is compared.

3.3.1 Recursive Least Squares identifier

RLS is one of the simplest methods with good convergence properties for online identification. The recursive identification method is followed in most adaptive systems because recursive identification requires less memory as it does not store any data. Also, the storage of data will not increase in time [76].

The control action is based on the most recent model because it becomes the central part of the adaptive systems. The controller adapts to the changes in the plant based on the online estimation of the parameters. The scheme followed for online identification of the system is

shown in Fig.3.3 in which the plant model is shown in chapter 2, Fig.2.7. In order to identify the system, equation (3.1) can be rewritten in the form:

$$y(t) = \theta^T(t).\phi(t) + \zeta(t) \qquad (3.9)$$

where

$$\theta(t) = [\, a_1 \;\; a_2 \;\; .....a_{n_a} \; b_1 \;\; b_2 \;\; .... \; b_{n_b} \,]^T \qquad (3.10)$$

$\theta(t)$ is the parameter vector , $\varphi(t)$ is the measurement vector

$$\varphi(t) = [\; -y(t-1) \;\; ..... \;\; -y(t-n_a) \;\;\; u_i(t-l-1) \;\; ..... \;\; u_i(t-l-n_b) \;\;]^T \qquad (3.11)$$

The predicted value of the system output, $\hat{y}(t)$, for the actual system output, $y(t)$, can be calculated as:

$$\hat{y}(t) = \hat{\theta}(t-1).\varphi(t) \qquad (3.12)$$

The predicted error is:

$$e(t) = y(t) - \hat{y}(t) \qquad (3.13)$$

Equations (3.14) through (3.16) represent the RLS algorithm [76]:

$$K(t) = \frac{P(t-1).\varphi(t)}{\lambda(t) + \varphi(t).P(t-1).\varphi(t)} \qquad (3.14)$$

$$P(t+1) = \frac{P(t-1) - K(t).P(t-1).\varphi(t)^T}{\lambda} \tag{3.15}$$

`

$$\hat{\theta}(t+1) = \hat{\theta}(t) + K(t).e(t) \tag{3.16}$$

where P is the Covariance matrix

K is the gain vector

λ is the forgetting factor

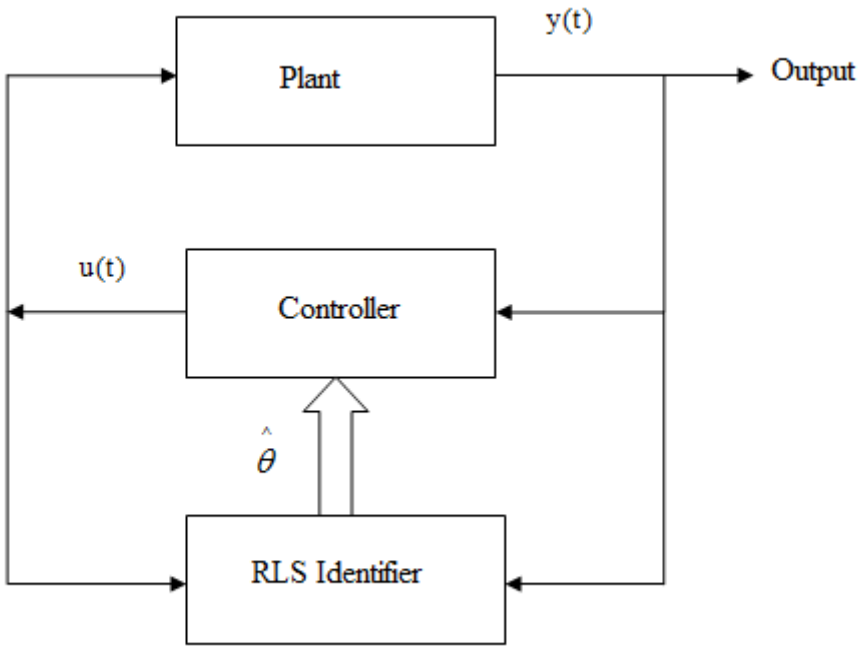

Fig.3.3. Scheme for RLS Identifier

Theoretically, the RLS algorithm is developed for time invariant systems. When it is used for the time varying systems, it exhibits some problems. For example, when time increases in a

time invariant system $\hat{\theta}(t)$ converges to the desired value and the prediction error, gain vector, covariance matrix approach zero. In a time variant system, because of this phenomenon the plant parameters to be estimated deteriorate and it results in a poor control signal. In this dissertation, the self-tuning approach is followed so, when RLS is applied to a time varying system, problems arise with the estimation of parameters. When RLS algorithm is applied in the STC, K(t) decreases with time that significantly affects the parameter tracking. This problem could be addressed by keeping the P(t) matrix constant at the fixed initial value or resetting to the latest values [77].

3.3.1.1 Variable Forgetting factor

In real time, by introducing a variable forgetting factor the RLS algorithm gives more importance to the recent information by gradually forgetting the older information. For smaller values of $\lambda(t)$, data from the previous information will be forgotten very quickly. However, with proper excitation fixed forgetting factors are used in many practical applications to track the parameters for the time varying systems. In power systems, during the normal operating condition the system is poorly excited, but when there is an abnormal operating condition such as large disturbances then the system is over excited. In this case, the fixed forgetting factor has some problems because it is very difficult to select the exact value of λ for the proper estimation of parameters from the plant. In the case of large disturbances smaller value of λ helps in proper estimation of parameters, but it makes it more vulnerable to noise. On the other hand, for steady state operation larger value of λ helps in estimating the parameters smoothly, but the tracking speed gets very slow. When the systems is operated at steady state for long time with a fixed

forgetting factor (λ<1) a blow up of the covariance matrix can occur, and if it tends to infinity that can result in the improper estimation of parameters. This problem can be addressed by some methods such as by keeping the covariance matrix constant in the iteration or imposing limits on it, switching the values of λ depending on the operating conditions like steady state, large disturbances, etc. However, the most efficient way to estimate the parameters is to keep λ as a variable [78, 79, 80, 81].

The forgetting factor in equation (3.15) is updated online by the following equation [81]:

$$\lambda(t) = 1 - \frac{\left[1 + \varphi^T(t-1).K(t)\right] e^2(t)}{\sum} \qquad (3.17)$$

where $\sum$ is a constant value between 0 and 1

When the system operates at steady state or normal state the error $e(t)$ will be zero or small. This helps in preventing the covariance matrix blowing up to infinity. On the other hand, when there is an abnormal condition due to disturbances λ decreases as $e(t)$ increases. So, λ changes according to the environment and it help in the tracking ability of the RLS identifier and proper estimation of the parameters of the plant.

3.3.2 Kalman filter estimator

In 1960, R.E Kalman published a paper on finding a solution to discrete data linear filtering problems [82]. Since then, due to the advances in digital computing, the Kalman filter has become an extensive part of research and is widely used in the area of automation and

navigation. The Kalman filter is a linear, discrete recursive data processing algorithm that helps to estimate the parameters by minimizing the mean square error. It has good convergence properties and requires simple calculations. So it can be easily implemented in real time [83]. The scheme followed to estimate the parameters of the system online is shown in Fig.3.4 in which the plant model is shown in chapter 2, Fig 2.7.

In order to identify the system, equation 3.1 can be rewritten in the form

$$y(t) = \theta^T(t).\phi(t) + \zeta(t) \tag{3.18}$$

where

$\theta(t)$ is the parameter vector, $\varphi(t)$ is the measurement vector

$$\theta(t) = [\, a_1 \;\; a_2 \;\; .....a_{n_a} \; b_1 \;\; b_2 \;\; .... \, b_{n_b} \,]^T \tag{3.19}$$

$$\varphi(t) = [\; -y(t-1) \;\; ..... \;\; -y(t-n_a) \;\;\; u_i(t-l-1) \;\; ..... \;\; u_i(t-l-n_b) \;\;]^T \tag{3.20}$$

The predicted error is calculated as:

$$e(t) \;\; = y(t) - \hat{y}(t) \tag{3.21}$$

where

$\hat{y}(t)$ is the predicted value of the system output

The recursive Kalman filter identification algorithm is described in the equations (3.22) through (3.24) [76].

$$k(t) = \frac{P(t-1).\phi(t)}{1+\phi^T(t).P(t-1).\varphi(t)} \tag{3.22}$$

$$P(t) = P(t-1) - \frac{P(t-1).\varphi(t).\varphi^T(t).P(t-1)}{[1+\varphi^T(t).P(t-1).\phi(t)]} + R \tag{3.23}$$

$$\hat{\theta}(t) = \theta(t-1) + K(t).e(t) \tag{3.24}$$

where P is the Covariance matrix

K is the gain vector

R is the error covariance matrix

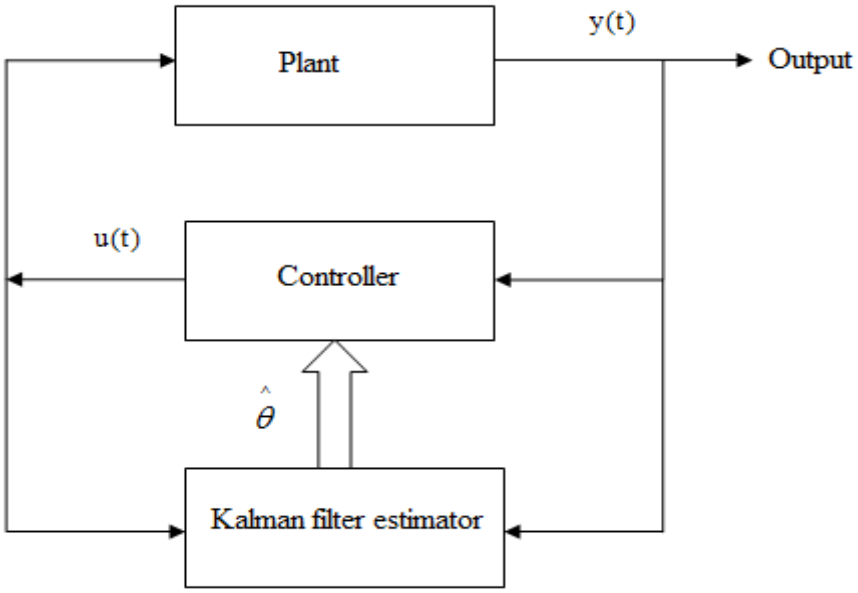

Fig.3.4. Scheme for Kalman filter estimator

Chapter Four: Variable pole shift feedback control

4.1 Introduction

In the previous chapter, online identifiers using recursive least squares and Kalman filter are discussed. In this chapter, an overview of the adaptive pole shifting control algorithm that combines the advantages of both MV and PA control algorithms is provided.

4.2 Background

Power systems are highly nonlinear. So the phase advance network or CPSS with fixed parameters cannot adapt to changes according to the varying operating conditions. An adaptive controller is the best solution to overcome this problem because it adapts to the changes in the system by tuning its parameters online. As discussed in chapter 1, the PS control has significant advantages over MV, GMV, PA, PZA, LQR controllers. It ensures and establishes closed loop stability and it does not assign the closed loop poles to some fixed locations in the z plane. It rather shifts the open loop poles closer to the center of the unit circle in the z-plane and the variable PS control algorithm self-searches the optimal value of α during the optimization process. In order to ensure the closed loop stability, it keeps the closed loop poles within the unit circle in the z – plane. Unlike the CPSS, the APSS does not need any manual tuning and by adapting to any changes in the operating condition, it overcomes the drawbacks of CPSS thus providing a better control performance over different operating conditions.

4.2.1 Pole shifting control

Consider the system, as shown in Fig.4.1, modeled by the discrete equation as:

$$A(z^{-1}).y(t) = z^{-1}B(z^{-1}).u_i(t) + \xi(t) \qquad (4.1)$$

where

$y(t)$ is the system output

$u_i(t)$ is the system input

$\xi(t)$ is the white noise

$A(z^{-1}), B(z^{-1})$, polynomials in the delay operator z^{-1}, are given by:

$$A(z^{-1}) = 1 + a_1 z^{-1} + a_2 z^{-2} + \ldots\ldots + an_a z^{-n_a} \qquad (4.2)$$

$$B(z^{-1}) = b_1 z^{-1} + b_2 z^{-2} + \ldots\ldots + b_n z^{-n_b} \qquad (4.3)$$

$n_a \geq n_b$

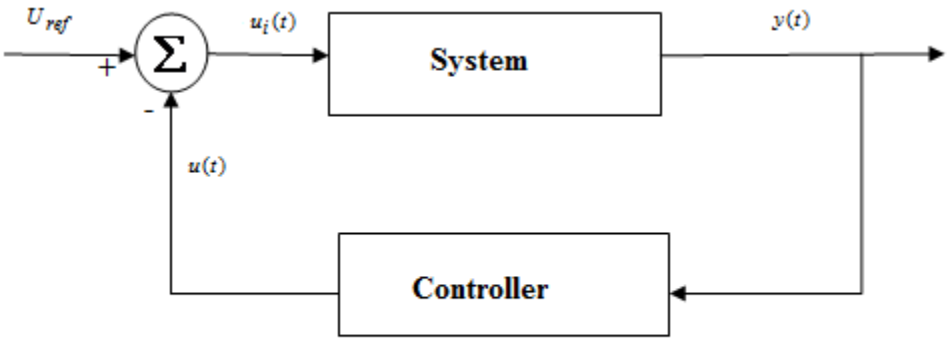

Fig.4.1 Generalized model with a feedback control

Assuming that system parameters a_i, b_i are obtained online from the RLS or the Kalman based identifiers, the control signal $u(t)$ is calculated by using pole-shifting algorithm as discussed below [23, 81].

By assuming that the feedback loop has the form:

$$\frac{u(t)}{y(t)} = -\frac{G(z^{-1})}{F(z^{-1})} \tag{4.4}$$

where

$$G(z^{-1}) = g_o z^{-1} + g_1 z^{-2} + ... + g_{n_g} z^{-n_b} \tag{4.5}$$

$$F(z^{-1}) = 1 + f_1 z^{-1} + f_2 z^{-2} + ... + f_i z^{-i} + an_a z^{-n_a} \tag{4.6}$$

$$n_f = n_b - 1, \; n_g = n_a - 1 \tag{4.7}$$

the closed loop characteristic polynomial $T(z^{-1})$ *can be written as:*

$$T(z^{-1}) = A(z^{-1})F(z^{-1}) + B(z^{-1})G(z^{-1}) \tag{4.8}$$

In the pole shift control algorithm, $T(z^{-1})$ takes the form $A(\alpha z^{-1})$ and the locations of the poles are shifted by the variable pole shift factor, α ,

$$A(z^{-1})F(z^{-1}) + B(z^{-1})G(z^{-1}) = A(\alpha z^{-1}) \tag{4.9}$$

Expanding equation (4.9) on both sides results in (4.10):

$$\begin{bmatrix} 1 & 0 & . & 0 & b_1 & 0 & . & 0 \\ a_1 & 1 & . & 0 & b_2 & b_1 & . & 0 \\ . & a_1 & . & . & . & b_2 & . & 0 \\ a_{n_a} & . & . & 1 & b_{n_b} & . & . & b_1 \\ 0 & a_{n_a} & . & a_1 & 0 & b_{n_b} & . & b_2 \\ . & 0 & . & . & . & 0 & . & . \\ . & . & . & . & . & . & . & . \\ 0 & 0 & . & a_{n_a} & 0 & 0 & . & b_{n_b} \end{bmatrix} \begin{bmatrix} f_1 \\ . \\ . \\ f_{n_f} \\ g_o. \\ . \\ . \\ g_{n_g} \end{bmatrix} = \begin{bmatrix} a_1(\alpha-1) \\ a_2(\alpha^2-2) \\ . \\ .. \\ a_{n_a}(a^{n^a}-1) \\ 0 \\ . \\ 0 \end{bmatrix} \qquad (4.10)$$

Equation (4.10) can be written in matrix form as in Equation (4.11):

$$M.w(\alpha) = L(\alpha) \qquad (4.11)$$

The system parameters a_i, b_i are calculated by on-line identifier and the control parameters f_i, g_i can be solved to calculate the control signal $u(t)$ with the pole shifting factor α. If the pole shifting factor α is fixed then it falls in the special case called 'Pole Assignment' control algorithm (PA). As α plays an important role in the PS control algorithm, it is modified online according to the operating condition.

$$u(t,\alpha) = X_C^T(t).w(\alpha) = X_C^T(t).M^{-1}L(\alpha) \qquad (4.12)$$

where

$$X_C^T = [-u(t-1) - u(t-2)....-u(t-n_f)..-y(t) - y(t-1) - y(t-2)..-y(t-n_g)^T] \quad (4.13)$$

is the measurement vector.

4.2.2 Taylor series expansion of the control signal

The Taylor series can be used to express the control signal $u(t,\alpha)$ in terms of factor α

$$u(t,\alpha) = u(t,\alpha_0) + \sum_{i=1}^{\infty} \frac{1}{i!}\left[\frac{\partial^i u(t,\alpha)}{\partial \alpha^i}\right]_{a=\alpha_0} (a-\alpha_0)^i \qquad (4.14)$$

The i[th] order differential of $u(t,\alpha)$ with respect to pole shifting factor α is:

$$\left[\frac{\partial^i u(t,\alpha)}{\partial \alpha^i}\right]_{a=\alpha_0} = X_C{}^T(t).M^{-1}L^{(i)}(a_0) \qquad (4.15)$$

From equation (4.14), let a_0 = 0. Then $L^{(i)}(0)$ becomes:

$$L^{(i)}(0) = [0.....0\ i!a_i\ 0.....0]^T \qquad i \underline{<} n_a \qquad (4.16)$$

The i[th] order sensitivity constant s_i can be defined as

$$S_i = \frac{1}{i!}\left[\frac{\partial^i u(t,\alpha)}{\partial \alpha^i}\right]_{a=\alpha_0} = \frac{1}{i!} X_C{}^T(t)M^{-1}L^i(0) = p_i a_i \qquad i \underline{<} n_a \qquad (4.17)$$

where p_i is the i^{th} term of the row vector $X_C{}^T(t)M^{-1}$. Equation (4.14) can be written as:

$$u(t,a) = u(t,0) + \sum_{i=1}^{n_a} s_i a^i \qquad (4.18)$$

4.2.3 System output pred*iction*

The output of the system $\hat{y}(t+1)$ can be predicted at time (t) if the control signal $u(t,\alpha)$ at time t is known [84].

Then $\hat{y}(t+1)$ can be written as:

$$\hat{y}(t+1) = X_i^T(t)\beta + b_1 u(t,\alpha) \quad (4.19)$$

where

$$X_C^T = [-u(t-1) - u(t-2)....-u(t-n_f)..-y(t) - y(t-1) - y(t-2)..-y(t-n_g)^T] \quad (4.20)$$

is the measurement vector, and

Equation (4.18) is substituted in (4.19) and it is expressed as a function of a

$$\hat{y}(t+1) = X_i^T(t)\beta + b_1[u(t,0) + \sum_{i=1}^{n_a} s_i a^i] \quad (4.21)$$

$$\beta = [-b2 - b3 ..... - bn_b \ a_1 \ a_2 \ a_3 \ ....a_{n_a}]^T \quad (4.22)$$

is an identified parameter vector.

4.2.4 Performance index and constraints

Performance index, chosen to obtain the optimum control signal, can be expressed as:

$$\min_a J(t+1,a) = E\left[\hat{y}(t+1) - y_{ref}(t+1)\right]^2 \quad (4.23)$$

where

$y_{ref}(t+1)$ is the system output reference.

Equation (4.21) is substituted in (4.23) and it results in equation (4.24), and in terms of $u(t,a)$ it can be expressed as in equation (4.25).

$$\min_{a} \hat{j}(t+1,a) = \left[X^T(t)\beta + b1\left\{ u(t,0) + \sum_{i=1}^{n_a} s_i a_i \right\} - y_{ref}(t+1) \right]^2 \quad (4.24)$$

$$\min_{u(t,a)} \hat{j}(t+1,u(t,a)) = \left[X^T(t)\beta + b_1 u(t,a) - y_{ref}(t+1) \right]^2 \quad (4.25)$$

4.2.4.1 Constraints

The following constraints have to be followed during the minimization with respect to a such that the controller tries to keep the system stable in the closed loop.

- All roots of the closed loop characteristic polynomial, $A(a\,z^{-1})$, must lie within the unit circle on z- plane. By assuming that λ_C is the absolute value of the largest characteristic root of $A(z^{-1})$, $a \,.\, \lambda_C$ is the largest characteristic root of $A(a\,z^{-1})$. In order to ensure the closed loop stability of the system a should satisfy equation (4.26).

$$-\frac{1}{\lambda_c} < \alpha < \frac{1}{\lambda_c} \quad (4.26)$$

- The control limits should be considered in order to avoid servo saturation. The optimal solution for a should satisfy equation (4.27):

$$u_{\min} \le u(t,0) + \sum_{i=1}^{n_a} S_i \alpha^i < u_{\max} \quad (4.27)$$

where,

$u_{\min}$ is the lower control limit of the controller

$u_{\max}$ is the upper control limit of the controller

4.2.5 Properties of PS Algorithm

The main objective of the PS control algorithm is to push the closed loop poles closer towards the center of the unit circle in the z – plane. The pole shifting factor helps to achieve this by shifting the open loop poles towards the center of the unit circle. The pole shifting strategy is shown in Fig 4.2. The varying range of the pole shifting factor α has to be within the range - $\frac{1}{\lambda_C} < a < \frac{1}{\lambda_C}$. The behaviour of α changes according to the operating conditions such as [85]:

- When the open loop system is unstable $(\lambda_C > 1)$. The controller behaves like a PA controller and it places the largest closed loop poles within the unit circle to maintain the stability of the closed loop system and its performance is improved by optimization.
- When the open loop system is stable $(\lambda_C < 1)$ then the range of PS factor is larger than (0, 1) and it helps in obtaining better performance.

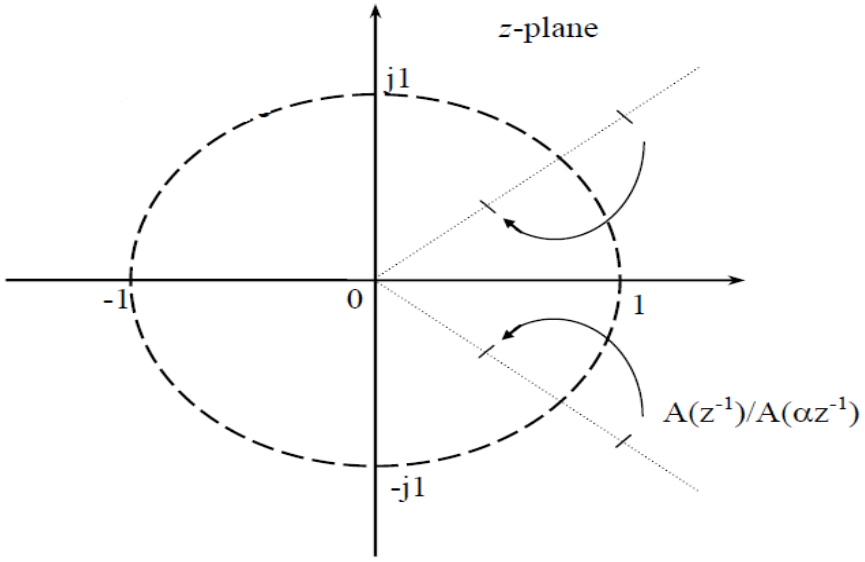

Fig.4.2 Pole shifting process in the unit circle [23]

4.2.6 Optimization

The optimization scheme can be explained from Fig. 4.3. The performance index is a quadratic function of the control, *u (t, a*). So the control obtained by optimizing the performance index $\hat{J}(t+1,\alpha)$ with the stability constraints can be at three possible locations only. As shown in Fig. 4.3, the control at point `a` is within the limits so it can be applied to the system to be controlled, while the controls at points, b, c, fall outside the limits and cannot be used by the controller. The optimal substitutions for the control at point b and c are b' ($U_{\min}$), c' ($U_{\max}$). The optimal value of the pole shifting factor $\alpha_{opt,}$ is obtained by optimizing $\hat{J}(t+1,\alpha)$ within the stability constraints [86].

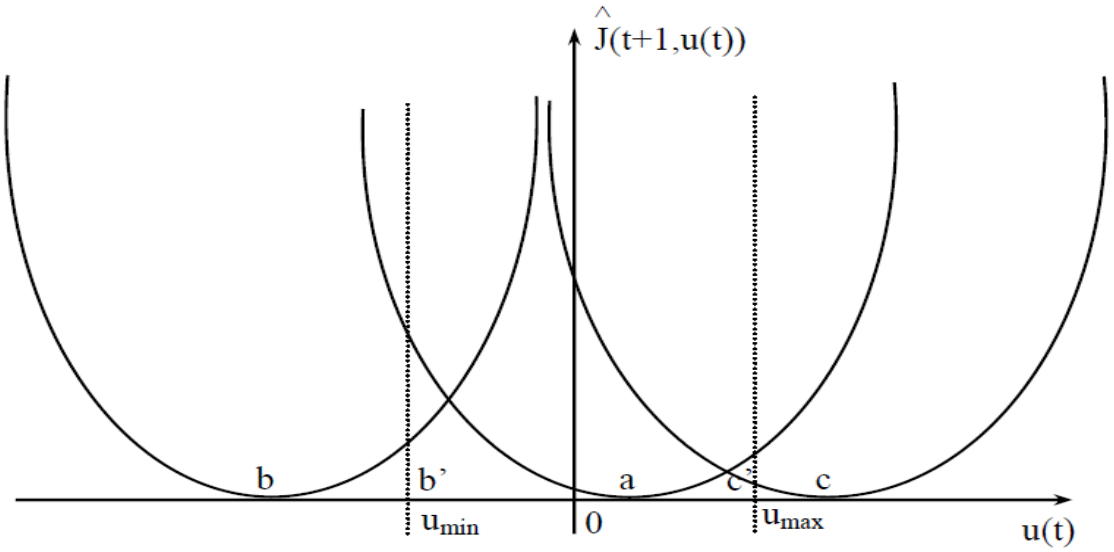

Fig 4.3 Illustration of performance index [23]

Controls versus pole shifting factor curves at different sampling times are shown in Fig. 4.4. The pole shifting factor, α, is 1.0 when there is no control signal. In case when the open loop is stable $(1/\lambda_c > 1.0)$ the optimal value of PS factor, $a_{opt,}$ can be obtained by optimizing $\hat{j}(t+1,a)$ and by following the stability constraints such as ($-1/\lambda_c < a_{opt} < 1.0$ *or* $1.0 < a_{opt} < 1/\lambda_c$). Suppose, if the control signal $u(t,a)$ is outside the limit $u(t,a_{opt}) < u_{min} < 0$ *or* $0 < u_{max} < u(t, a_{opt})$ then the upper or lower limit of the control signal is applied and the corresponding a_{limit} is used. The control signal $u(t,a)$ is a continuous single value function in terms of PS factor a. By applying the mean value theorem of continuous functions, a_{limit} should satisfy equation (4.28).

$$-\frac{1}{\lambda_c} < \alpha_{opt} < \alpha_{\text{limit}} < 1 \quad or \quad 1 < \alpha_{\text{limit}} < \alpha_{opt} < \frac{1}{\lambda_c} \tag{4.28}$$

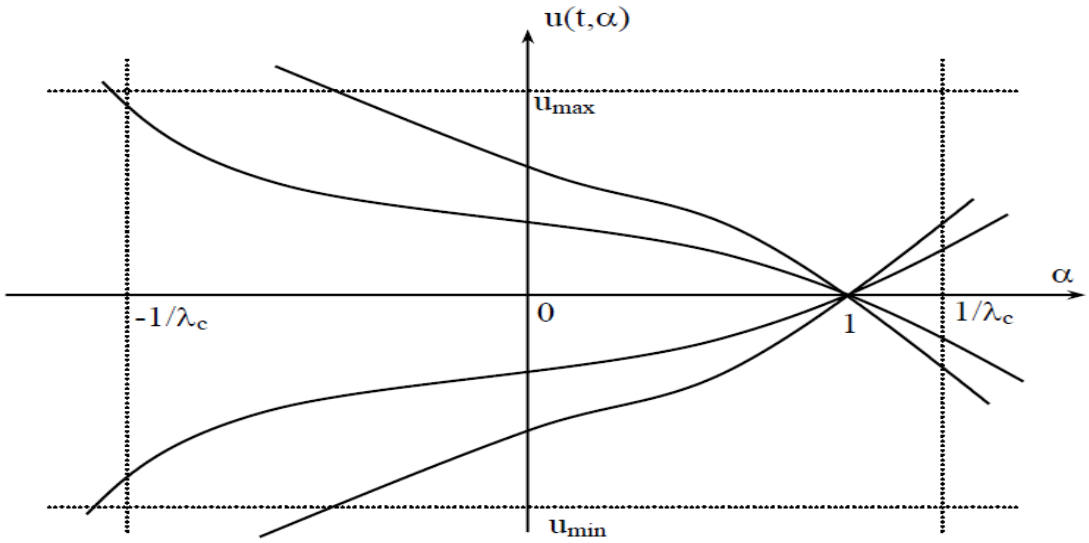

Fig 4.4 Illustration of Control signal [23]

It indicates that a_{limit} is within the range $\left(\frac{1}{\lambda_c}, \frac{1}{\lambda_c}\right)$ so it assures the closed loop stability of the system. In the case for open loop unstable system, control has to move the unstable poles inside the unit circle in the z-plane. These strategies simplify the optimization scheme and its optimizing time. Also, when the control signal reaches its limits, in that situation the control limit itself is the best control signal and it helps to maintain the closed loop stability without losing its stability. The most important priority of this algorithm is an emphasis on the closed loop stability. In case of linear systems, when the model of the system is of the same order as well and the identified parameters converge to their true values, the closed loop stability is assured by the algorithm. In non-linear systems, if the model of the system is of a lower order or that model is

of the same order as a linear system, the identified parameters do not converge to their true values and equation (4.26) is modified as in equation (4.29):

$$-\frac{1}{\lambda_c}(1-\sigma) < \alpha < \frac{1}{\lambda_c}(1-\sigma) \qquad (4.29)$$

where

σ is the security coefficient

The value of σ can be chosen anywhere between 0 % and 100 %. During this case, the controller acts in attentive mode and it satisfies the corresponding security coefficient [85, and 86].

Chapter Five: System Identification Studies

5.1 Introduction

In chapter 3, RLS and Kalman filter for the identification of parameters are discussed. In this chapter those two algorithms are applied to an SCG connected to an infinite bus to identify the parameters of the system recursively at each sampling interval as the PS controller uses the ARMA parameters obtained online to calculate the control signal. For a time varying system the tracking ability of the system and preciseness of the identified parameters are vital to obtain the control signal. Various types of disturbances are applied to the system to study the performance of the identification algorithm.

5.2 System configuration

The system is described as a third order discrete model as:

$$A(z^{-1}).y(t) = z^{-1}B(z^{-1}).u_i(t) + \xi(t) \qquad (5.1)$$

where

$A(z^{-1}), B(z^{-1})$ are polynomials with the delay operator z^{-1} in which

$$A(z^{-1}) = 1 + a_1 z^{-1} + a_2 z^{-2} + a_3 z^{-3} \qquad (5.2)$$

$$B(z^{-1}) = b_1 z^{-1} + b_2 z^{-2} + b_3 z^{-3} \qquad (5.3)$$

Parameters (a_i , b_i) are estimated using recursive identification techniques. Although numerous techniques are available for updating the parameters, two algorithms, Kalman and RLS, have been used here for identifying the parameters online with a sampling rate of 20 Hz. The single machine infinite bus system, Fig.2.7, is used for the studies.

5.2.1 Online identification using RLS, Kalman algorithm

Rewriting equation (5.1) as:

$$y(t) = \theta^T(t).\varphi(t) + \zeta(t) \tag{5.4}$$

where $\theta(t)$ is the parameter vector, $\varphi(t)$ is the measurement vector

$$\theta(t) = [\, a_1 \;\; a_2 \;\; a_3 b_1 \;\; b_2 \;\; b_3 \,]^T \tag{5.5}$$

$$\varphi(t) = [\, -y(t-1) \;\; -y(t-2) \;\; -y(t-3) \;\; u_1(t-1) \; u_1(t-2) \; u_1(t-3) \;\;]^T \tag{5.6}$$

The parameter vector $\theta(t)$ is calculated by RLS with a variable forgetting factor and by the Kalman filter techniques as discussed in chapter 3.

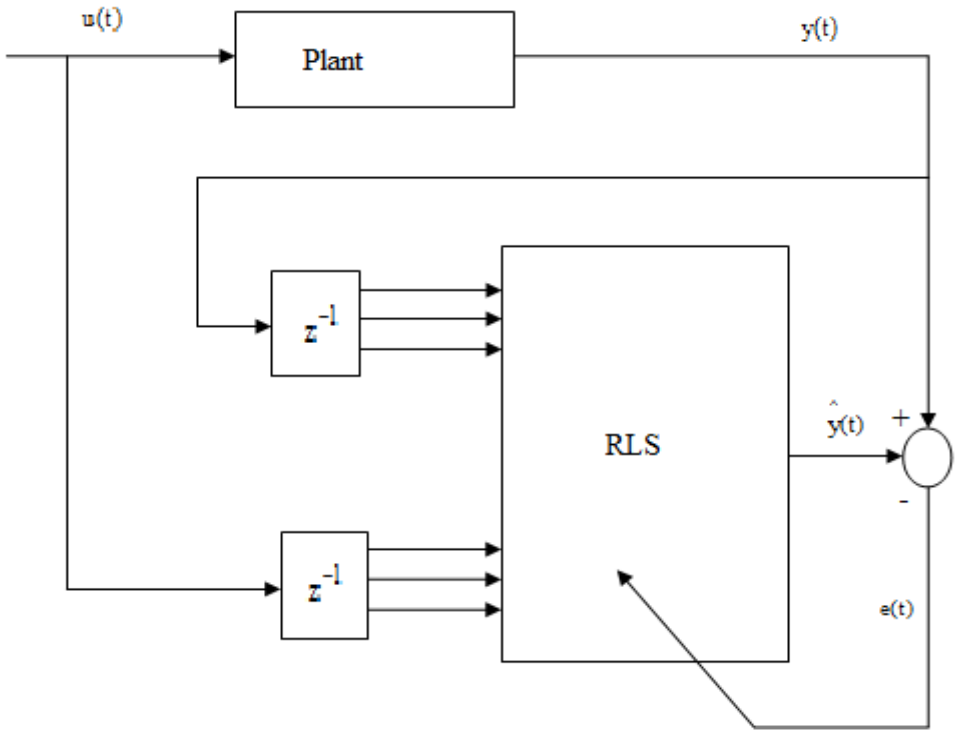

Fig 5.1 Online identification of parameters using RLS

5.2.2 Performance studies using RLS algorithm

In this section, RLS algorithm with a variable forgetting factor is used to track the parameters of the system or plant as shown in Fig.5.1 at the sampling rate of 20 Hz. Then the output of the system is compared with the RLS identifier conditions for various disturbances and different operating conditions.

5.2.2.1 Normal load

In this experiment, the SCG was operated at P = 0.7 p.u, pf = 0.85 lag. A 0.1 p.u step increase of initial mechanical torque is applied at 0.5 s. How RLS identifier tracks the output of the system is shown in Fig. 5.2.

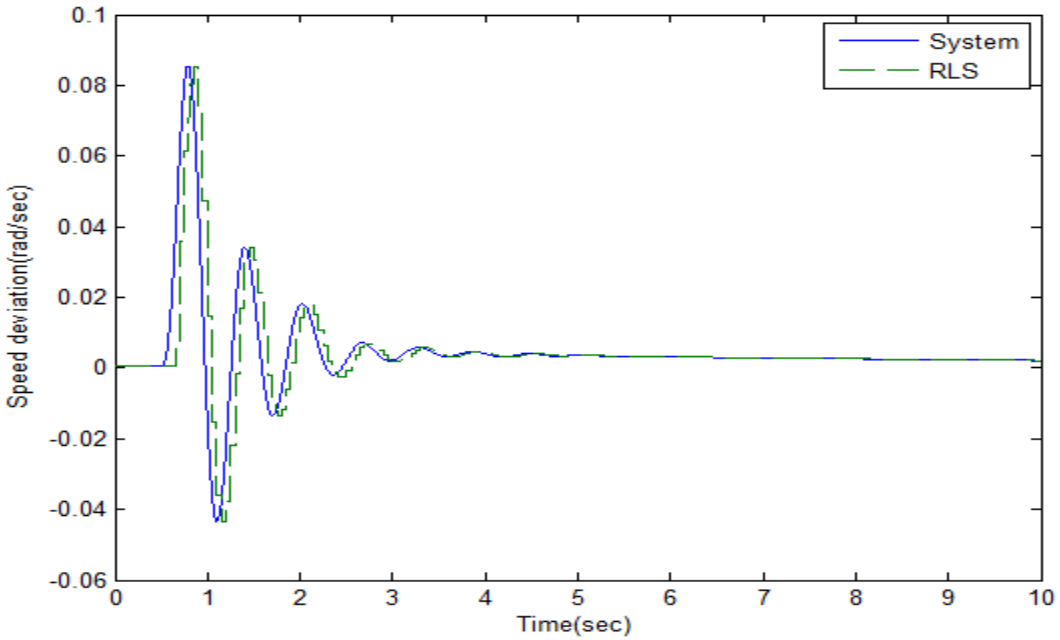

Fig.5.2 System output and RLS identifier response to a 0.1 p.u step increase in intial mechanical torque under normal load condition

5.2.2.2 Voltage reference change

The caliber of the RLS identifier for a step increase in reference voltage is studied here. The SCG operated at P = 0.7 p.u, pf = 0.85 lag, and a 0.1 p.u step increase of the initial terminal voltage is applied at 0.5 s as shown in Fig.5.3.

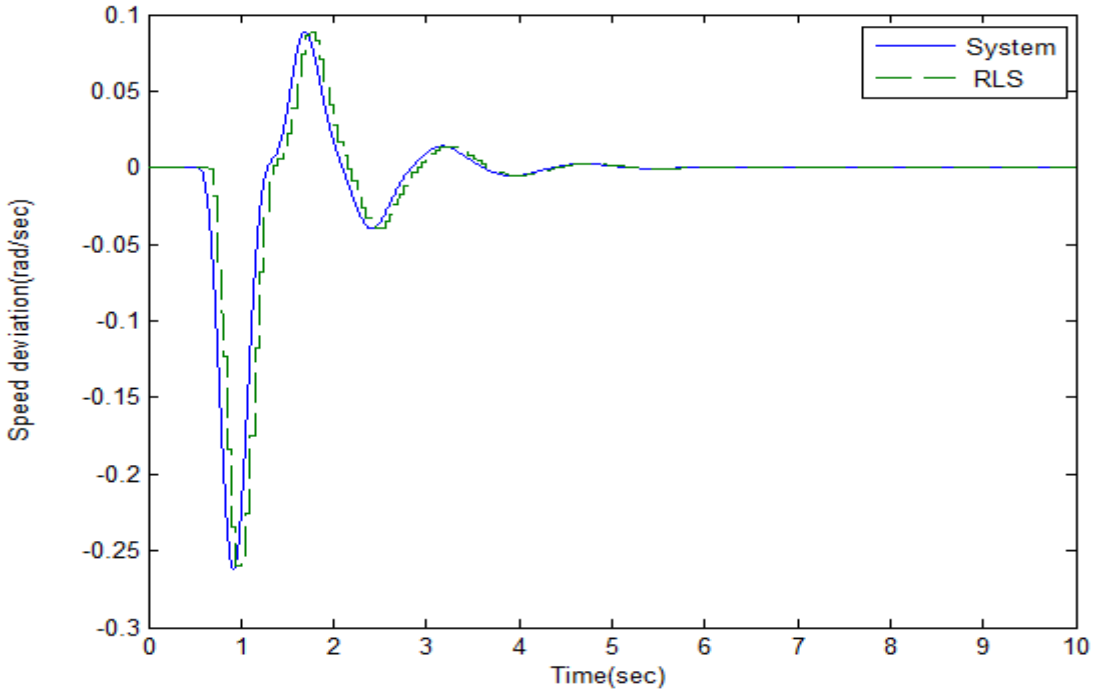

Fig.5.3 System output and RLS identifier response to a 0.1 p.u step increase in reference terminal voltage under normal load condition

5.2.2.3 Light load

The system was operated at a light load condition of P = 0 .2 p.u, pf = 0.85 lag, and a 0.2 p.u step increase in initial mechanical torque is applied at 0.5 s. The system response is shown in Fig.5.4.

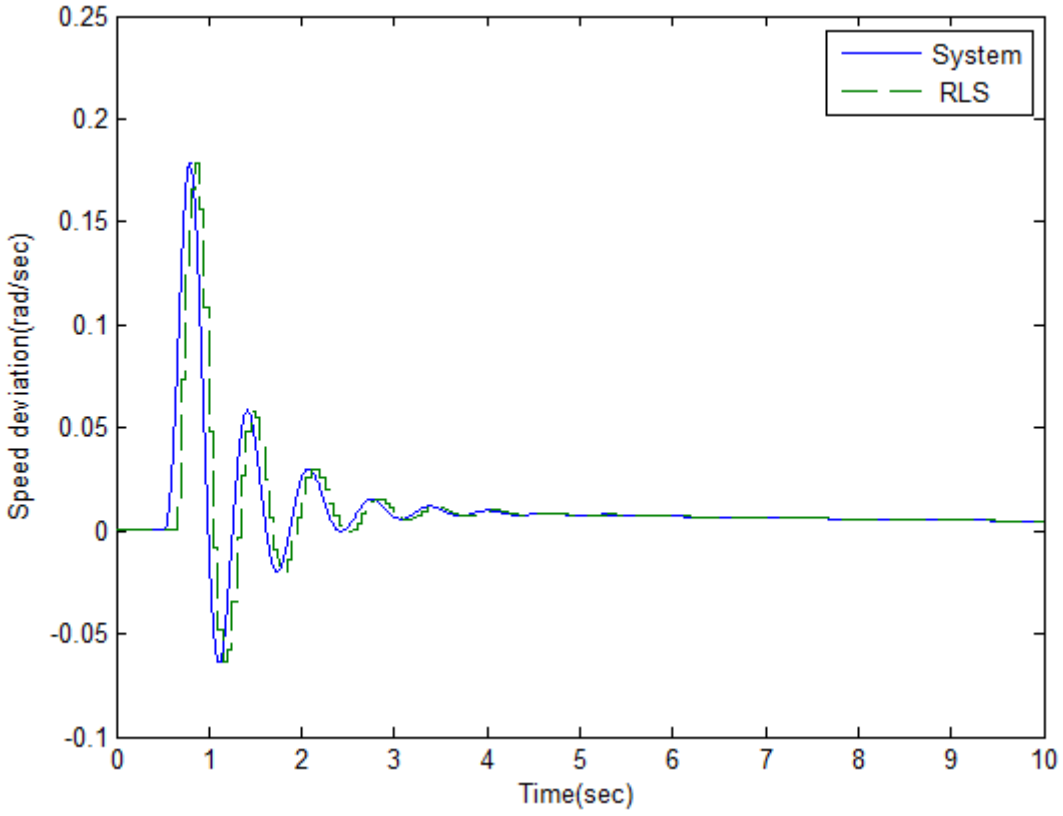

Fig.5.4 System output and RLS identifier response to a 0.2 p.u step increase in intial mechanical torque under light load condition

5.2.2.4 Leading power factor operation

The SCG was operated at P = 0.3 p.u, pf = 0.85 lead, and a 0.1 p.u step increase of initial mechanical torque is applied at 0.5 s. The response of the output of the plant and the RLS identifier is shown in Fig. 5.5.

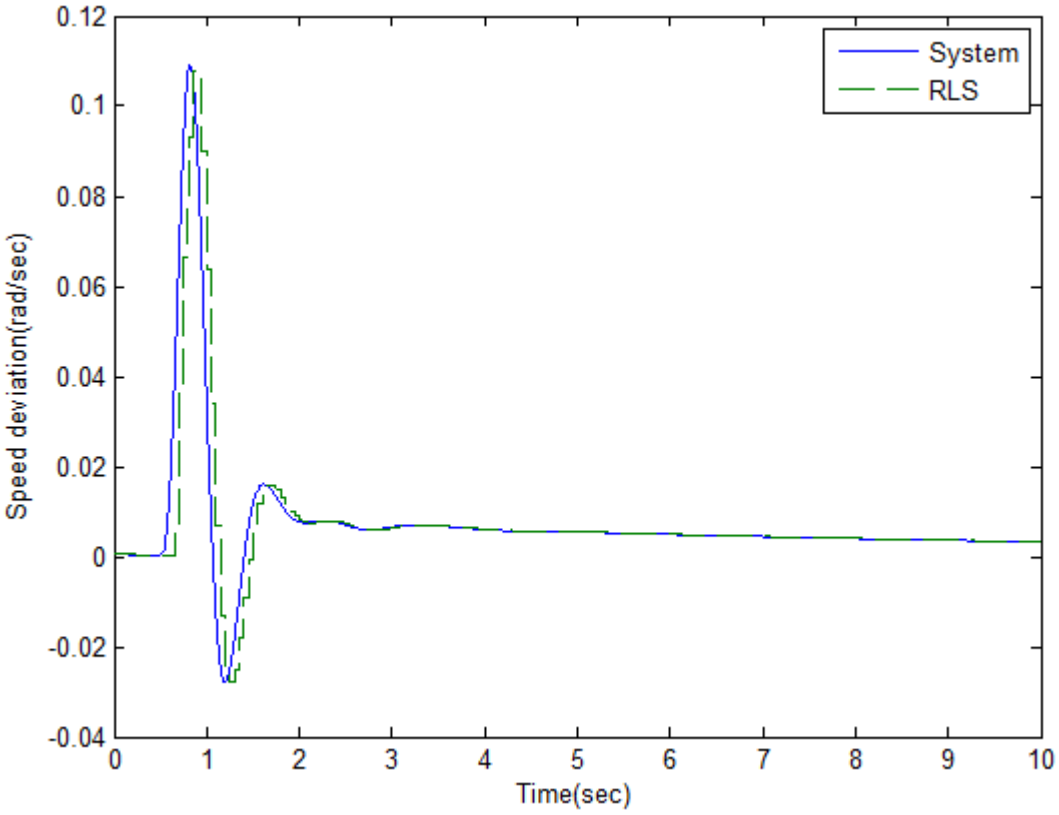

Fig 5.5 System output and RLS identifier response to a 0.1 p.u step increase in intial mechanical torque under leading load condition

5.2.2.5 Three phase shortcircuit test

In order to verify the ability of the RLS identifier under a transient condition two test cases were carried out as given below

Case1:

The SCG was operated at P = 0.9 p.u, pf = 0.8 lag and a three phase fault is applied at 0.5 s at the midddle of the transmission line connecting the generator to the infinte bus as shown in chapter 2, Fig.2.7. The fault is cleared at 50 ms by operating the circuit breakers. The response

of RLS tracking the system output during case 1 is shown in Fig.5.6 and the online variation of forgetting factor is shown in Fig.5.7.

Case 2:

With the SCG operating at P = 0.7 p.u , pf = 0.85 lag, a three phase fault is applied at 0.5s at the midddle of the transmission line connecting the generator to the infinte bus as shown in chapter 2, Fig 2.7, and it is cleared at 50 ms by operating the circuitbreaker to bring back to original condition at 7 s. The ability of RLS to track the output of the system during case 2 is shown in the Fig.5.8 and the online variation of a, b parameters is shown in Figs. 5.9 and 5.10.

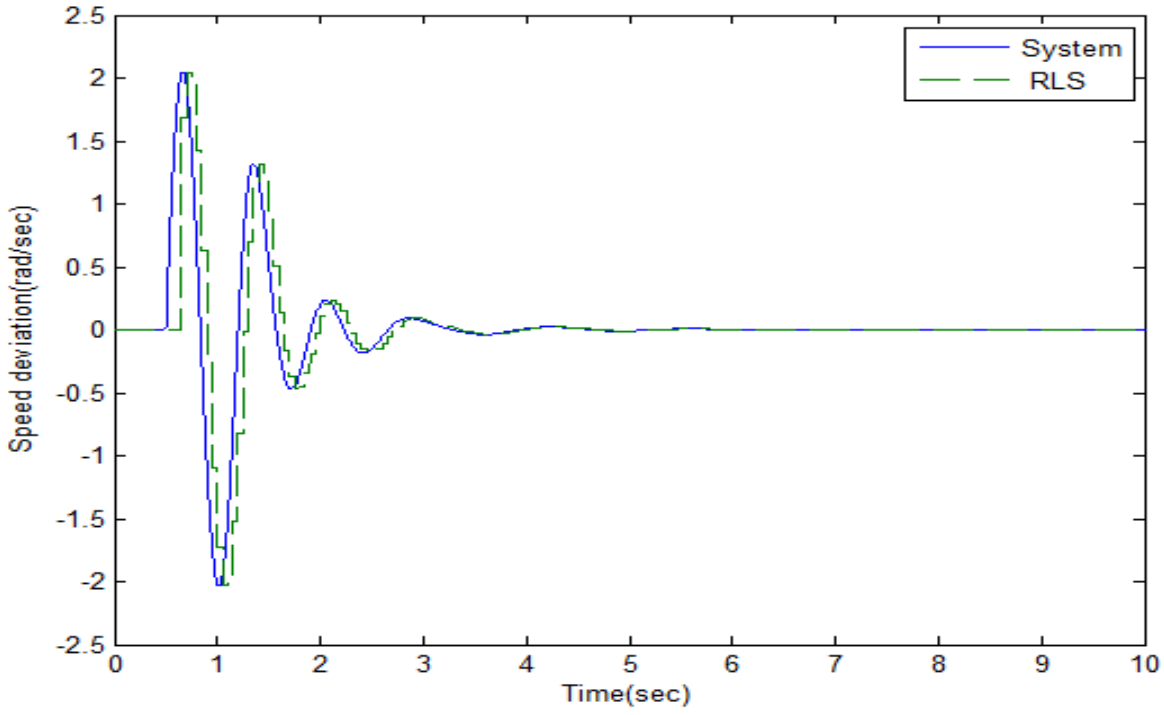

Fig.5.6 System output and RLS identifier response to a three phase to ground fault at the operating condition P = 0.9 p.u , pf = 0.8 lag

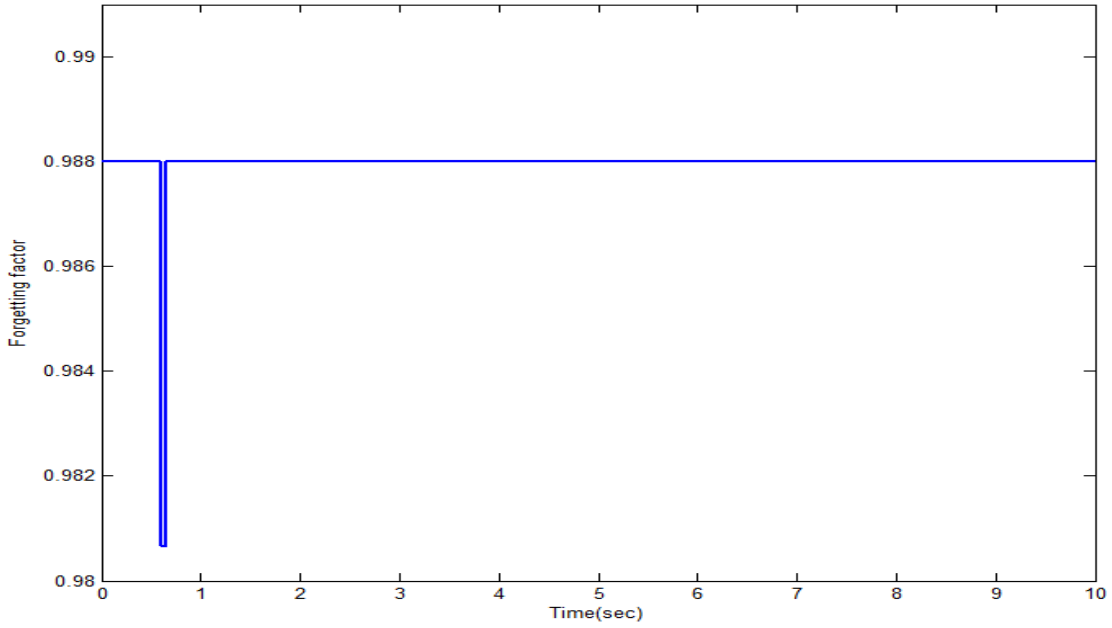

Fig.5.7 Variation of forgetting factor during the three phase to ground fault (case 1)

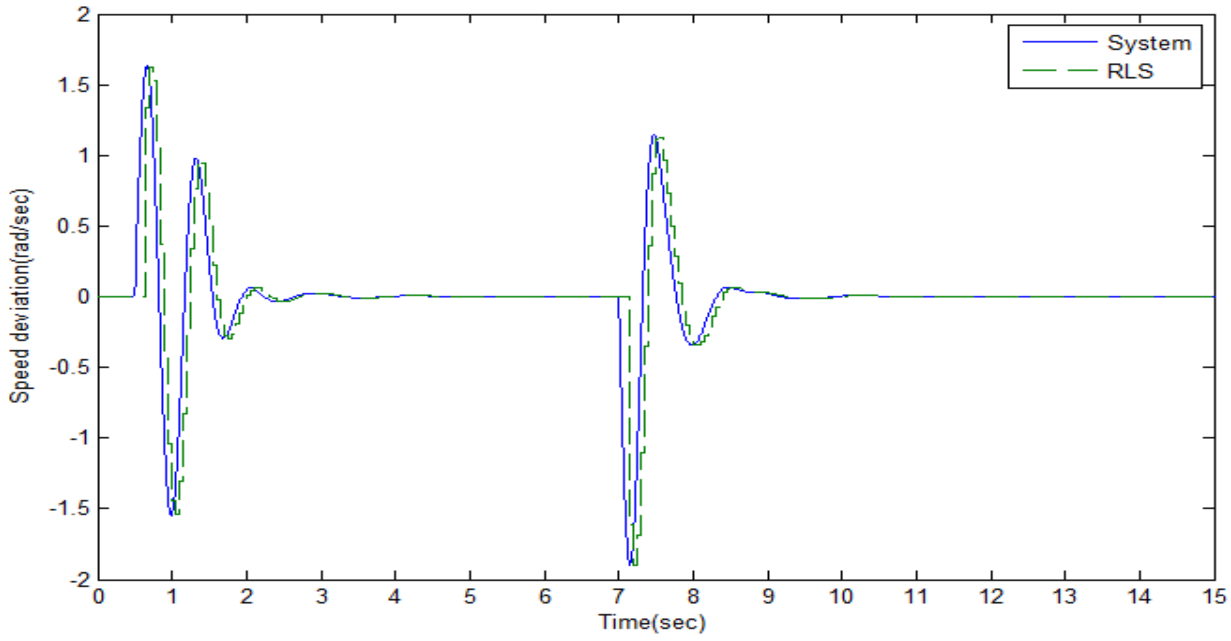

Fig.5.8 System output and RLS identifier response to a three phase to ground fault at the operating condition P = 0.7 p.u , pf = 0.85 lag

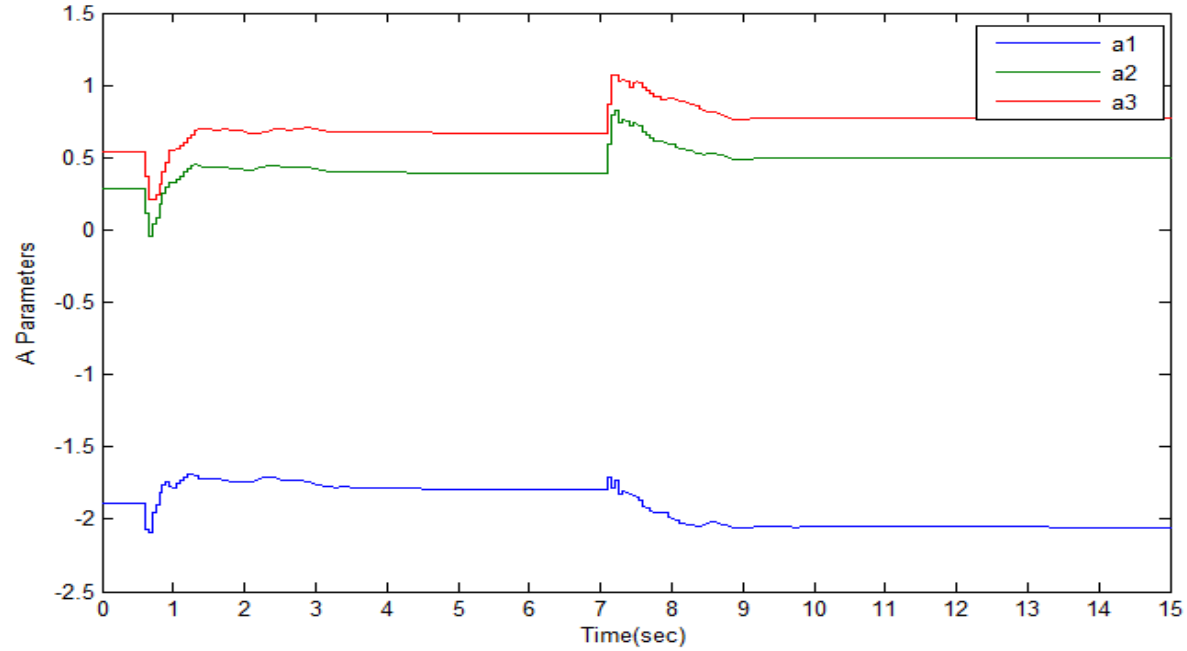

Fig.5.9 Online variation of A parameters during a three phase to ground fault at the operating condition P = 0.7 p.u , pf = 0.85 lag

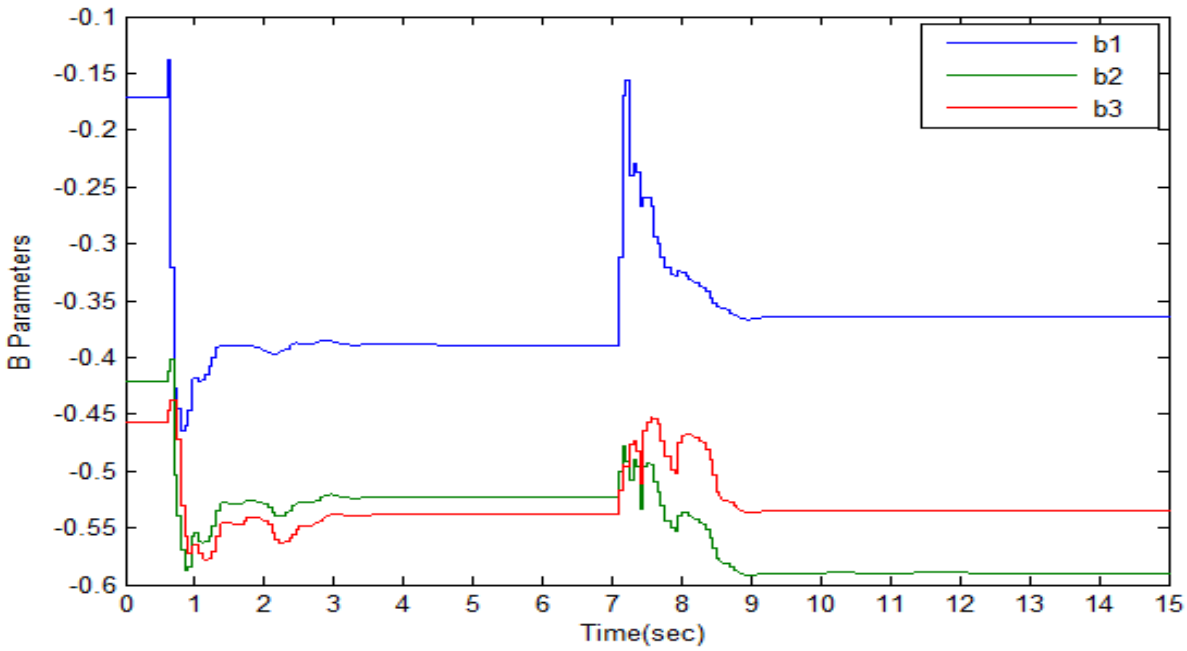

Fig.5.10 Online variation of B parameters during a three phase to ground fault at the operating condition P = 0.7 p.u , pf = 0.85 lag

5.2.2.6 Slower, higher frequency condition, and demonstration of white noise

In this experiment, the SCG was operated at P = 0.7 p.u, pf = 0.85 lag. A 0.1 p.u step increase of initial mechanical torque is applied at 0.5 s. How RLS identifier tracks the output of the system for 10 Hz, 20 Hz, 50 Hz, and 100 Hz respectively without and with white noise are shown in Fig 5.11 to 5.15.

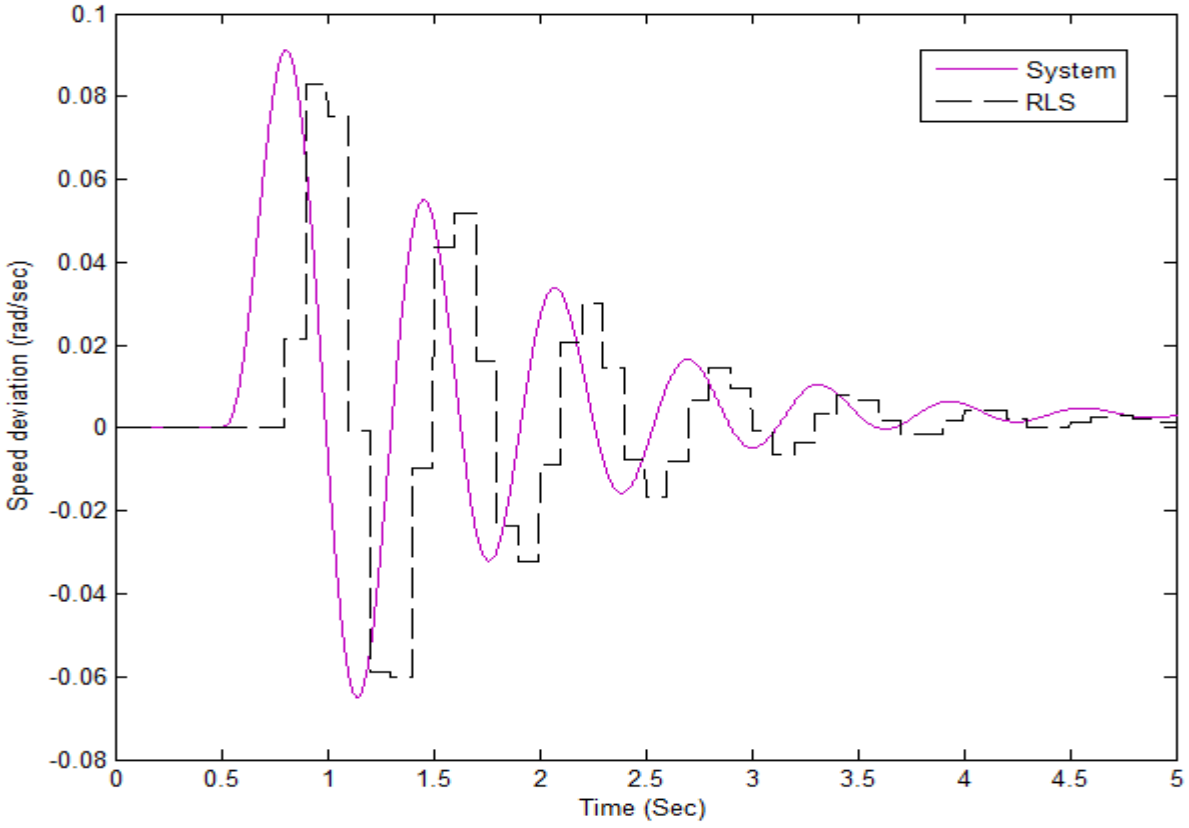

Fig 5.11 System output and RLS identifier response to a 0.1 p.u step increase in intial mechanical torque under normal load condition for sampling frequency 10 Hz, without white noise

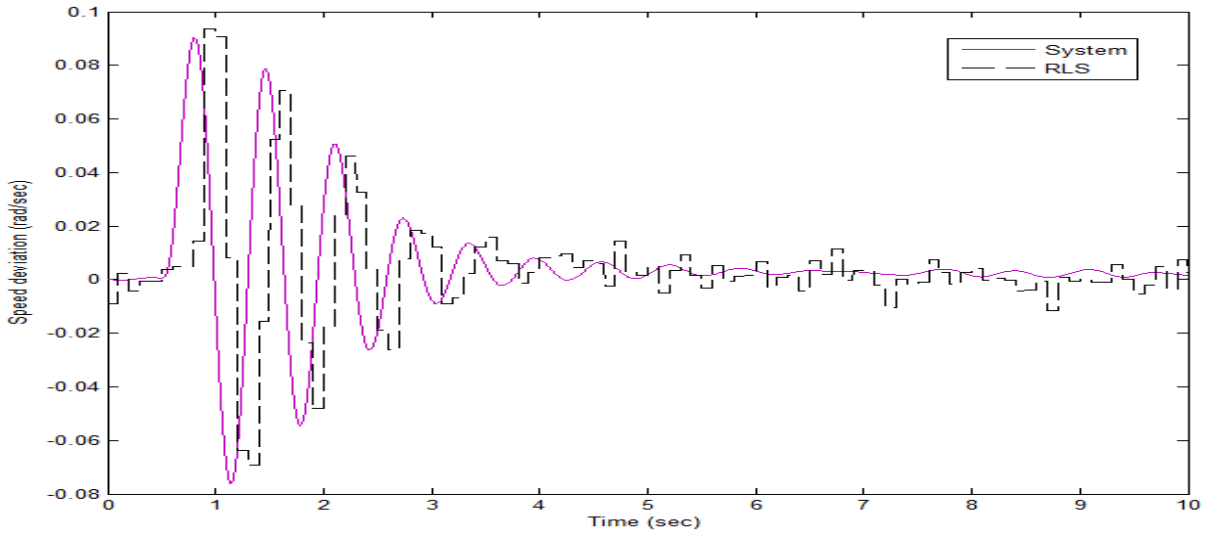

Fig. 5.12 System output and RLS identifier response to a 0.1 p.u step increase in intial mechanical torque under normal load condition for sampling frequency 10 Hz, with white noise

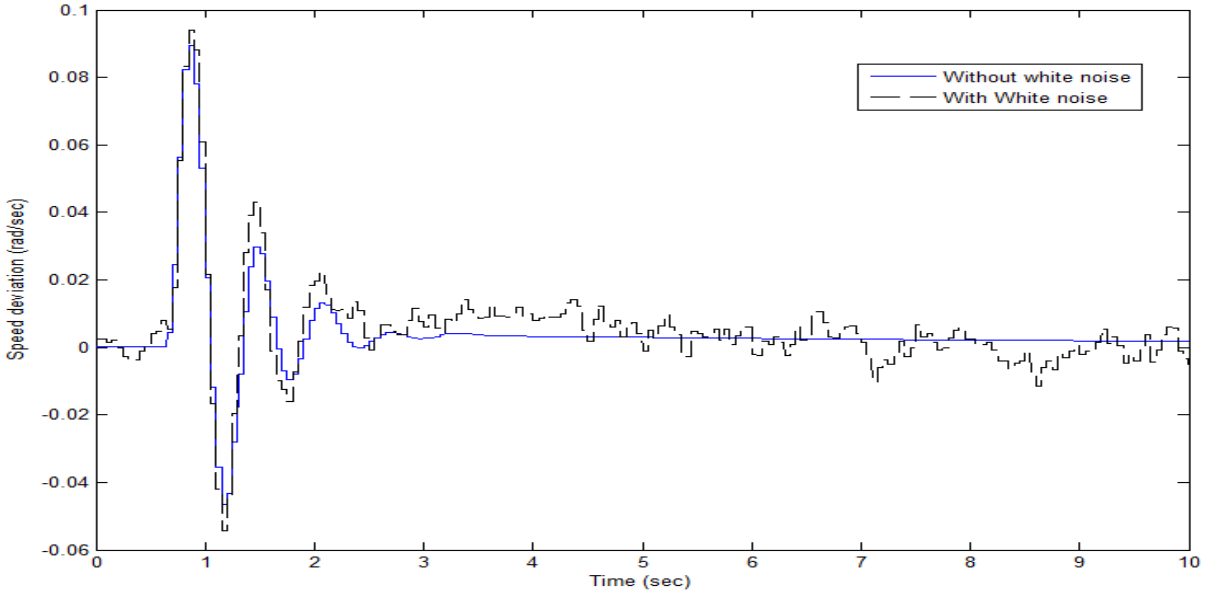

Fig 5.13 Comparison of RLS identifier response to a 0.1 p.u step increase in intial mechanical torque under normal load condition for sampling frequency 20 Hz, with and without white noise

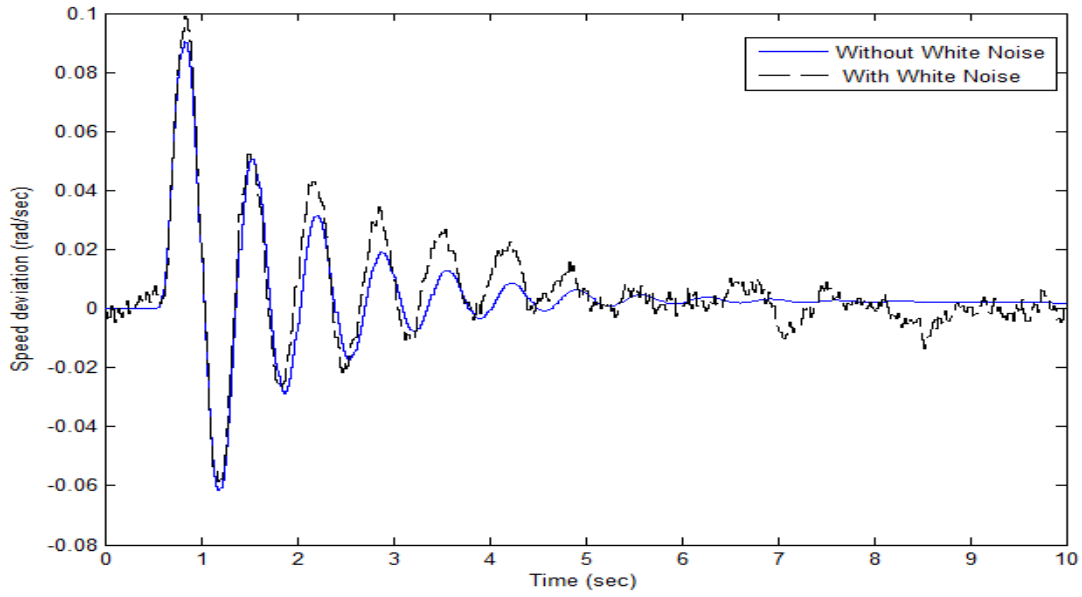

Fig 5.14 Comparison of RLS identifier response to a 0.1 p.u step increase in intial mechanical torque under normal load condition for sampling frequency 50 Hz, with and without white noise

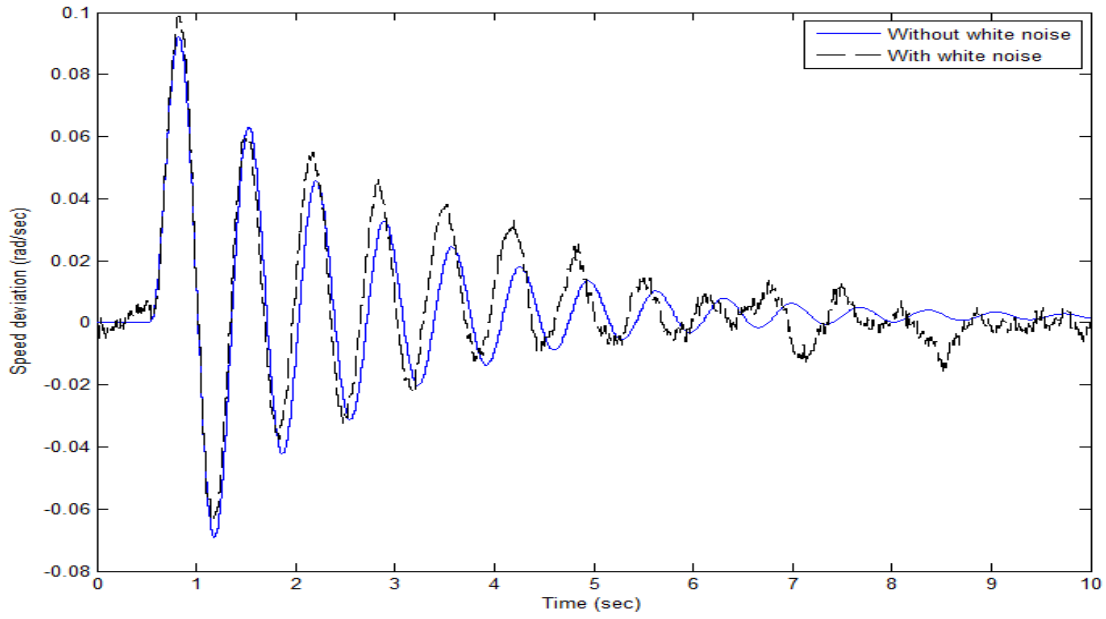

Fig 5.15 Comparison of RLS identifier response to a 0.1 p.u step increase in intial mechanical torque under normal load condition for sampling frequency 100 Hz, with and without white noise

5.2.3 Performance studies using Kalman identifier

In the previous section, response of the RLS identifier is studied with respect to the output of the system for different types of operating conditions and disturbances. In this section Kalman filter is used to track the parameters of the output of the system at the sampling rate of 20 Hz. From the performance, the best among the two can be selected to update the controller.

5.2.3.1 Normal load condition

The SCG was operated at P = 0.7 p.u, pf = 0.85 lag. A 0.1 p.u step increase of initial mechanical torque is applied at 0.5 s and brought back to the normal condition by removing the step increase in initial mechanical torque at 7 s. The response of the output of the plant and the Kalman identifier is shown in Fig. 5.16.

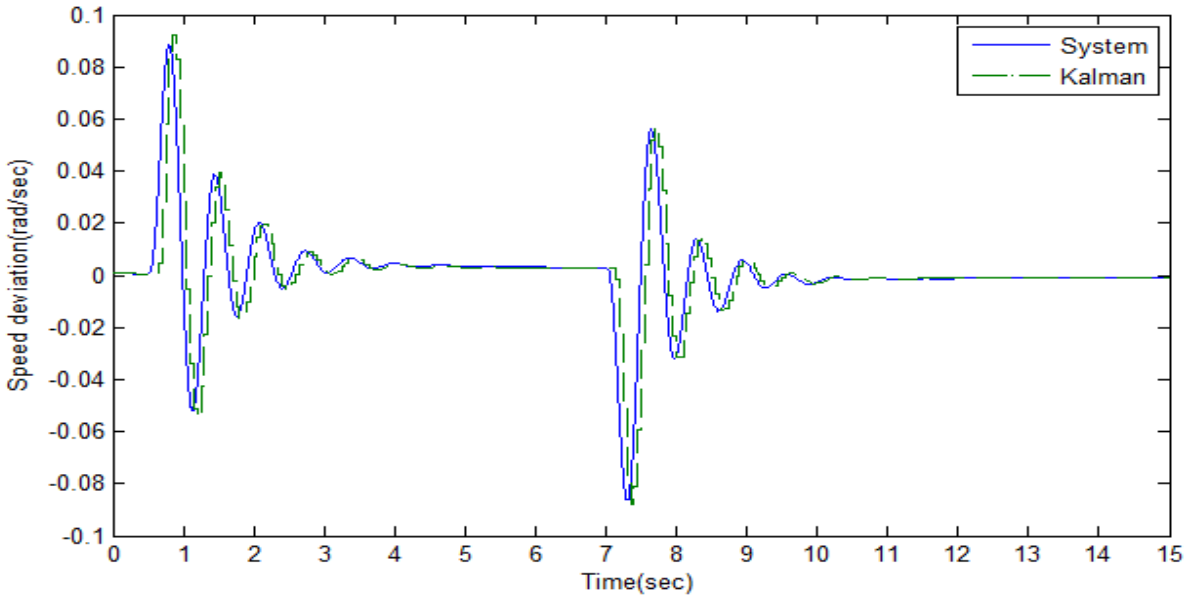

Fig.5.16 System output and Kalman identifier response to a 0.1 p.u step increase of intial mechanical torque and return to original condition under normal load condition

5.2.3.2 Voltage reference change

The performance of Kalman identifier for a step increase in reference voltage is carried out in this experiment. The SCG was operated at P = 0.7 p.u, pf = 0.85 lag. A 0.2 p.u step increase of the reference terminal voltage at 0.5 s and brought back to the original condition by removing the step increase in reference terminal voltage at 7 s as shown in Fig.5.17.

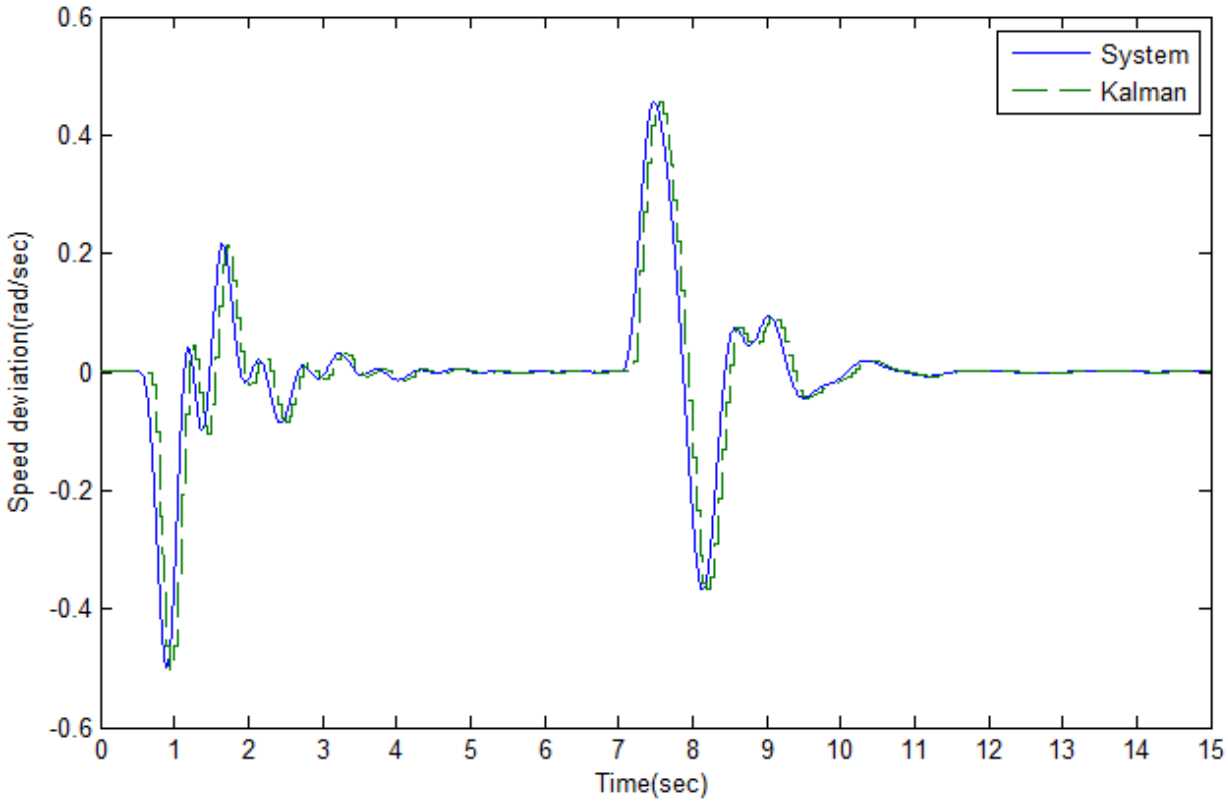

Fig.5.17 System output and Kalman identifier response to a 0.2 p.u step increase in refernce terminal voltage and return to original condition under normal load condition

5.2.3.3 Light load condition

The ability of Kalman identifier under a light load condition to track the variations of the plant due to a disturbance is studied here. The SCG was operated at P = 0.2, pf = 0.85 lag. Response to a step increase of 0.2 p.u in initial mechanical torque applied at 0.5 s and step increase removed at 7 s to bring back to the original condition is shown in Fig.5.18.

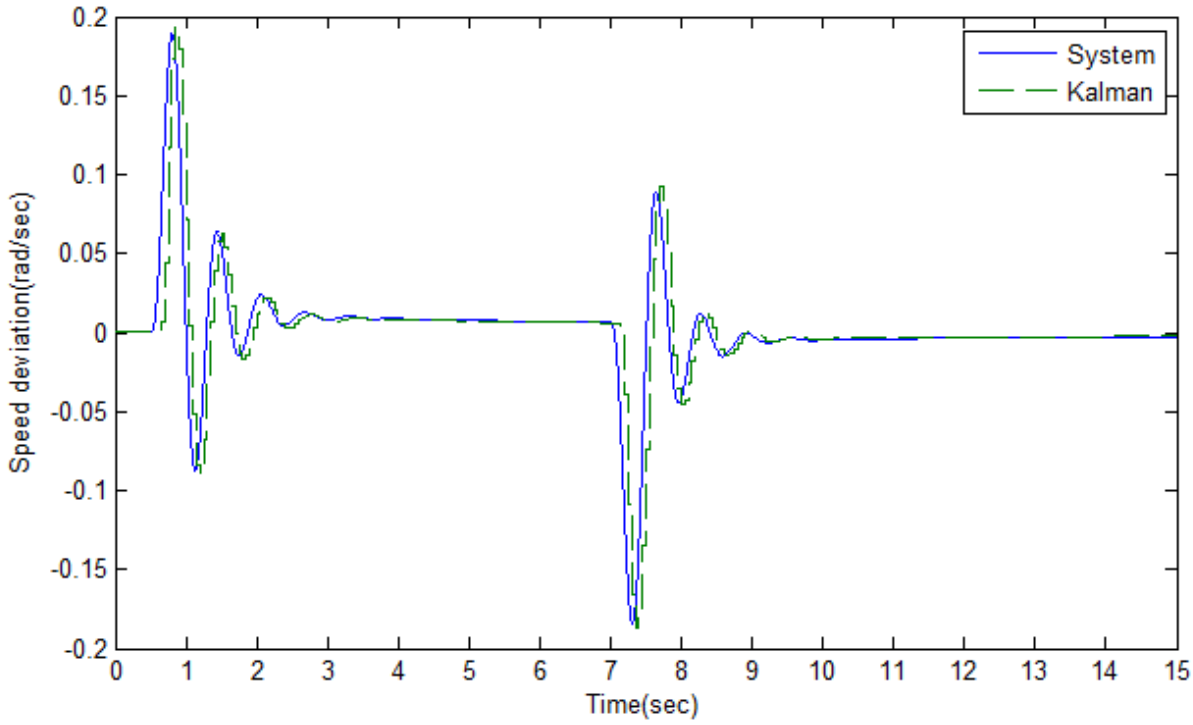

Fig.5.18 System output and Kalman identifier response to a 0.2 p.u step increase in intial mechanical torque and return to original condition under light load condition

5.2.3.4 Three phase short circuit test

Tracking performance during the three phase fault with a Kalman identifer is studied here. With the SCG operating at P = 0.8 p.u , pf = 0.85 lag, a three phase fault is applied at 0.5 s at the midddle of the transmission line connecting the generator to the infinte bus as shown in chapter 2, Fig.2.7. The fault is cleared at 50 ms by operating the circuitbreakers and the results are shown in Fig.5.19. The online variation of a, b parameters during the three phase fault is shown in Figs.5.20 and 5.21.

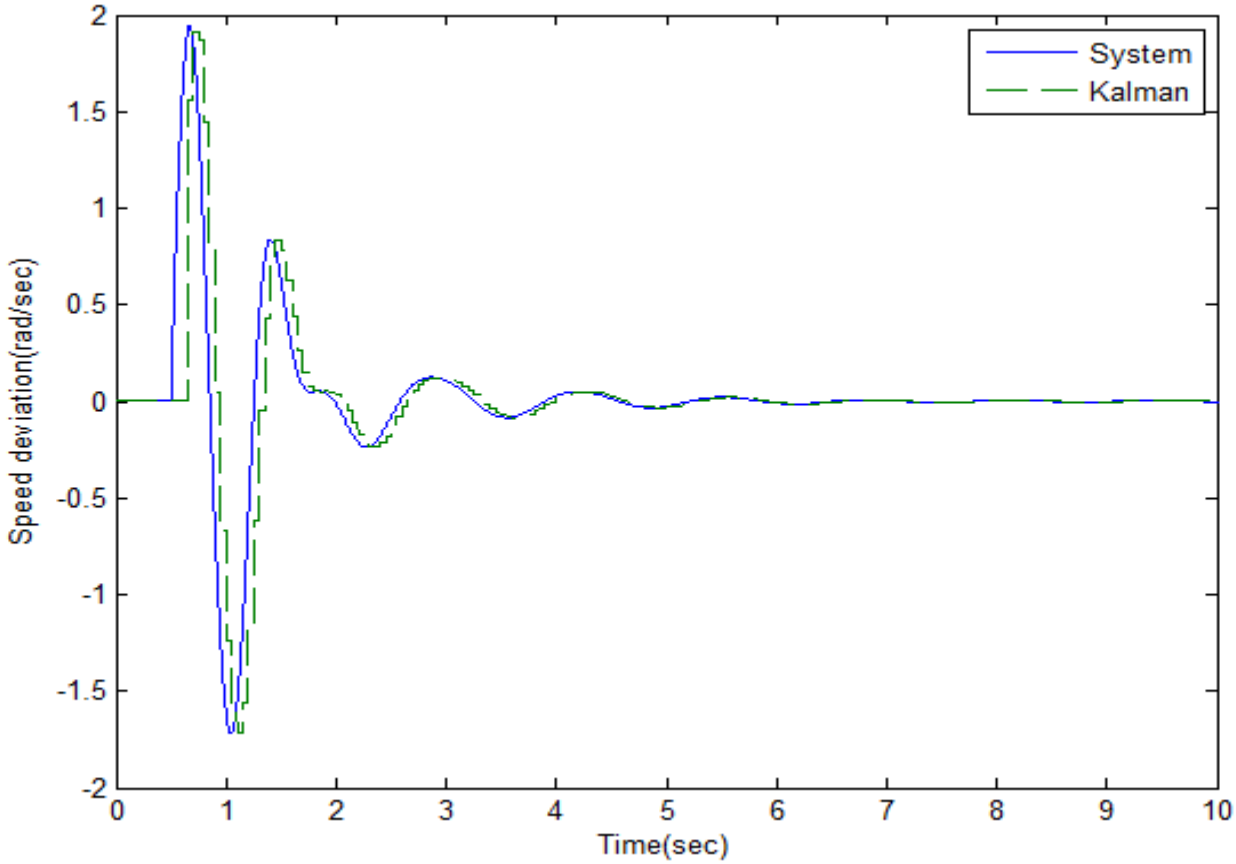

Fig.5.19 System output and Kalman identifier response to a three phase to ground fault at the operating condition P = 0.8 p.u , pf = 0.85 lag

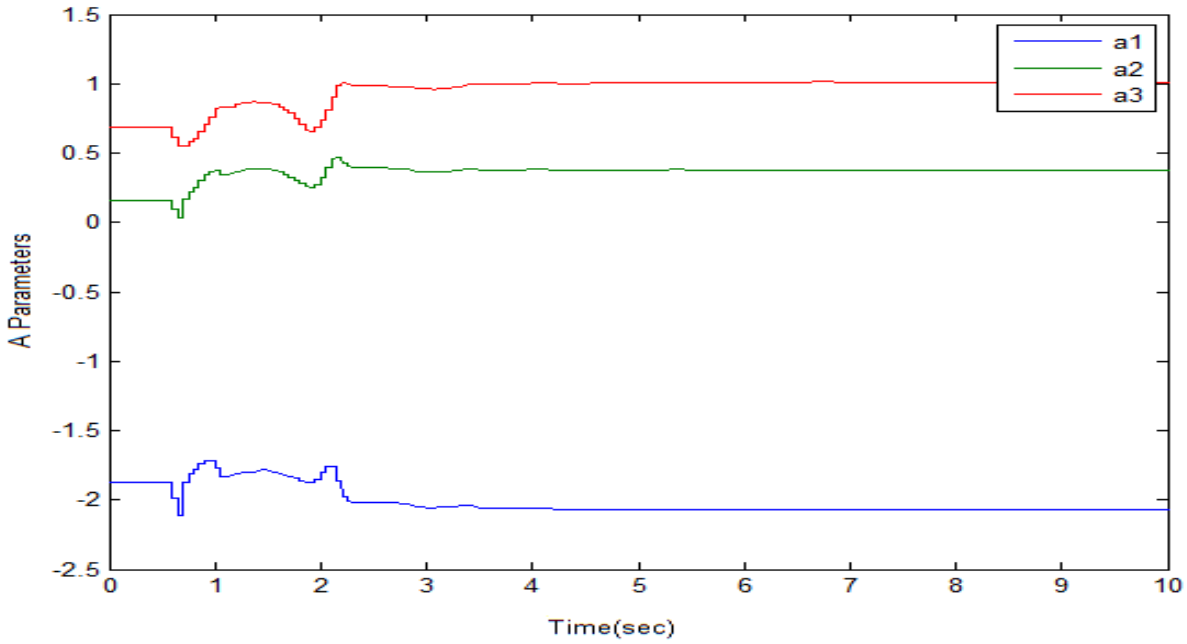

Fig.5.20 Online variation of A parameters during a three phase to ground fault at the operating condition P = 0.8 p.u , pf = 0.85 lag with Kalman identifier

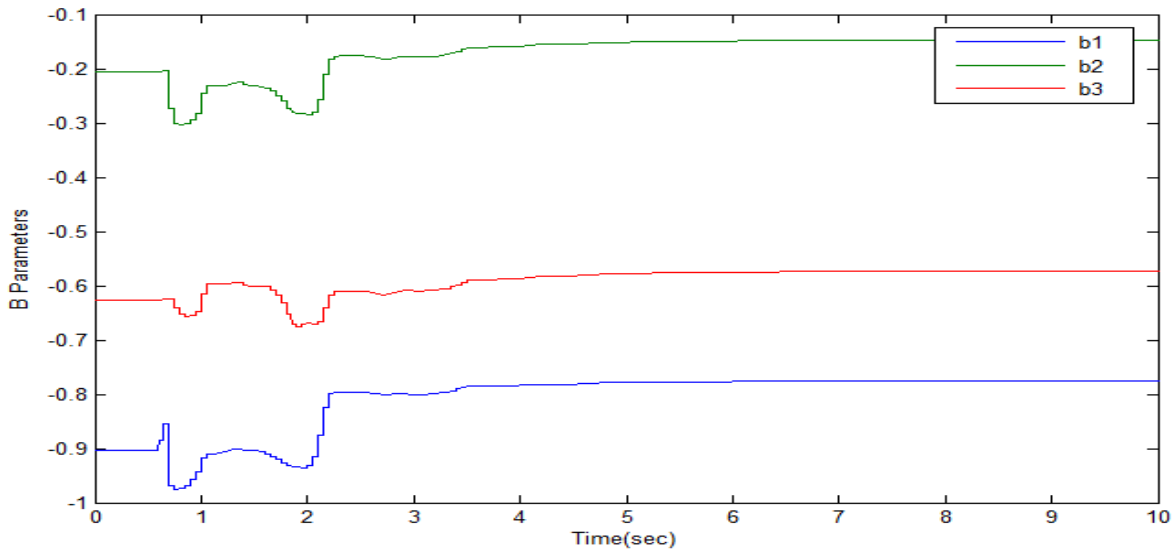

Fig.5.21 Online variation of B parameters during a three phase to ground fault at the operating condition P = 0.8 p.u , pf = 0.85 lag with Kalman identifier

5.2.3.5 Slower, higher frequency condition, and demonstration of white noise

In this section Kalman filter is used to track the parameters of the output of the system for 10, 20, 50, and 100 Hz respectively without and with white noise are shown in Fig 5.22 to Fig 5.26.

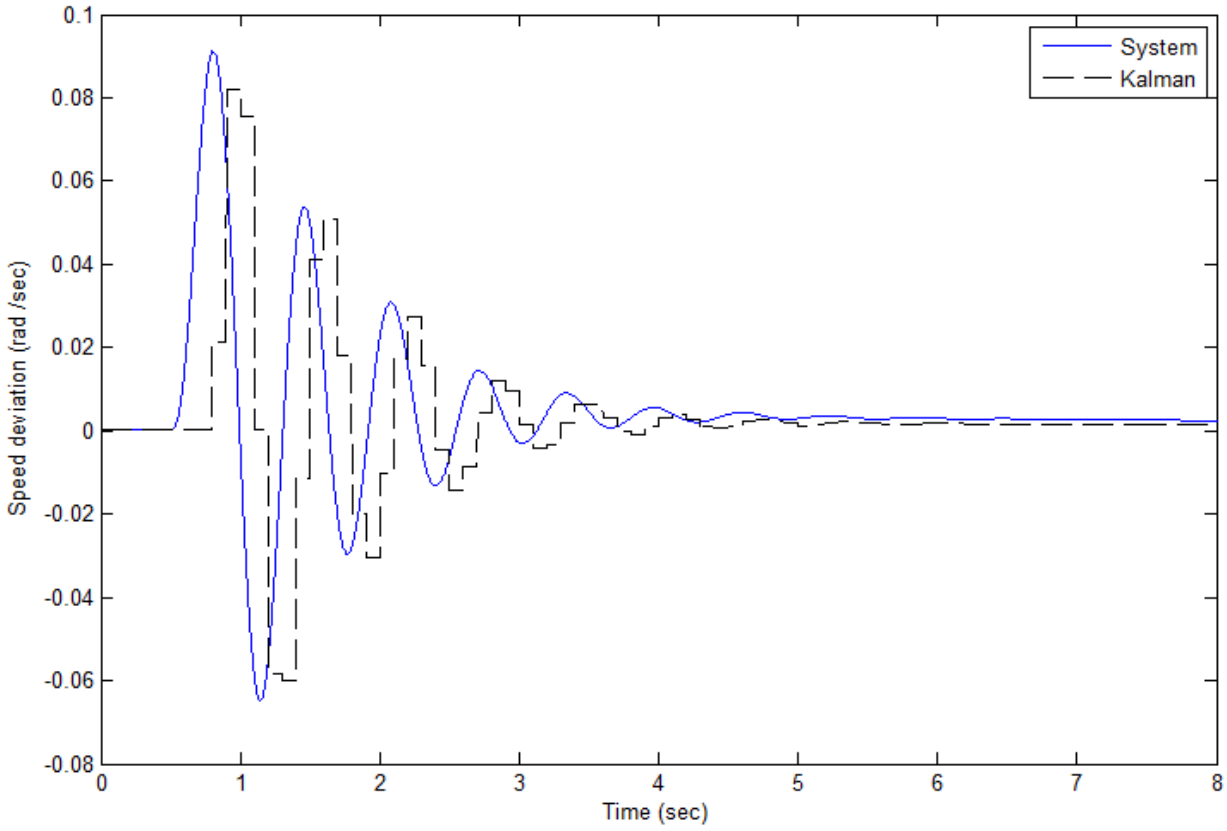

Fig 5.22 System output and Kalman identifier response to a 0.1 p.u step increase of intial mechanical torque under normal load condition for sampling frequency 10 Hz, without white noise

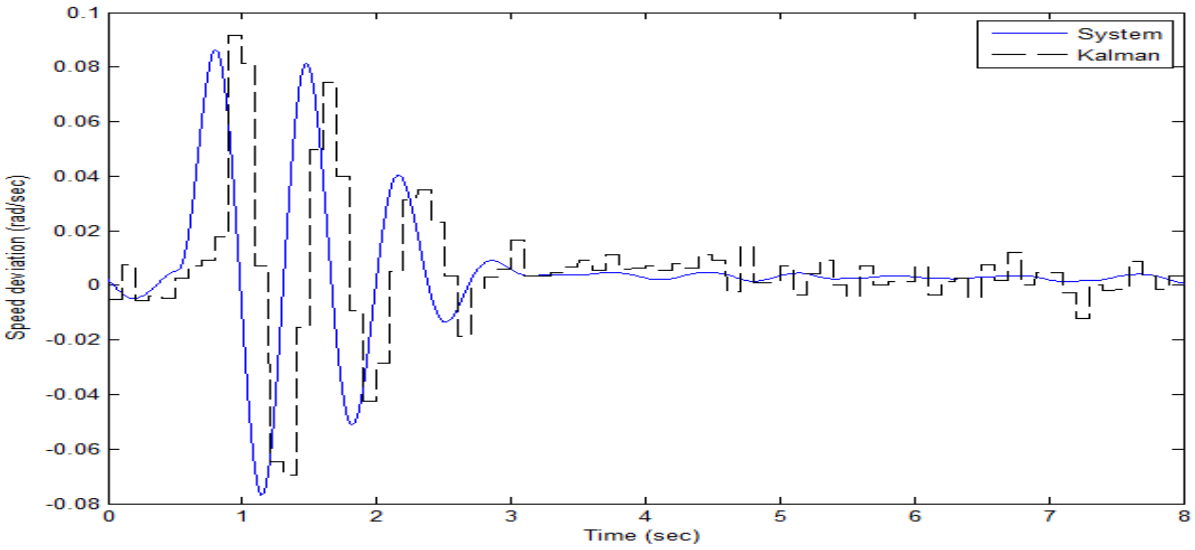

Fig 5.23 System output and Kalman identifier response to a 0.1 p.u step increase of intial mechanical torque under normal load condition for sampling frequency 10 Hz, with white noise

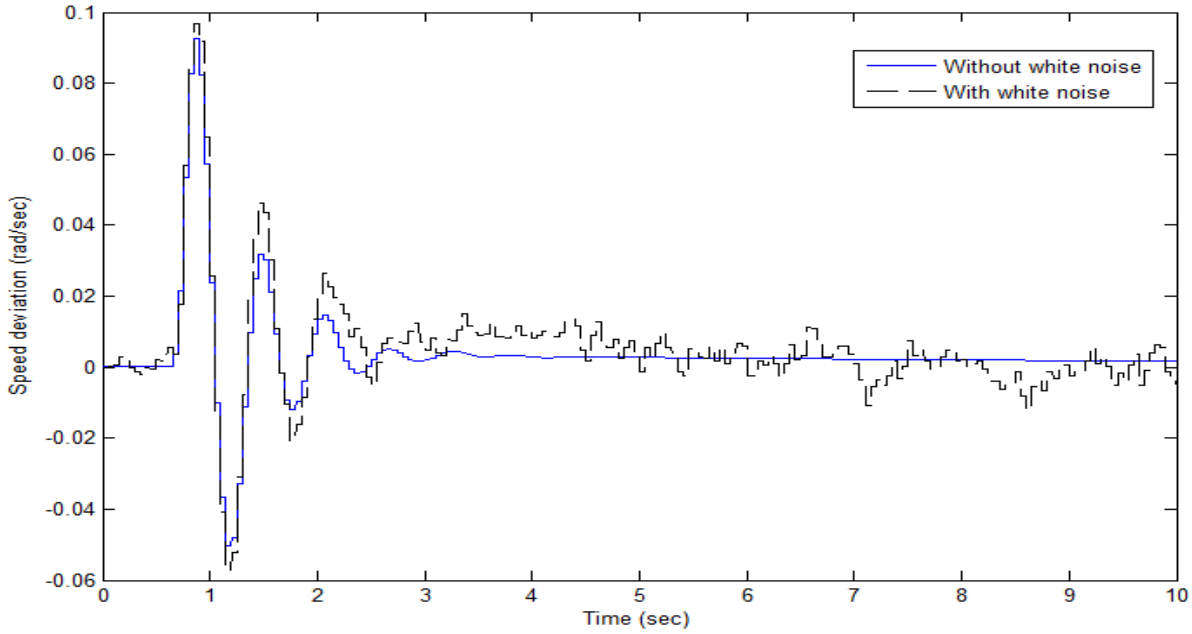

Fig 5.24 Comparison of Kalman identifier response to a 0.1 p.u step increase of intial mechanical torque under normal load condition for sampling frequency 20 Hz, with and without white noise

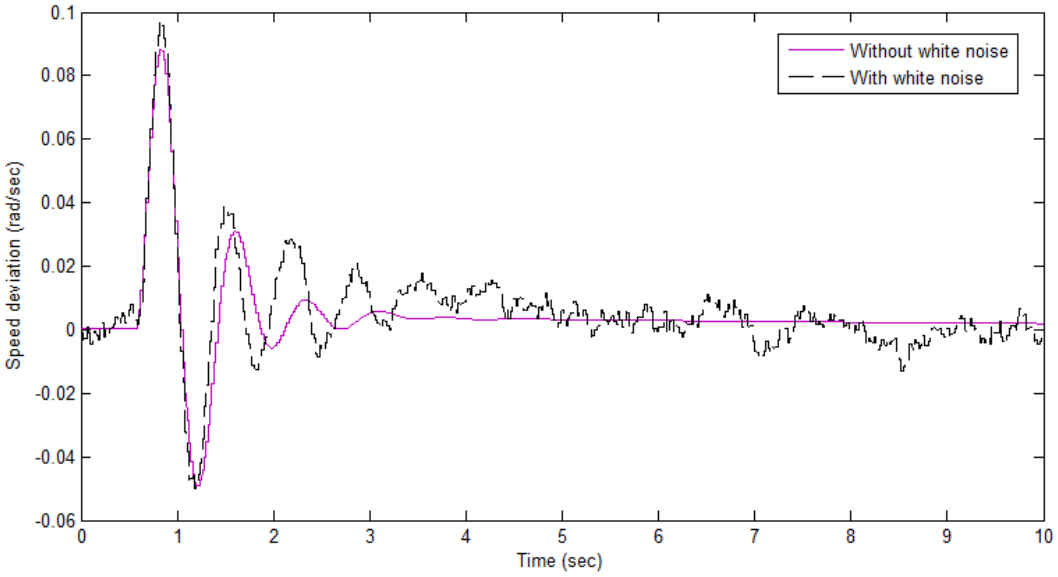

Fig 5.25 Comparison of Kalman identifier response to a 0.1 p.u step increase of intial mechanical torque under normal load condition for sampling frequency 50 Hz, with and without white noise

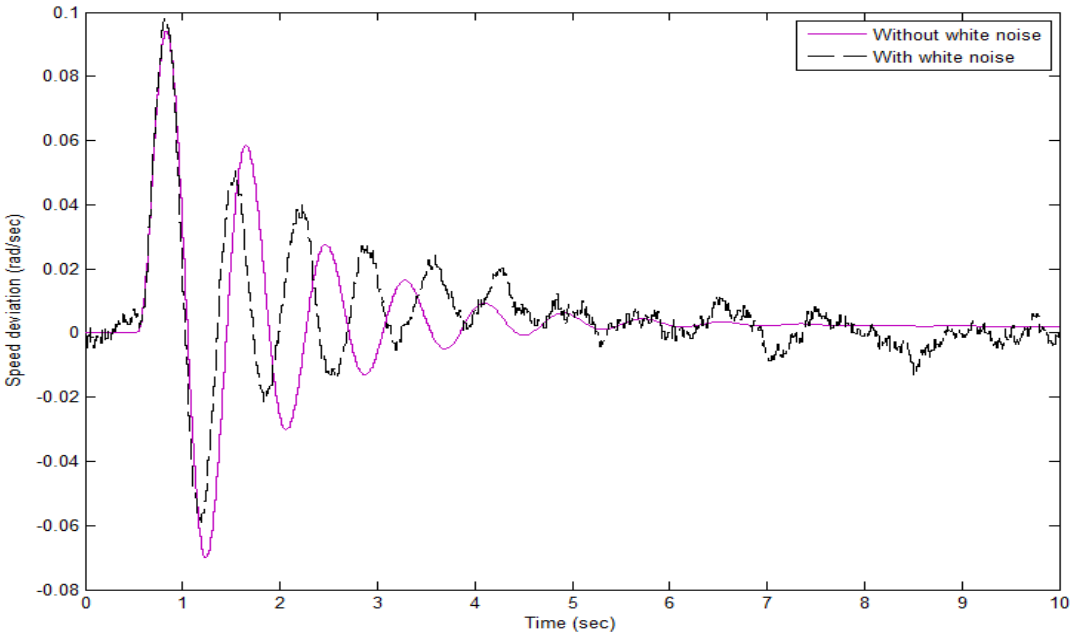

Fig 5.26 Comparison of Kalman identifier response to a 0.1 p.u step increase of intial mechanical torque under normal load condition for sampling frequency 100 Hz, with and without white noise

5.3 Discussion

In the previous sections simulation studies have been carried out with the RLS and Kalman filter algorithms to identify the parameters of the system under different operating conditions with disturbances. The results obtained from the simulation studies show that both RLS and Kalman filter have very good tracking capability and the same level of accuracy in reflecting the output of the system. The results show that both algorithms are suitable for estimating the parameters online to update the PS controller to obtain the control signal. However, RLS algorithm employed with variable forgetting factor has good convergence time (0.012s) over the Kalman filter (0.024 s). Preference is, therefore, given to RLS with a variable forgetting factor to update the system parameters in the simulation studies for APSS in chapter 6.

Chapter Six: Application of indirect adaptive pole shift control to an SCG

6.1 Introduction

Power systems are highly non-linear and never operate in steady state. They are also subject to many disturbances. The CPSS, the commonly used controller, does not have the characteristics to adapt to the changes in the environment so the parameters have to be tuned according to the operating condition of the system. It is desired to have an adaptive controller that is flexible in adapting its parameters on-line according to the operating condition of the system. In this chapter, results of simulation studies of an indirect adaptive pole shift controller using self-optimizing technique applied to the electro-hydraulic governor of an SCG, connected to an infinite bus through a transmission line, are discussed.

6.2 PS Control strategies

Parameters of the third order model of the system are identified with the help of an identification algorithm. After that the control signal is calculated based on the discrete model using equation (5.1). If the feedback loop has the form:

$$\frac{u(t)}{y(t)} = -\frac{G(z^{-1})}{F(z^{-1})} \qquad (6.1)$$

where

$$G(z^{-1}) = g_o + g_1 z^{-1} + g_2 z^{-2} \qquad (6.2)$$

$$F(z^{-1}) = 1 + f_1 z^{-1} + f_2 z^{-2} \quad (6.3)$$

the closed loop characteristic polynomial $T(z^{-1})$ is written as

$$T(z^{-1}) = A(z^{-1})F(z^{-1}) + B(z^{-1})G(z^{-1}) \quad (6.4)$$

In pole shift control algorithm, $T(z^{-1})$ takes the form $A(\alpha z^{-1})$ and the locations of the poles are shifted by the variable pole shift factor, α

$$A(z^{-1})F(z^{-1}) + B(z^{-1})G(z^{-1}) = A(\alpha z^{-1}) \quad (6.5)$$

On expanding equation (6.5) on both sides, results in (6.6):

$$\begin{bmatrix} 1 & 0 & b_1 & 0 & 0 \\ a_1 & 1 & b_2 & b_1 & 0 \\ a_2 & a_1 & b_3 & b_2 & b_1 \\ a_3 & a_2 & 0 & b_3 & b_2 \\ 0 & a_3 & 0 & 0 & b_3 \end{bmatrix} \begin{bmatrix} f_1 \\ f_2 \\ g_0 \\ g_1 \\ g_2 \end{bmatrix} = \begin{bmatrix} a_1(\alpha - 1) \\ a_2(\alpha^2 - 1) \\ a_3(\alpha^3 - 1) \\ 0 \\ 0 \end{bmatrix} \quad (6.6)$$

Equation (6.6) can be written in matrix form as in Equation (6.7):

$$M.w(\alpha) = L(\alpha) \quad (6.7)$$

The control signal $u(t)$ is calculated as a function of α , and it is modified online according to the operating condition of the system.

$$u(t,\alpha) = X_C{}^T(t).w(\alpha_t) = X_C{}^T(t).M^{-1}L(\alpha) \qquad (6.8)$$

where

$$X_C{}^T = [-u(t-1) - u(t-2) - y(t) - y(t-1) - y(t-2)] \qquad (6.9)$$

The properties, constraints, optimization techniques of the control algorithm are discussed in chapter 4.

6.3 Simulation studies

To investigate the capability of the pole shift based APSS, studies have been performed on the system shown in Fig 6.1. The RLS identifier with a variable forgetting factor, used for the identification of the parameters, and the variable pole shifting linear control algorithm, used as a controller, are applied to the electro-hydraulic governor of the SCG with a three stage turbine and connected to an infinite bus through a transmission line. The speed deviation is sampled at the rate of 20 Hz for parameter identification and control computation. The sampling frequency of 20 Hz is chosen to give enough time for updating the identifier and control computation. The output of the controller is limited with upper limit, + 0.1p.u and lower limit, - 0.1p.u.

6.3 Normal load condition

In this experiment, with the SCG operating at normal operating condition P = 0.7 p.u, pf = 0.85 lag, a 0.1 p.u step increase of initial mechanical torque was applied at 0.5 s. The studies were carried out by comparing the response of speed deviation, rotor angle, valve position and

terminal voltage with APSS, CPSS and without any supplementary control (OPEN). The results are shown in Figs. 6.2 through 6.5.

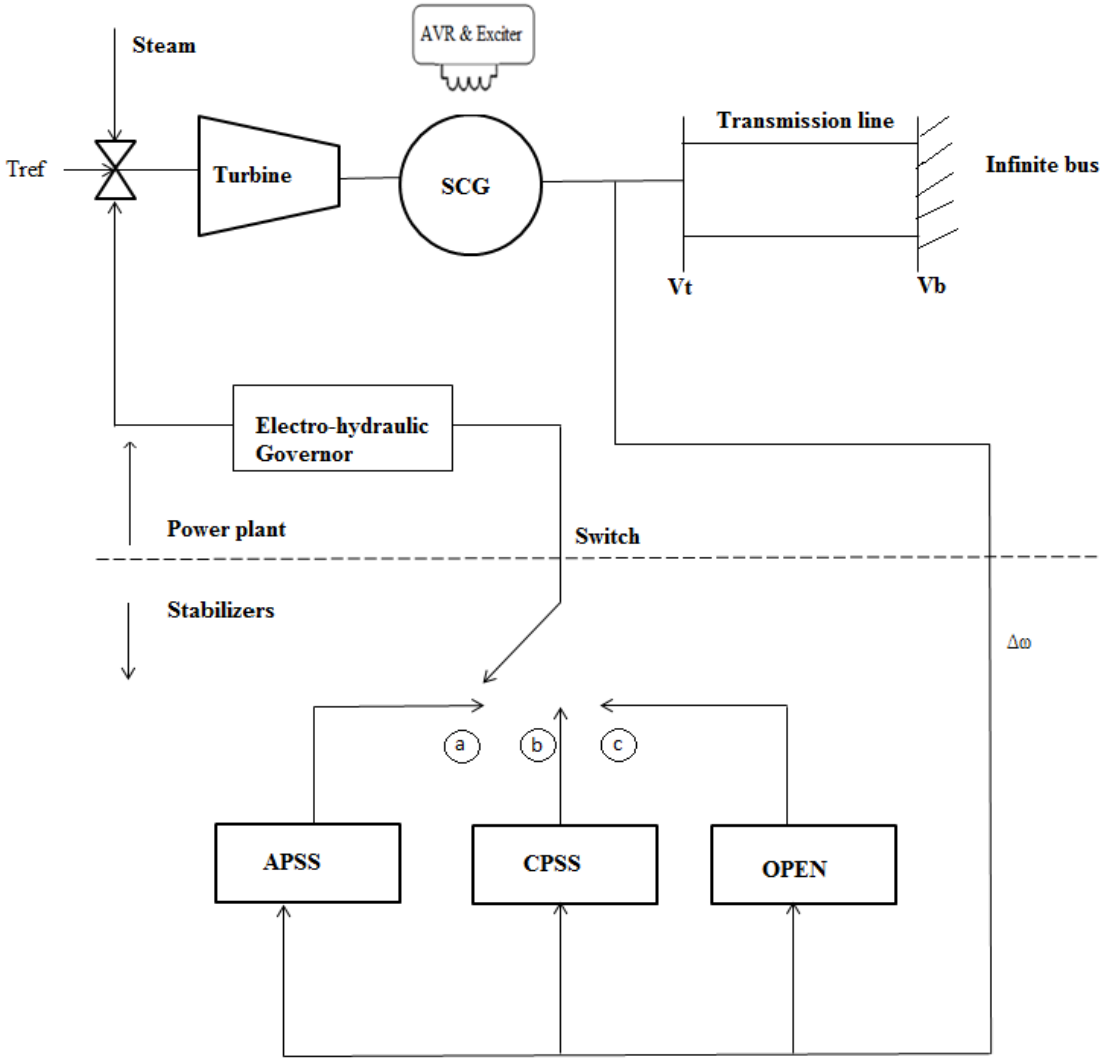

Fig.6.1 System used for simulation studies

It can be seen from Fig. 6.2 that the pole shift based APSS provides fast damping with the settling time of 1.5 s where it is 3.5 s with the CPSS. Also, the peak over-shoot of the oscillation with APSS during the first swing and overshoots during successive swings are much

less than with the CPSS or OPEN. Position of the valve of electro hydraulic governor is shown in Fig. 6.3 and it can be seen that the position of the valve was controlled very quickly by the APSS within 1.6 s where as it took 3 s with the CPSS. This helps in controlling the amount of steam entering the turbine because the input mechanical power has been controlled to damp the oscillations encountered during the disturbance. Also, another test was conducted at normal condition P = 0.7 p.u, pf = 0.9 lag with a 0.2 p.u step increase of initial mechanical torque applied at 0.5 s and brought back to the original condition at 5 s. The results are shown in Figs. 6.6 and 6.7. It can be seen from Fig. 6.6 that the settling time with APPS on returning to the original condition is about 2 s vs 3s with CPSS. It shows that APSS damps the oscillations very effectively during the normal operating condition.

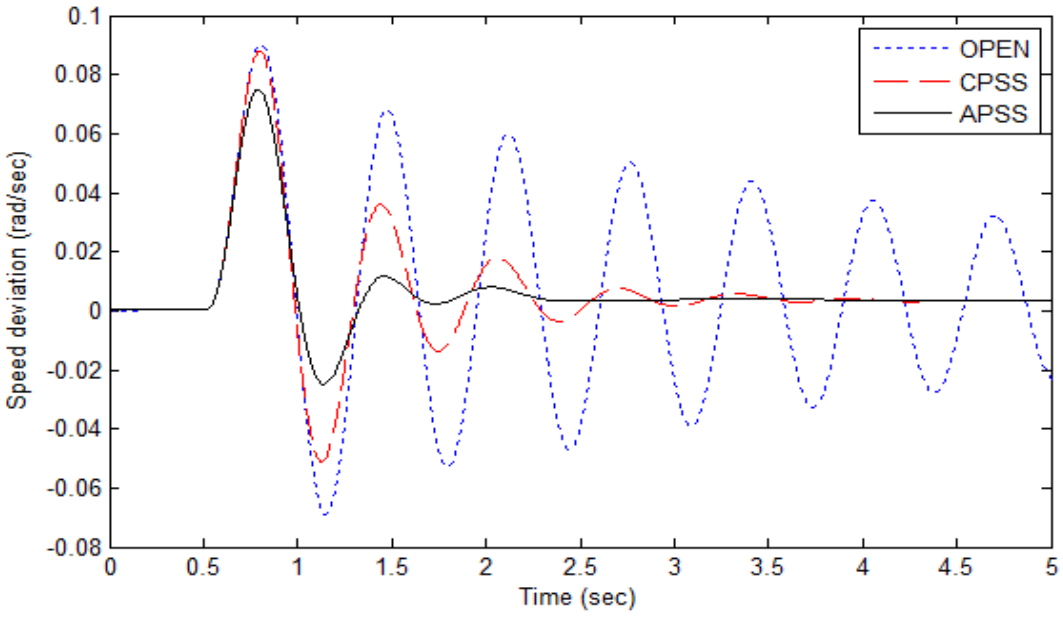

Fig.6.2 Speed deviation of the SCG in response to a 0.1 p.u step increase in the mechanical torque under normal operating condition P = 0.7 p.u, pf =0.85 lag

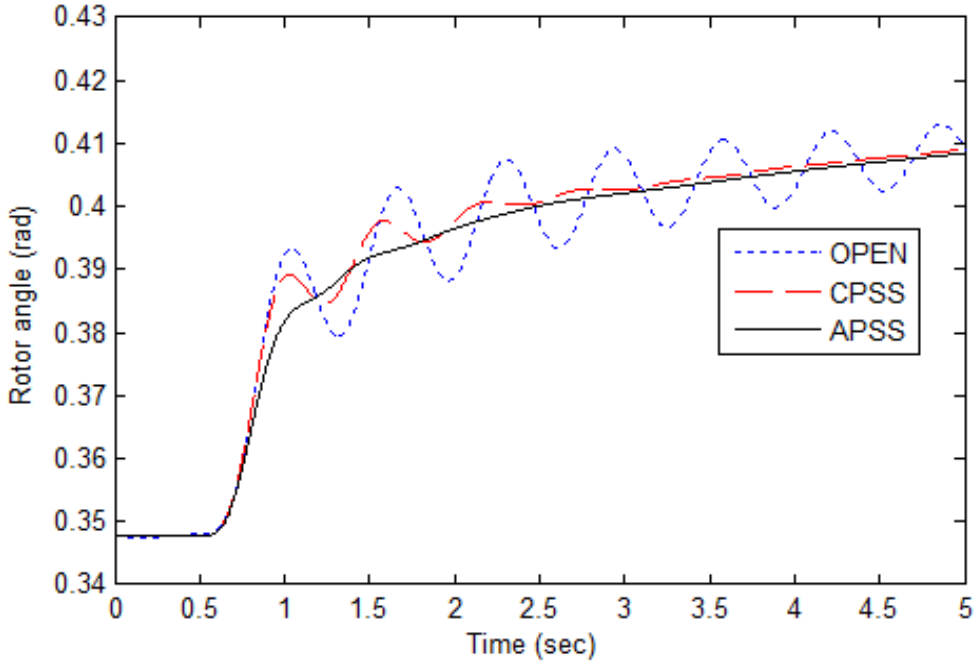

Fig.6.3 Rotor angle in response to 0.1 p.u step increase in the mechanical torque under normal operating condition P = 0.7 p.u, pf =0.85 lag

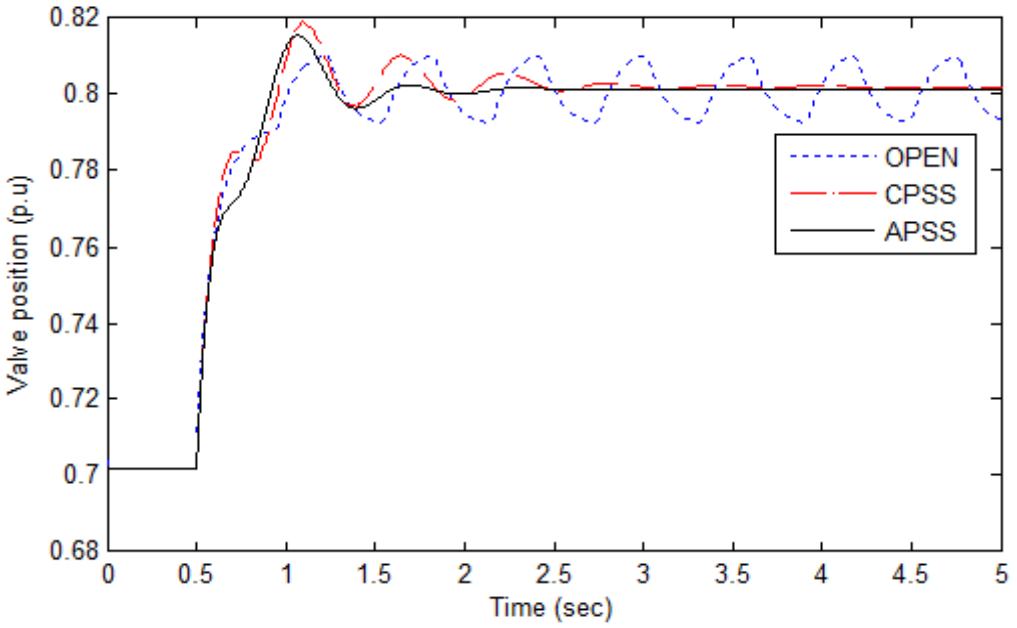

Fig. 6.4 position of the electro-hydraulic governor valve in response to 0.1 p.u step in the mechanical torque under normal operating condition P = 0.7 p.u, pf =0.85 lag

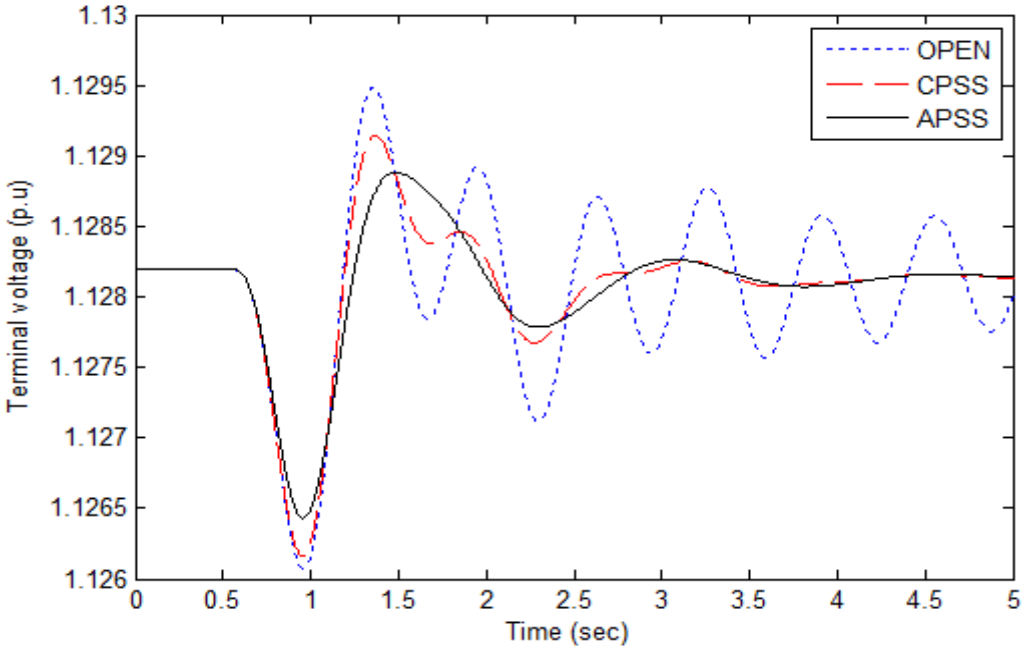

Fig.6.5 Terminal voltage of the SCG in response to 0.2 p.u step in the mechanical torque under normal operating condition P = 0.7 p.u, pf = 0.85 lag

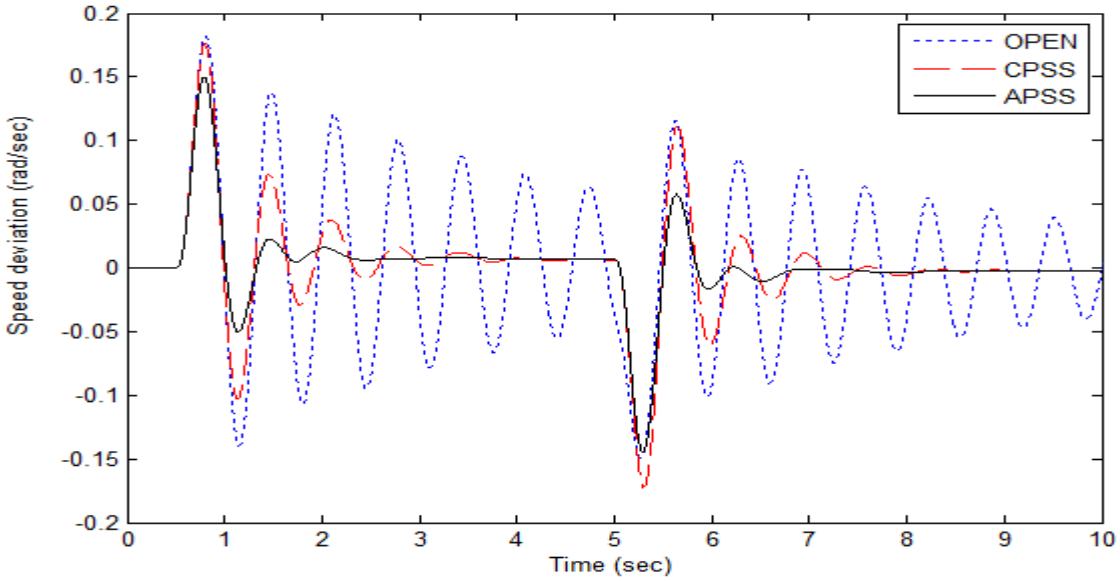

Fig.6.6 Speed deviation of the SCG in response to 0.2 p.u step increase in the mechanical torque under normal operating condition P = 0.7 p.u, pf =0.9 lag and return to original condition at 5 s

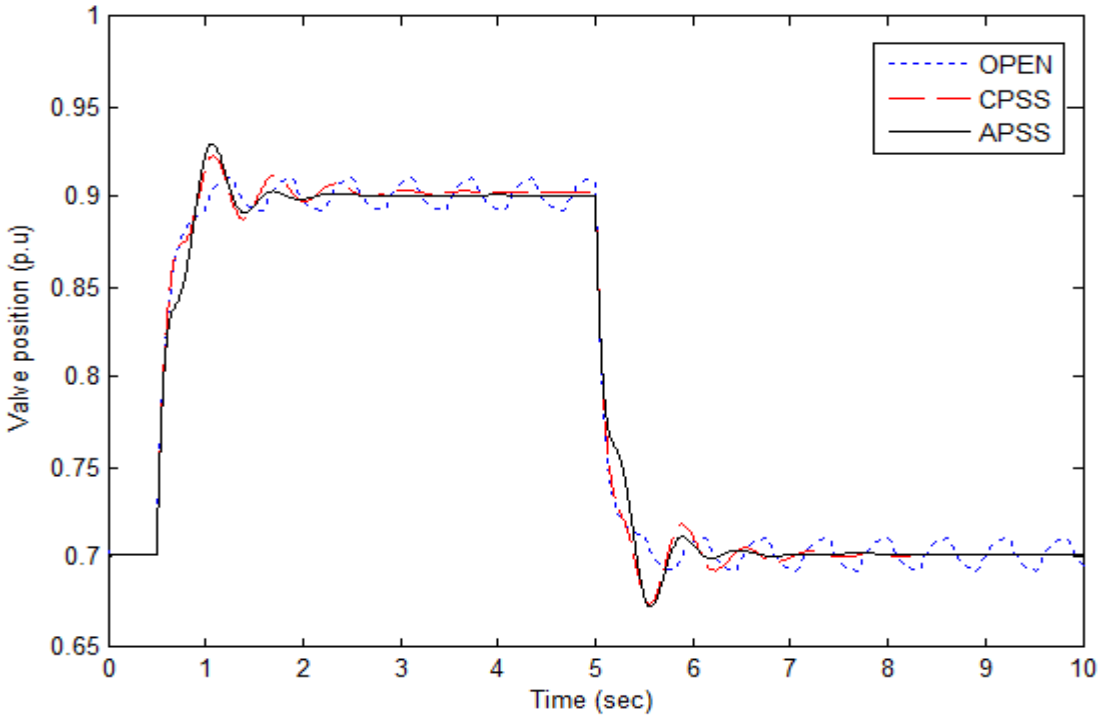

Fig.6.7 Position of the valve of electro-hydraulic governor in response to 0.2 p.u step increase in the mechanical torque under the normal operating condition P = 0.7 p.u, pf =0.9 lag and return to original condition at 5 s

6.4 Voltage reference test

In this test, the terminal voltage reference of the SCG was increased by 0.2 p.u while the generator was operating at P = 0.7 p.u , pf = 0.85 lag. The response of the speed deviation and rotor angle are shown in Figs. 6.8 and 6.9, respectively. It can be seen from Fig. 6.8 that the peak over-shoot with APSS is -0.46 p.u vs -0.5 p.u with CPSS and with the subsquent swing the peak over-shoot is much smaller than with CPSS. Also, the settling time of APSS is 3s where as 4s with the CPSS.

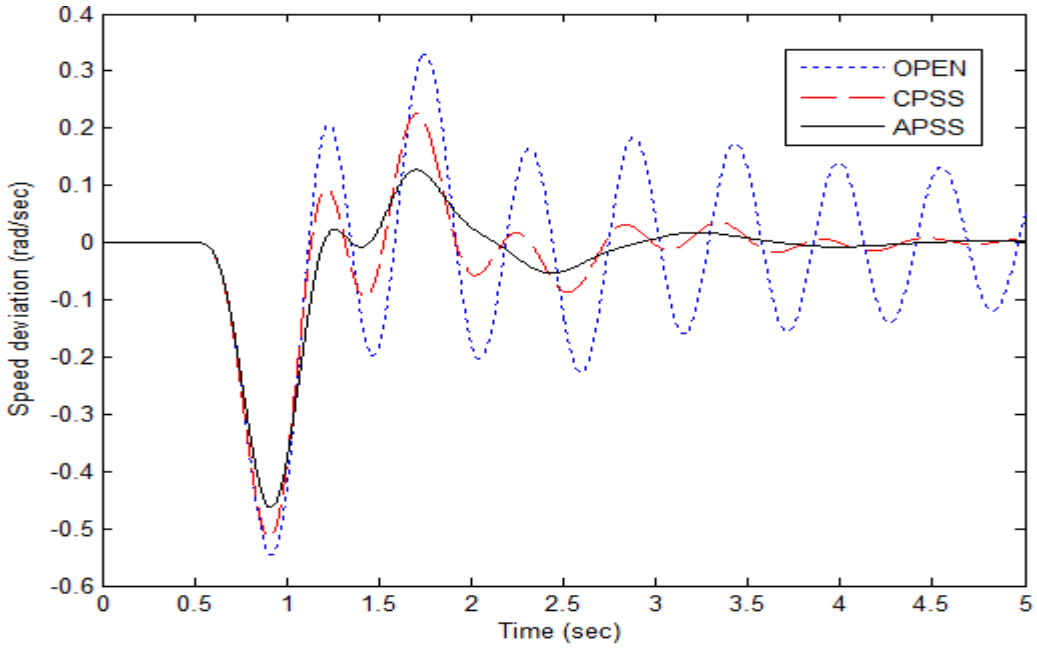

Fig.6.8 Generator speed deviation in response to a 0.2 p.u step increase in the terminal voltage reference

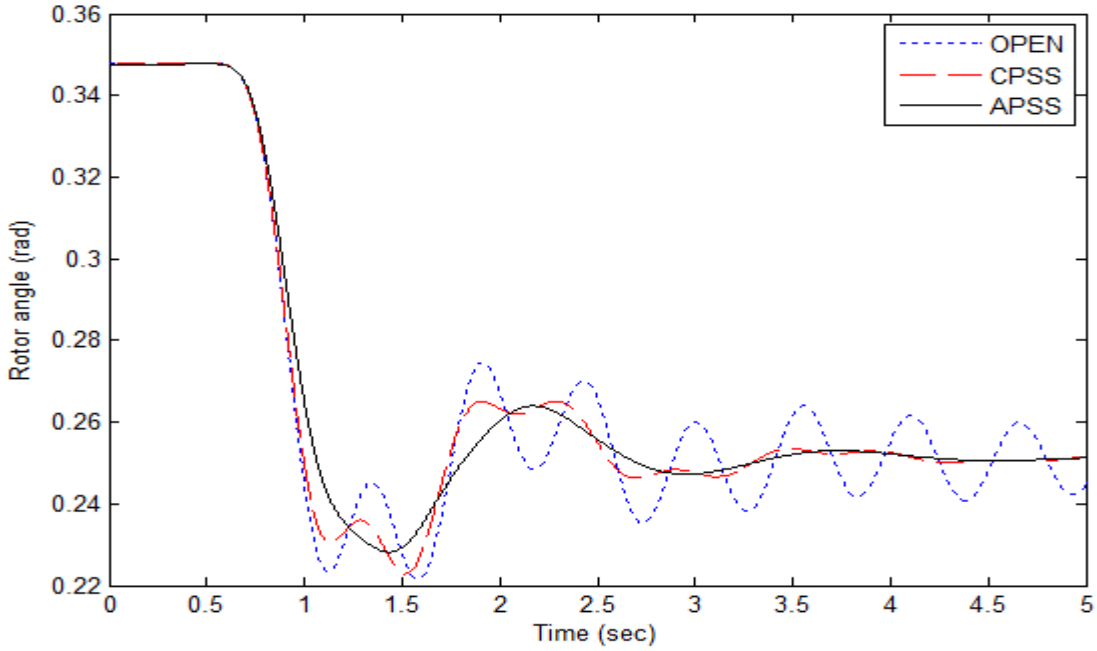

Fig.6.9 Rotor angle in response to a 0.2 p.u step increase in the reference terminal voltage

6.5 Light load condition

In this experiment, the system was operating under light load condition at P = 0.3 p.u, pf = 0.85 lag. A 0.2 p.u step increase in the intial mechnical torque was applied. The responses of the system are shown in Figs. 6.10 and 6.11. It can be seen from Fig. 6.10 that within the first swing the APSS damps out the oscillations very quickly, the peak over-shoot of the oscillation is 0.1 p.u lesser than with OPEN or CPSS. Also, it can be seen from Fig. 6.11 that the position of the valve was controlled very quickly within 1.5 s with the help of the APSS whereas it was 2.2 s with the CPSS. The very fast response of electro-hyrdualic governor with the help of the APSS helps in controlling the mechanical power faster than CPSS without any manual interventions like tuning the parameters. It can be concluded from the results that the adaptive controller damps out the oscillations in light load conditions effectively.

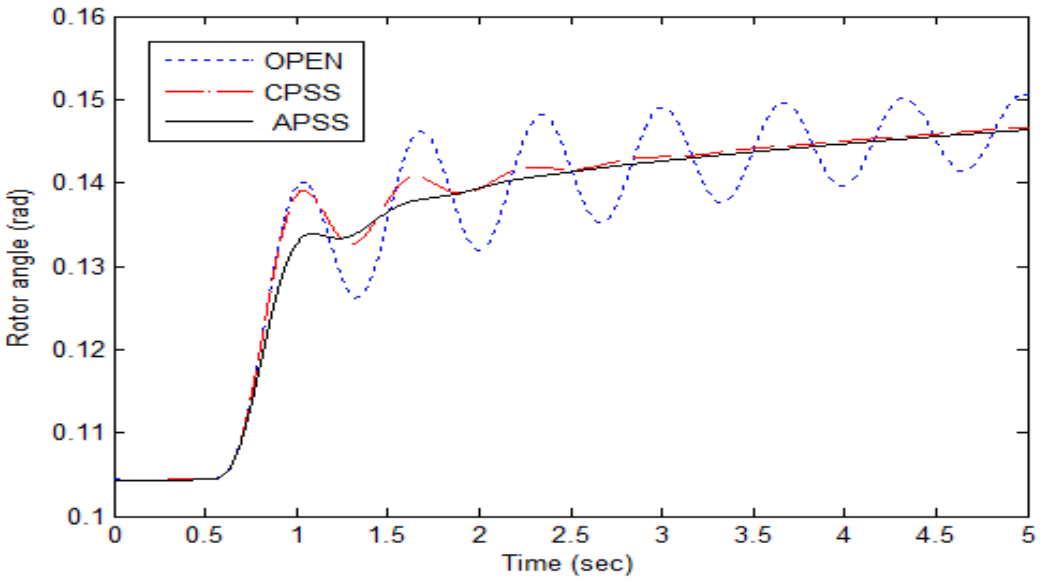

Fig 6.10 Rotor angle of the generator under a light load condition in response to a 0.2 p.u step increase in the mechanical torque

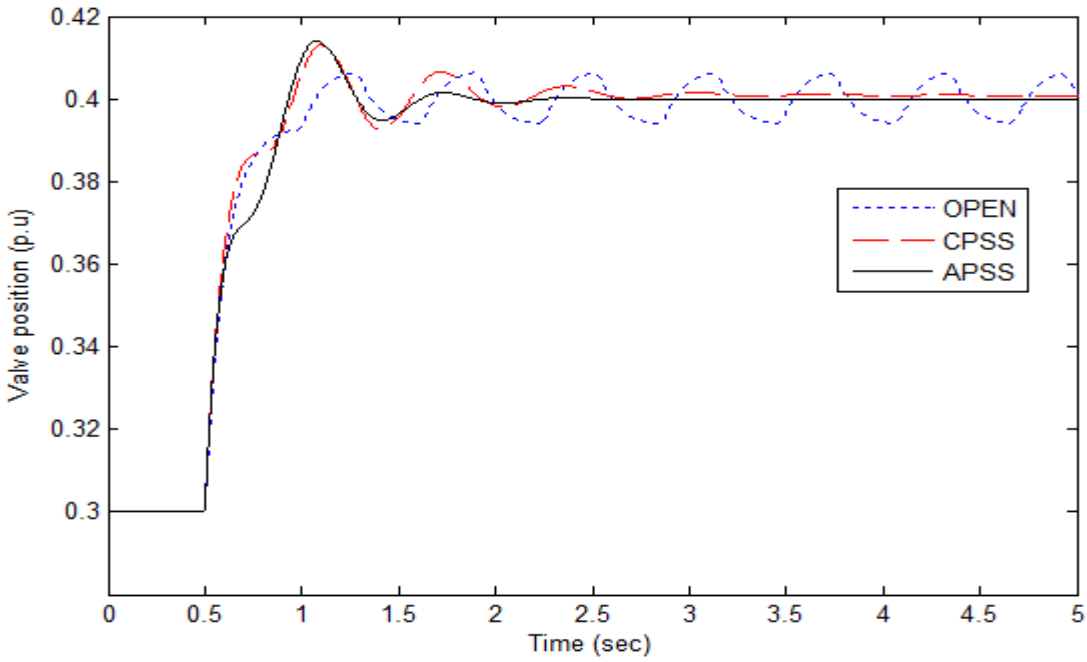

Fig.6.11 Position of the valve in response to light load condition 0.2 p.u step increase in mechanical torque

6.6 Leading power factor condition

In power systems sometimes the current leads the applied voltage due to the capacitive load. It is necessary to test under this condition to know the ability of the APSS to damp the oscillations during the leading power factor condition. Apparently, it is an extremely difficult situation for the controller to act as the stability margin has been reduced. Two cases carried out to know its effectiveness are given below.

Case 1:

The SCG was operated at P = 0.3 p.u, pf = 0.85 lead, and a step increase of 0.1 p.u of initial mechanical torque was applied at 0.5 s. The results are shown in Figs. 6.12 through 6.15. It can be seen from Figs. 6.12 and 6.13 that the peak over-shoot of the oscillation with the APSS

is much smaller than with OPEN or CPSS, and it damps the oscillation within the first swing. Also, it can be seen from Fig. 6.14 that the governor with the APSS acts fast within 1.8 s but it was 2.2 s with the CPSS.

Case 2:

The SCG was operated at P = 0.5 p.u, pf = 0.9 lead. A step increase of 0.2 p.u of initial mechanical torque was applied at 0.5 s and removed at 7s. The results shown in Figs. 6.16 through 6.18 illustrate the effectiveness of the APSS to damp oscillations during the leading power factor conditions.

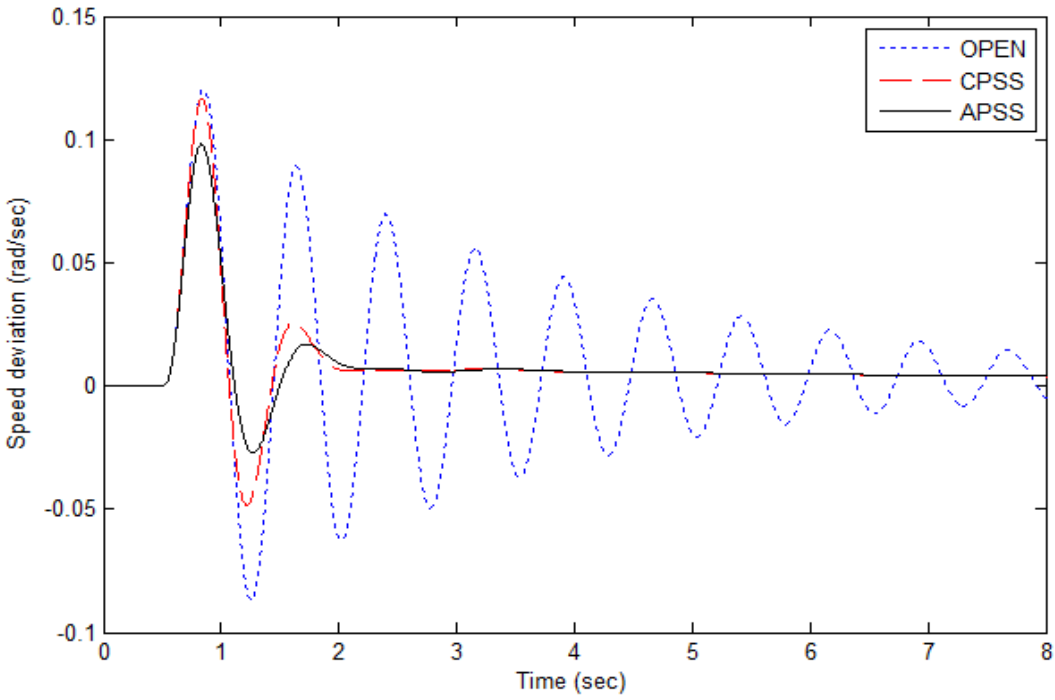

Fig. 6.12 Speed deviaiton of the SCG at P = 0.3 p.u, pf = 0.85 lead in response to a 0.1 p.u step increase in intial mechanical torque at 0.5s.

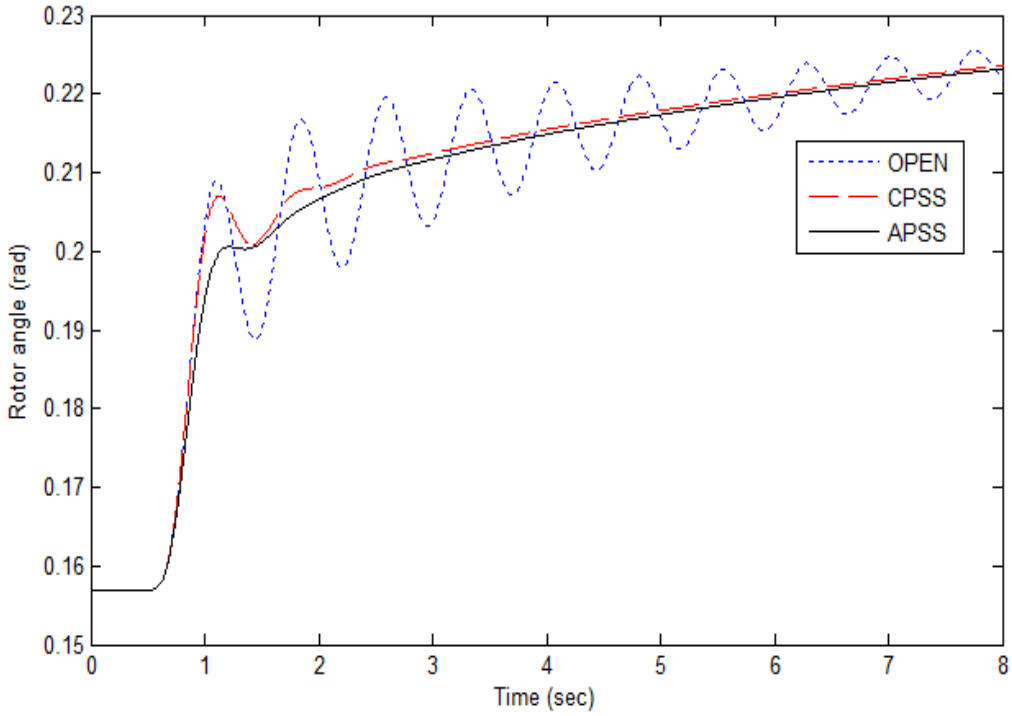

Fig.6.13 Rotor angle of the SCG at P = 0.3 p.u, pf = 0.85 lead in response to a 0.1 p.u step increase in intial mechanical torque at 0.5s.

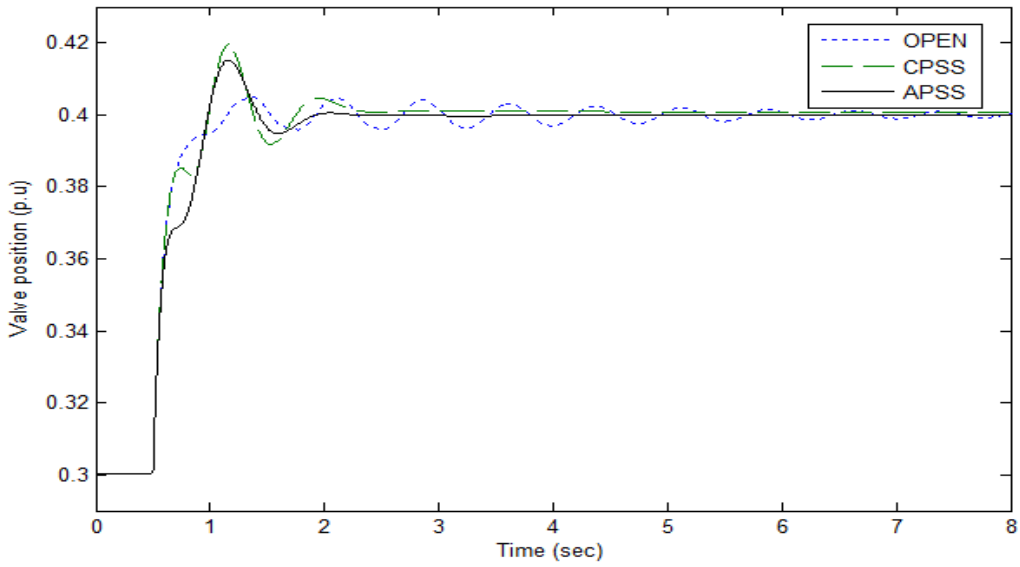

Fig.6.14 Position of the governor valve at P = 0.3 p.u, 0.85 lead in response to a 0.1 p.u step increase in intial mechanical torque at 0.5

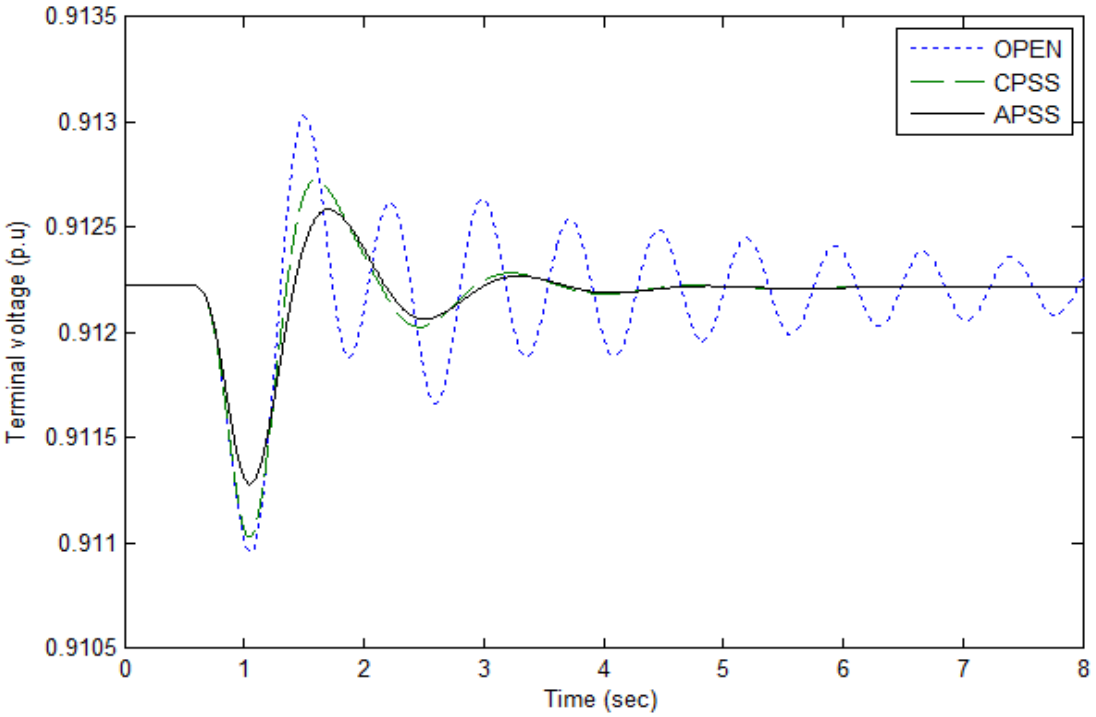

Fig.6.15 Terminal voltage of the SCG at P = 0.3 p.u, 0.85 lead in response to a 0.1 p.u step increase in intial mechanical torque at 0.5 s

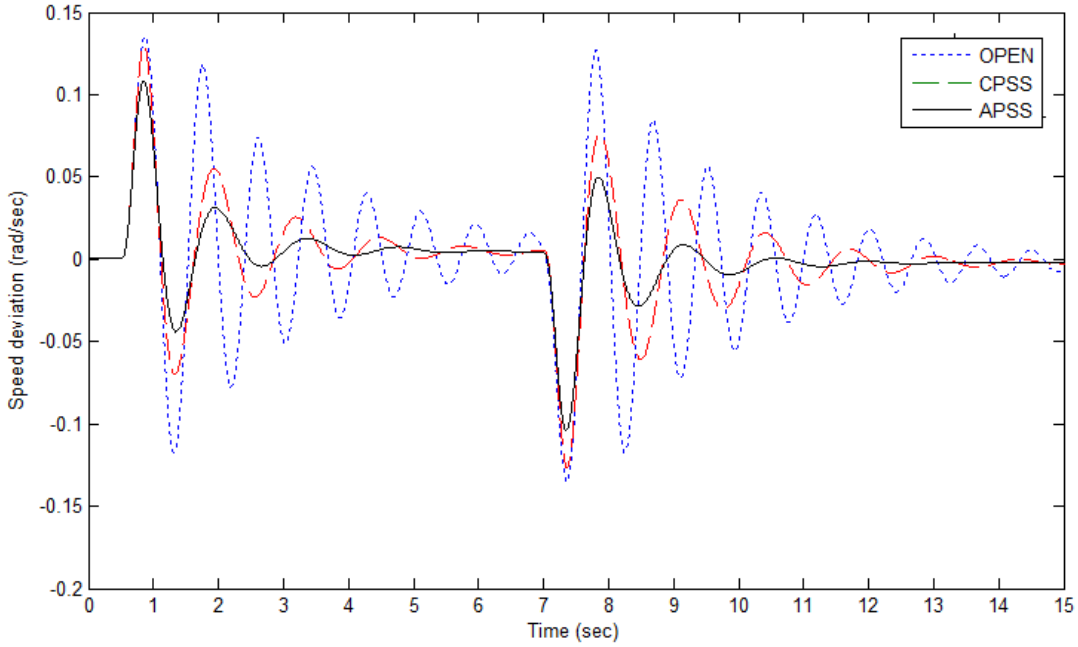

Fig.6.16 Speed deviaiton of the SCG at P = 0.5 p.u, pf = 0.9 lead in response to a 0.2 p.u step increase in intial mechanical torque at 0.5 s and return to the original condition

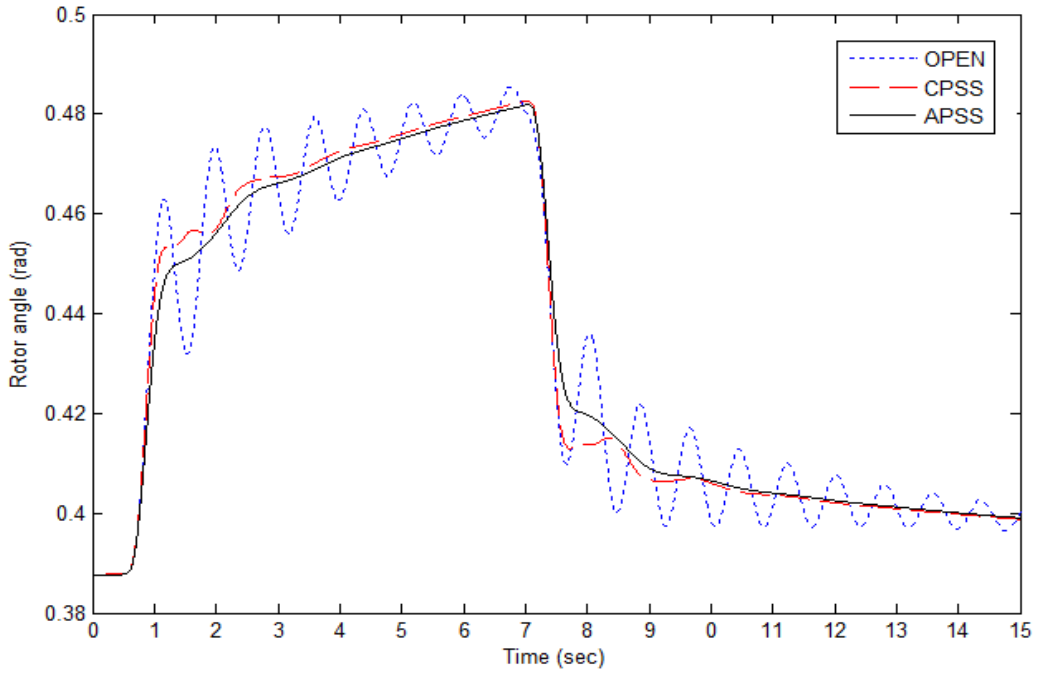

Fig.6.17 Rotor angle of the SCG at P = 0.5 p.u, pf = 0.9 lead in response to a 0.2 p.u step increase in intial mechanical torque at 0.5 s and return to the original condition

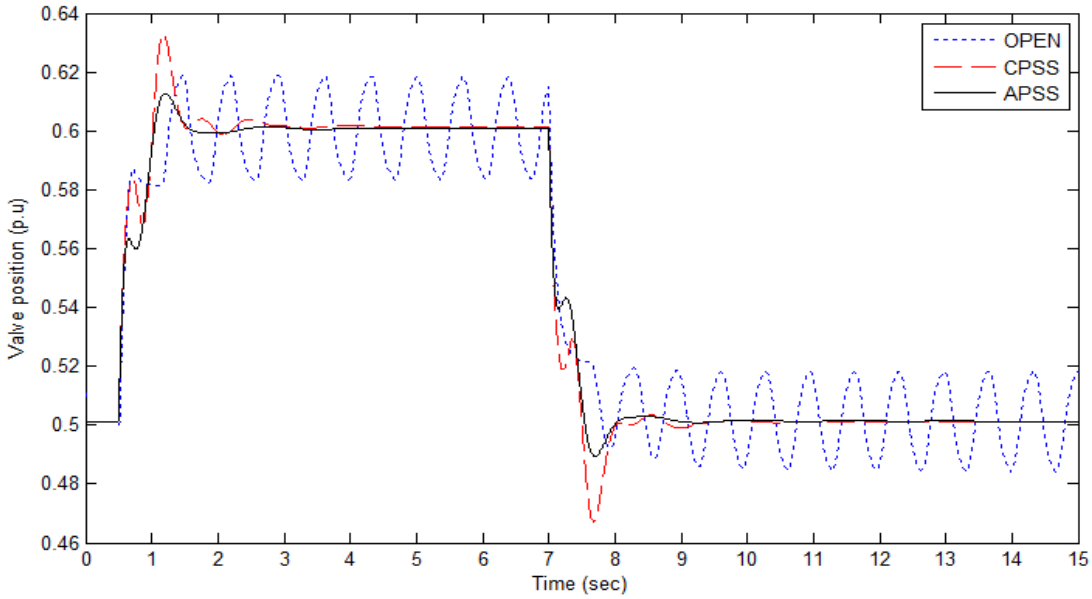

Fig.6.18 Valve position of the SCG at P = 0.5 p.u, pf = 0.9 lead in response to a 0.2 p.u step increase in intial mechanical torque at 0.5 s and return to the original condition

6.7 Three phase short circuit test

Short circuit faults occur quite commonly in power systems and it is considered to be one of the severe ones among different types of short circuits. In order to verify the performance of the controller, a three phase short circuit is applied on one of the transmission lines connecting the generator to the infinite bus in the system as shown in Fig. 6.1. The initial operating conditions are P = 0.7 p.u, pf = 0.85 lag. The fault occurs at 0.5s, cleared at 50 ms with the use of circuit breakers at both ends.

The responses of the system are shown in Figs. 6.19 through 6.21. It can be seen from Fig. 6.19 that the peak over-shoot of the oscillation with APSS within the first swing is much shorter than with the CPSS and it damps out the oscillation within 2 s. Also, it can be seen from Fig. 6.20 that the position of the valve is stretched out to the maximum when there is no control. However, with the help of APSS the response of the governor has been improved and it reacts faster than CPSS within 1.8 s. The terminal voltage of the SCG during the three phase fault is shown in Fig. 6.21. It can be seen that, with the help of the APSS, the terminal voltage is restored back to its actual value much faster than with CPSS or OPEN. From these results, the effectiveness of the controller is verified to damp the oscillations during a three phase fault.

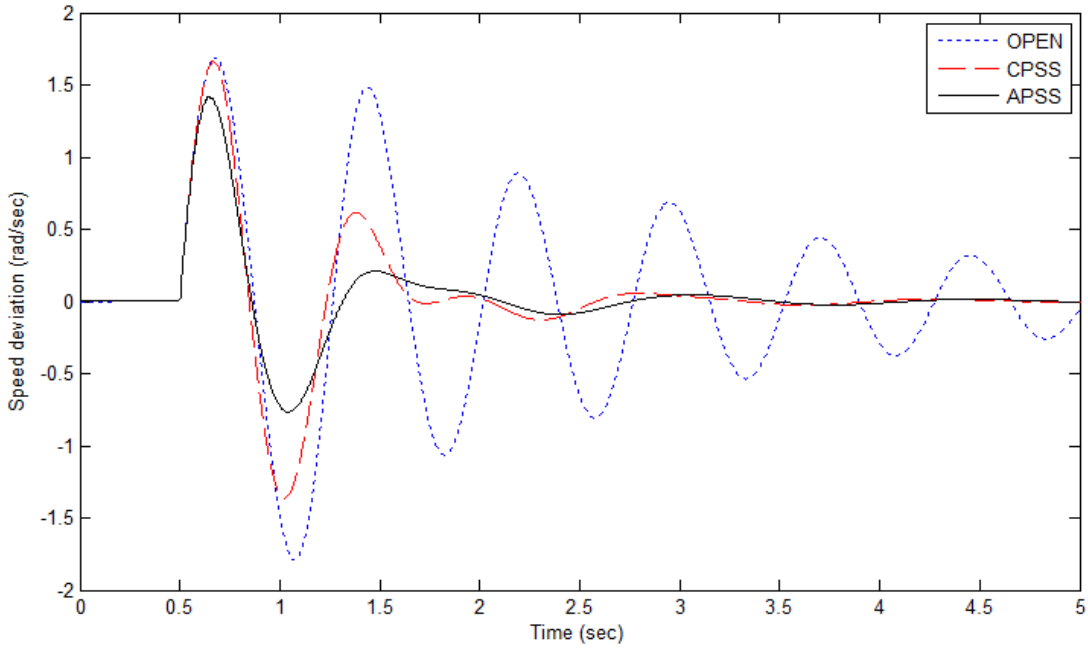

Fig. 6.19 Speed deviaiton of the SCG in response to a three phase short circuit test at P = 0.7 p.u , pf = 0.85 lag

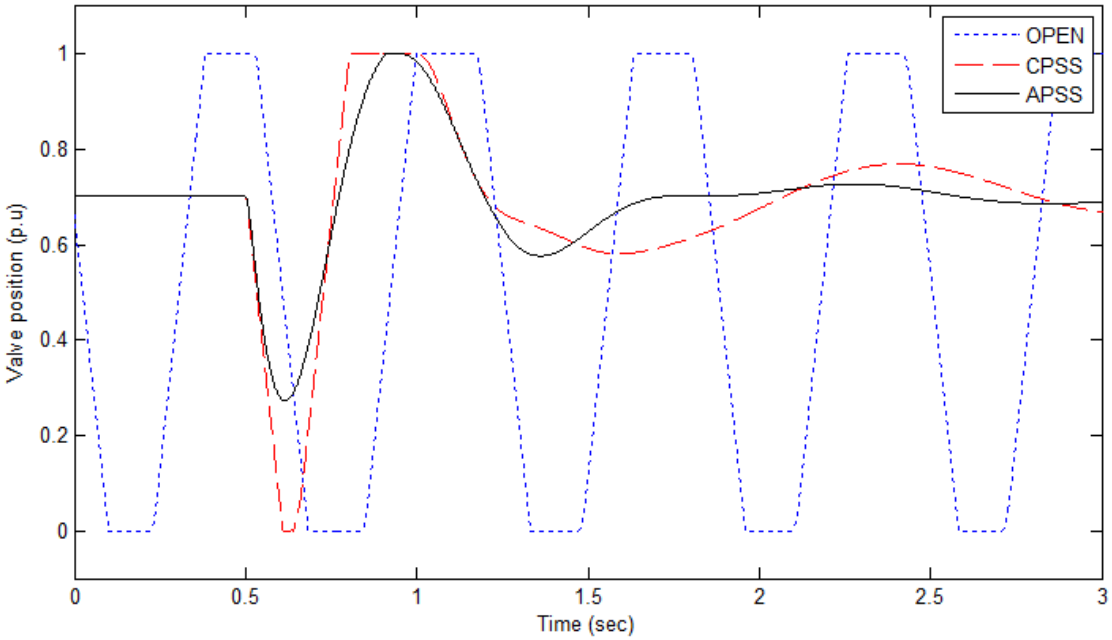

Fig.6.20 Position of the electro-hydraulic governor valve in response to a three phase short circuti test at P = 0.7 p.u, pf = 0.85 lag

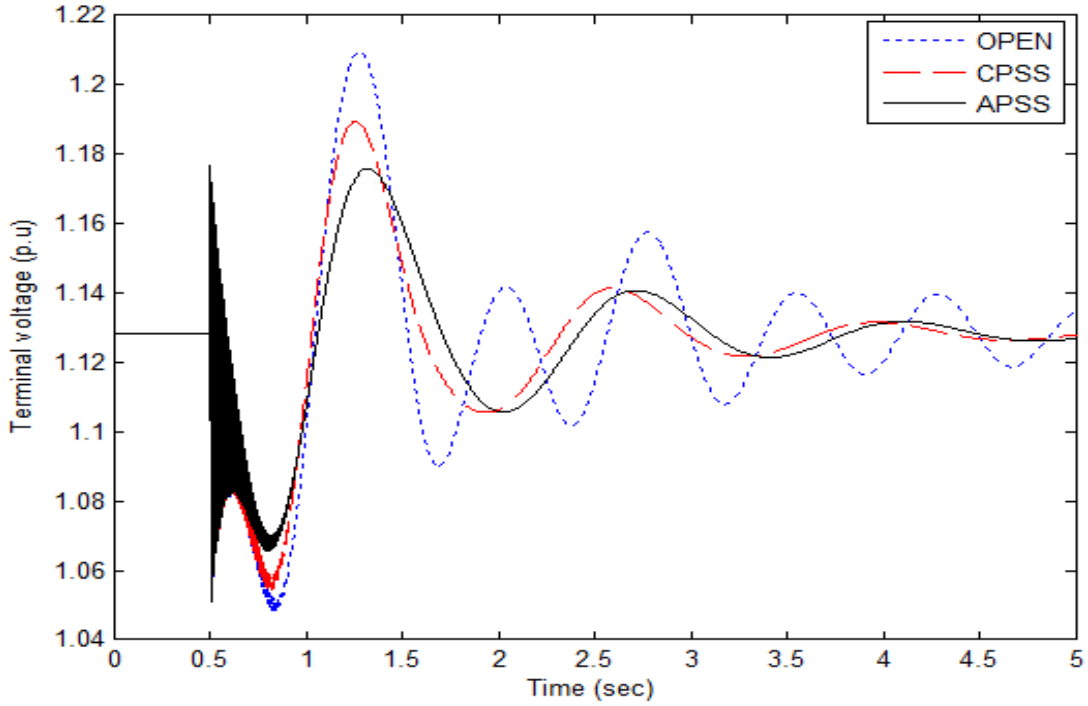

Fig.6.21 Terminal voltage of SCG in response to a three phase short circuit test at P = 0.7 p.u , pf = 0.85 lag

6.8 Three phase short circuit test with successful reclosure

In this test, a three phase short circuit takes place when P = 0.9 p.u, pf =0.9 lag, at 0.5 s and is cleared after 50 ms by opening the circuit breaker. The line is then connected back successfully at 7s. The results given in Fig.6.22 show that the APSS, provides more effective performance than the CPSS in damping the oscillations.

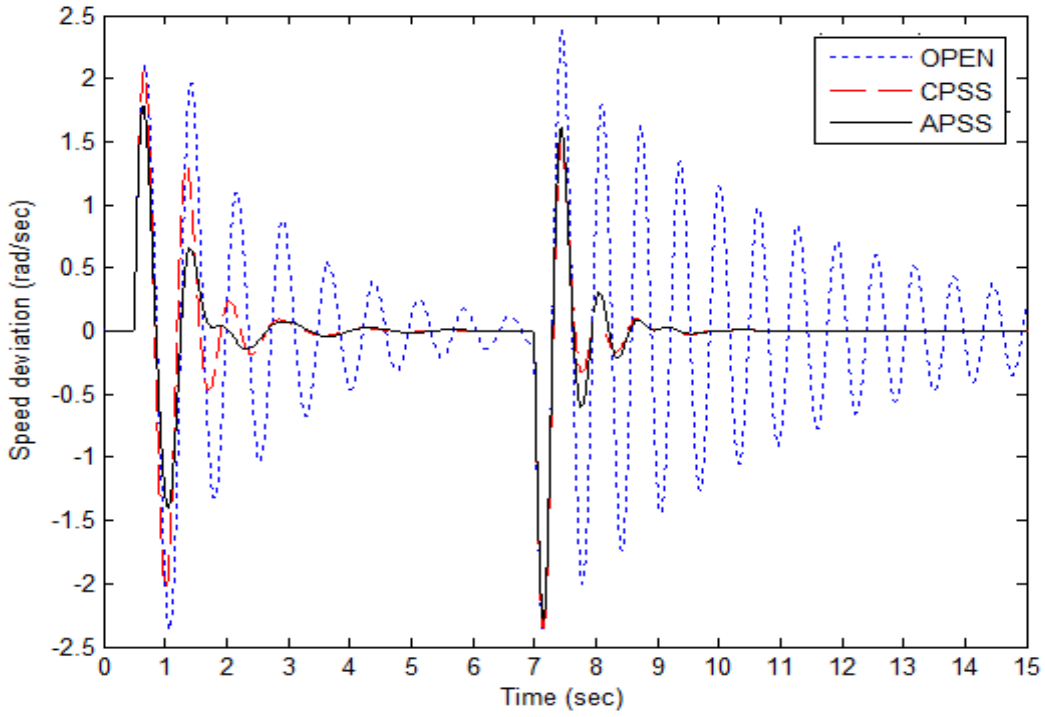

Fig.6.22 Speed deviaiton of the SCG at P = 0.9 p.u, pf = 0.8 lag in response to three phase short circuit fault at the middle of a transmission line and with succesful reclosure

6.9 Performance of the controller at slower, higher frequency, and with white noise

In this experiment, with the SCG operating at normal operating condition P = 0.7 p.u, pf = 0.85 lag, a 0.1 p.u step increase of initial mechanical torque was applied at 0.5 s. The studies were carried out by comparing the response of speed deviation with CPSS, and APSS for 10 Hz, 20 Hz, 50 Hz, and 100 Hz respectively without and with white noise are shown in Fig 6.23 to Fig 6.29. A simple low pass filter is added before the PSS signal as low frequency is the only concern.

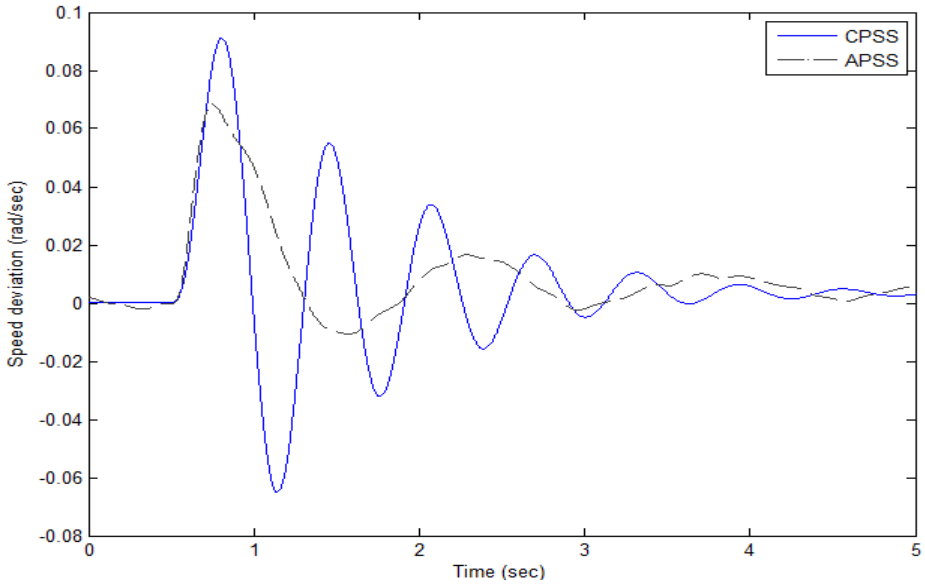

Fig 6.23 Speed deviation of the SCG in response to a 0.1 p.u step increase in the mechanical torque under normal operating condition P = 0.7 p.u, pf =0.85 lag, 10 Hz, without white noise

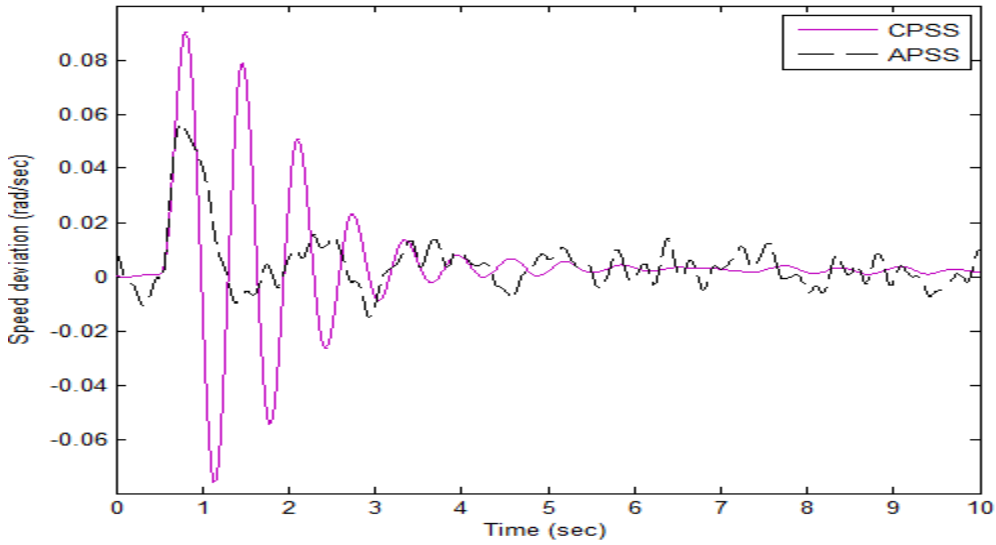

Fig 6.24 Speed deviation of the SCG in response to a 0.1 p.u step increase in the mechanical torque under normal operating condition P = 0.7 p.u, pf =0.85 lag, 10 Hz, with white noise

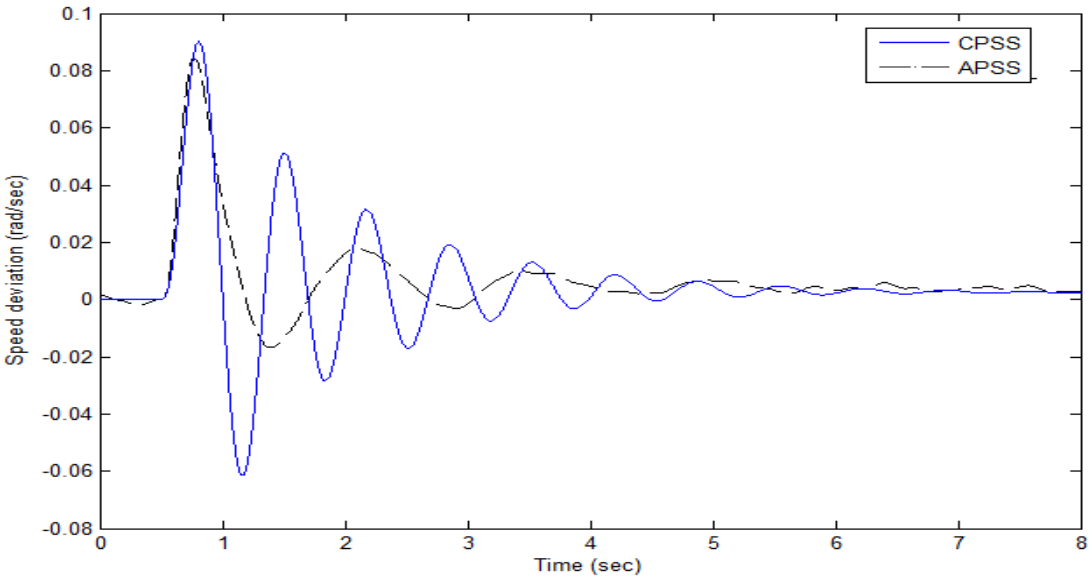

Fig 6.25 Speed deviation of the SCG in response to a 0.1 p.u step increase in the mechanical torque under normal operating condition P = 0.7 p.u, pf =0.85 lag, 50 Hz, without white noise

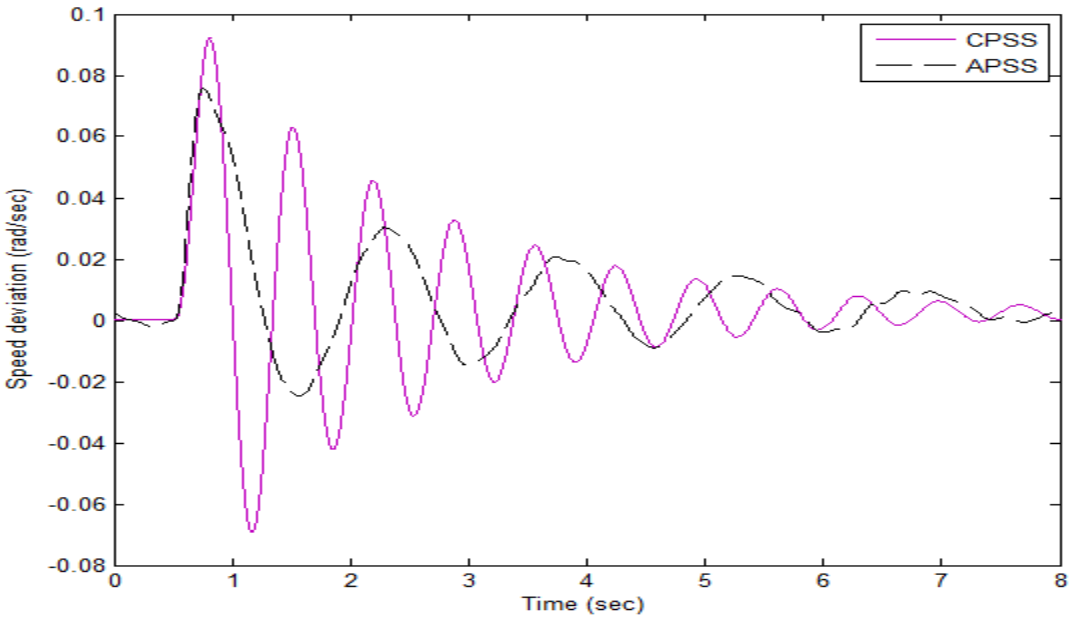

Fig 6.26 Speed deviation of the SCG in response to a 0.1 p.u step increase in the mechanical torque under normal operating condition P = 0.7 p.u, pf =0.85 lag, 100 Hz, without white noise

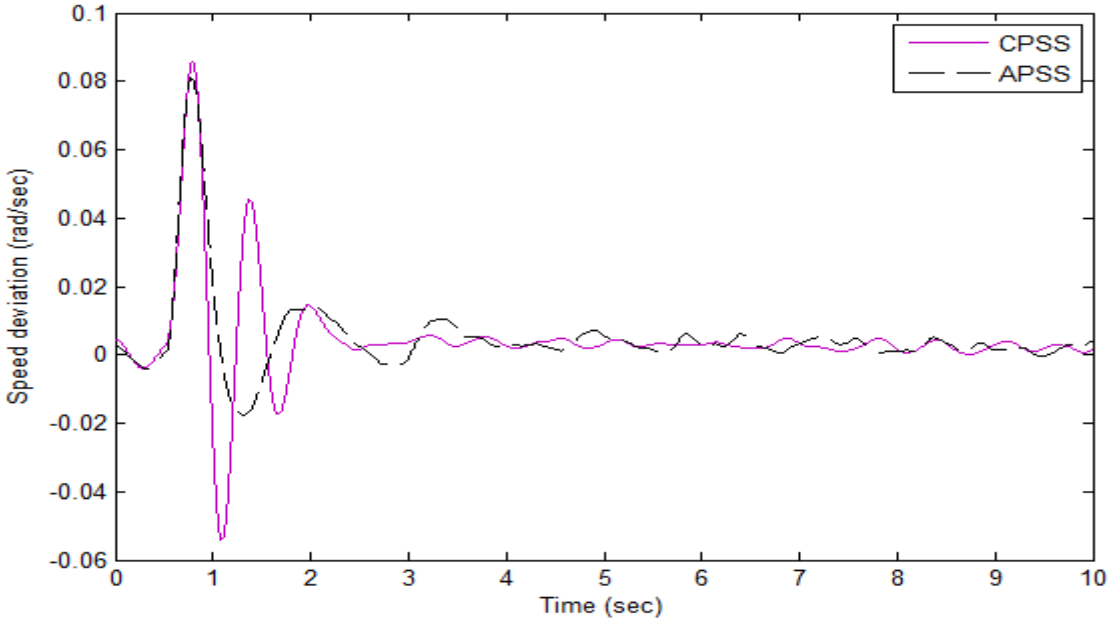

Fig 6.27 Speed deviation of the SCG in response to a 0.1 p.u step increase in the mechanical torque under normal operating condition P = 0.7 p.u, pf =0.85 lag, 20 Hz, with white noise

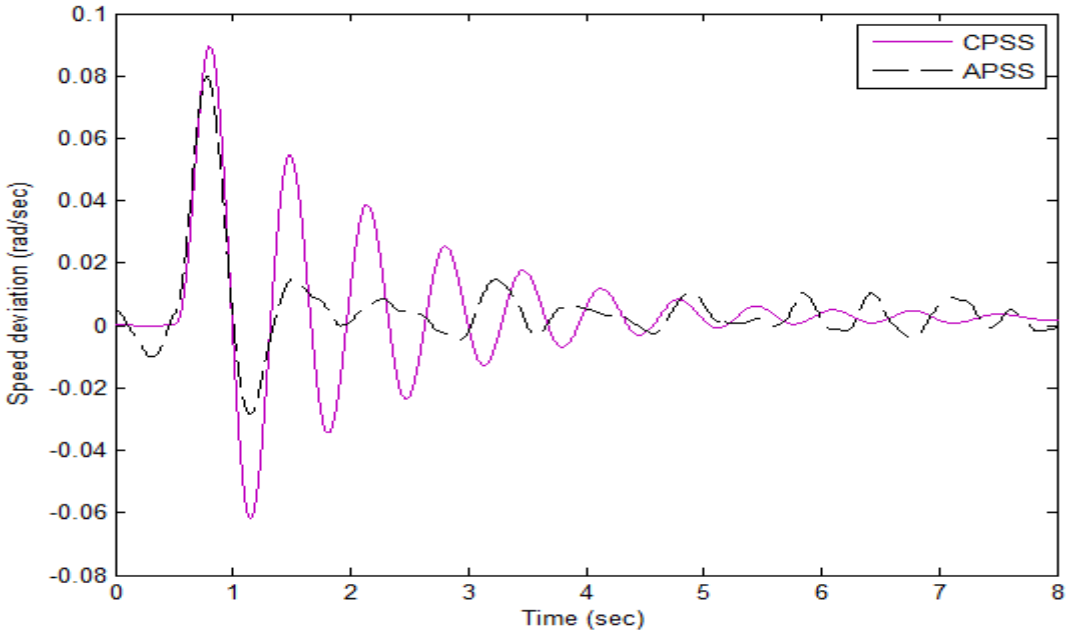

Fig 6.28 Speed deviation of the SCG in response to a 0.1 p.u step increase in the mechanical torque under normal operating condition P = 0.7 p.u, pf =0.85 lag, 50 Hz, with white noise

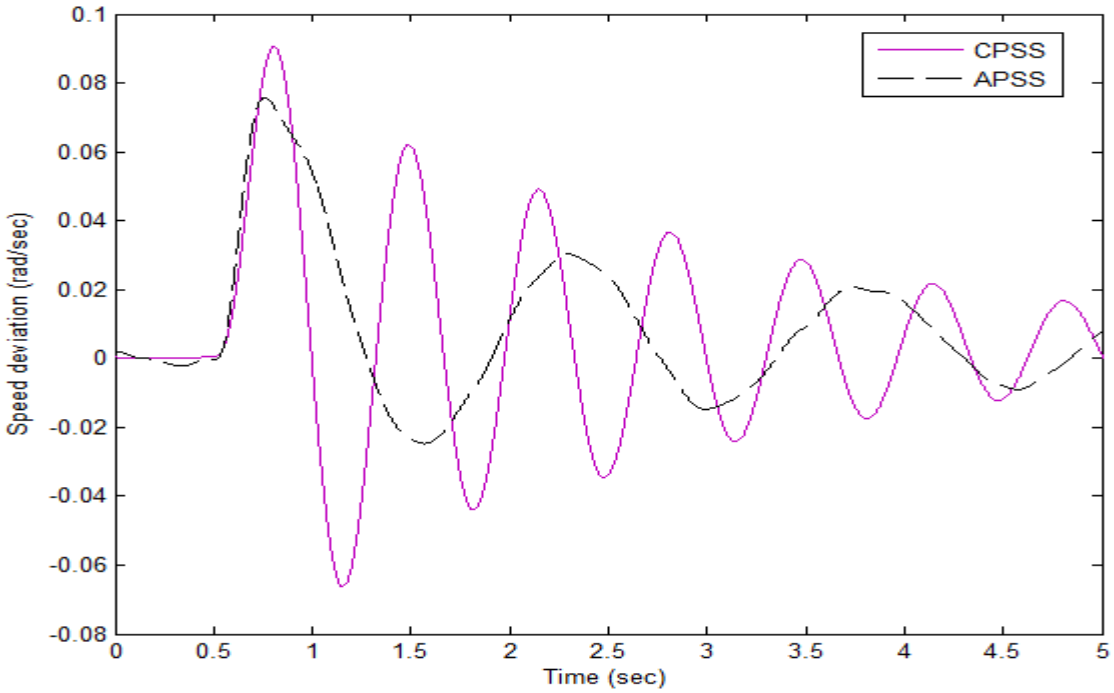

Fig 6.29 Speed deviation of the SCG in response to a 0.1 p.u step increase in the mechanical torque under normal operating condition P = 0.7 p.u, pf =0.85 lag, 100 Hz, with white noise

6.10 Stability test

In this experiment, the input mechanical torque applied to the SCG without any supplementary control, with CPSS and with APSS is increased at the rate of 0.05 p.u per second with the initial P = 1.6 p.u, pf = 0.9 lag until the system lost its stability. The results are shown in Fig. 6.23.The mechanical torque values for different types of control when the system lost stability are given in Table 6.1. From the results, the stability margin of SCG with an APSS is greater than with CPSS, and without any supplementary control.

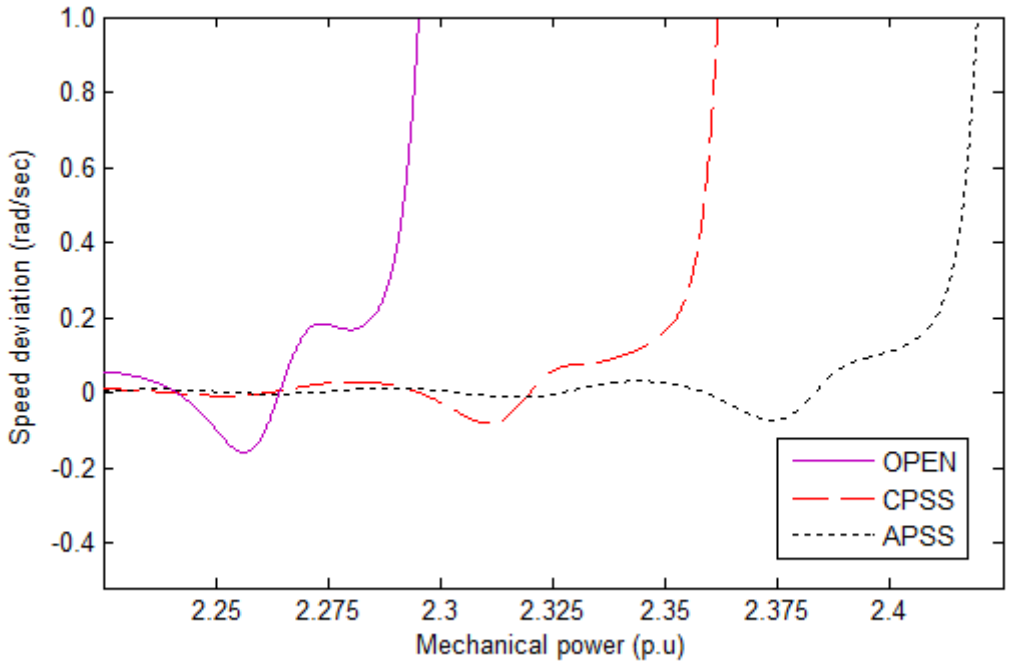

Fig. 6.30 Speed deviation of SCG at P = 1.6 p.u, pf = 0.9 lag in response to a increase in mechanical torque at the rate of 0.05 p.u per second

Types of control	OPEN	CPSS	APSS
Mechanical Torque (p.u)	2.275	2.35	2.4

Table 6.1 Mechanical torque values for different types of control when the system lost it stability

6.11 Summary of the chapter

The Performance of the indirect adaptive controller applied to the electro-hydraulic governor of the SCG with a three stage turbine connected to an infinite bus through a transmission line has been tested. The results obtained from the simulation studies show that the adaptive controller, not designed for any particular operating condition, gives good performance at any operating condition, fault conditions like 3 phase fault, and lagging or leading load without any manual tuning of its parameters. It offers higher stability margin and improved system stability than the CPSS. The linear feedback adaptive controller, tested here for the SCG, can be used for thermal based power plants like coal, co-generation, nuclear, and for a micro hydro.

Chapter Seven: Conclusions and recommendations for future work

Electric power systems have evolved with many changes in the recent past. Problems associated with the stability and control of conventional synchronous generators for power generation have been identified and successfully solved with the help of a PSS as a supplementary excitation controller. Extensive work has been done on the CPSS to improve the performance [12, 23, 39, 40, 42, and 47].

As energy needs keep on growing throughout the world, power producers who engage in business in deregulated markets like Alberta ISO, California ISO, and New York ISO are looking for higher efficiency, higher stability. The synchronous superconducting generator is a possible solution as it offers many potential advantages over the conventional machines for power generation such as improved steady state stability, better efficiency, less emissions, lower losses, smaller size and rating even beyond 2000 MVA possible. Despite the above advantages of SCG, the enhancement of power systems stability and control of SCG is a challenging task.

In early attempts investigators have proposed many methods to control the SCG to enhance power systems stability. Among so many techniques the excitation and governor control have gained importance because of their performance in damping the oscillations. However, the excitation control of SCG is ineffective due to the long-time constant of field winding and shielding effects of the rotor screen. Hence, the governor control becomes the only possible way to enhance the power system stability of SCG. The availability of fast valving and the electro-

hydraulic governor made it very effective in damping the power systems oscillations. However, the CPSS cannot provide good performance over wide operating conditions.

7.1 Conclusions

The simulation studies carried out show that the supplementary signal provided by the pole shift based adaptive controller to the electro-hydraulic governor can improve the stability effectively during the disturbances and it can be implemented in real time. On the other hand, artificial intelligence techniques are too complex to implement in real time because of unknown information on internal working. Here some of the issues that are focussed on in this dissertation are listed.

- Due to the ineffective nature of the excitation loop of SCG, the APSS was applied on the governor loop to damp the low frequency oscillations. The fast valving of electro –hydraulic governor helped further to obtain the quick response to enhance the stability.
- In real time, simpler controllers are easy to implement. So, the attention was focussed on the online based identifiers to estimate the parameters of the plant and the linear feedback PS control for the controller.
- Parameters of the plant are estimated online with the help of RLS with a variable forgetting factor, and Kalman estimator. A comparison between the two identification techniques shows that both algorithms are good in estimating the parameters of the plant. Preference is given to the RLS based variable forgetting factor identification technique because of its shorter convergence time.

- The variable pole shift algorithm with a variable pole shift factor is used for the controller. It adapts and self-searches the pole shift factor according to the operating condition to calculate the control signal. Unlike the CPSS, there is no need of manual intervention to tune its parameters. To the best of the author's knowledge this is the first attempt in the application of variable PS based adaptive power systems stabilizer to the electro-hydraulic governor of SCG with a three stage turbine, when exciter is in operation, with online system identification.

- To verify the effectiveness of the governor based adaptive power system stabilizer in a single machine infinite bus system, a ninth order generator model is used to represent the SCG connected to an infinite bus through a transmission line. Simulation studies were carried out for different operating conditions and the simulation results show that the pole shift based adaptive controller damps the low frequency oscillations very effectively to improve the stability of the system.

7.2 Future work and recommendations

In this thesis, the adaptive based governor control of SCG has been studied for power system stabilization. Based on this, the following topics are recommended for further research.

- The dynamics of the boiler (steam) is kept constant throughout the thesis. It can be modeled with nonlinear dynamics and the effectiveness of the governor control can be verified.
- The RLS with a variable forgetting factor was used to identify the parameters of the systems to update the variable PS controller. In recent years, techniques based on neural networks

have been developed. So any neural network based algorithm can be used to estimate the parameters of the plant as well as for the controller to know its effectiveness.

- The speed deviation of the generator, $\Delta\omega$, was used for the feedback signal to the stabilizer. Other signals, like acceleration, electric power, can be investigated.

REFERENCES

[1] "International Energy Outlook, September 2011", US Energy information (EIA) report DOE/EIA-0484 (2011), http://www.eia.gov/forecasts/ieo/pdf/0484(2011).pdf, Accessed on Jan, 2012.

[2] "US Department of energy report on smart grid, 2009", http://energy.gov/oe/technology-development/smart-grid, Accessed on Feb, 2012.

[3] Kalsi Swarn Singh, "*Applications of High temperature superconductors to electric power equipment*", Wiley- IEEE Press, 2011.

[4] "International Energy Agency, Energy statistics and balances of non –OECD countries energy statistics of OECD countries and United Nations, Energy Statistics Yearbook", http://www.iea.org/stats/index.asp, Accessed on Feb, 2012.

[5] Guohong Wu, Sakamoto.O, Nitta.T, Yokoyama.A, Uchida.N, "Increase of power transmission capacity in multi-machine power systems with introduction of superconducting generator", *Transmission and Distribution Conference and Exhibition 2002:* Asia Pacific. IEEE/PES, vol.1, 6-10, pp. 376- 381, Oct. 2002.

[6] Bumby J.R, *Superconducting rotating electrical machines*, Clarendon Press, Oxford 1983.

[7] Edmonds J, "Superconducting generator technology-an overview", *Magnetics, IEEE Transactions on*, vol.15, no.1, pp. 673- 679, Jan 1979.

[8] Parker J.H, Towne R.A, "Design of large superconducting turbine generators for electric utility Application", *Power Apparatus and Systems, IEEE Transactions on*, vol.PAS-98, no.6, pp.2241-2250, Nov. 1979.

[9] Machowski .J, Bialek J, Bumby. J, *Power Systems Dynamics and Control*, John Wiley & Sons, Oct 20, 1997.

[10] Kundur. P, *Power Systems Stability and Control*, McGraw hill, New York, 1994.

[11] Anderson P.M and Foud A.A, *Power System Control and Stability*, IEEE Press Piscataway, NJ, 1994.

[12] Tamer. A, "*Adaptive Fuzzy Logic Based Power System Stabilizer*", Department of Electrical and Computer Engineering, The University of Calgary, PhD. Dissertation, June 2005.

[13] Chan-Ki Kim, Vijay K. Sood, Gil-Soo Jang, Seong-Joo Lim, and Seok-Jin Lee, *HVDC Transmission*, John Wiley & Sons (Asia) Pte Ltd, 2009.

[14] Smed. T, Anderson. G, "Utilizing HVDC to damp power oscillations", *Power Delivery, IEEE Transactions on*, vol.8, no.2, pp.620-627, Apr 1993.

[15] Mittelstadt W.A, "Four Methods of Power System Damping", *Power Apparatus and Systems, IEEE Transactions on*, vol.PAS-87, no.5, pp.1323-1329, May 1968.

[16] Dash P.K, Puthal.B, Malik O.P, Hope G.S, "Transient stability and optimal control of parallel A.C.-D.C. power systems", *Power Apparatus and Systems, IEEE Transactions* on, vol.95, no.3, pp. 811- 820, May 1976.

[17] Narain G. Hingorani, "*Flexible AC Transmission", IEEE Spectrum*, vol.30, no.4, Apr, pp. 40-45, 1993.

[18] Cushing, E.W, Dressler G.E, Killgoar W.P, Marshall H.G, Stewart H.R, "Fast valving as an aid to power system transient stability and prompt resynchronization and rapid reload after full load rejection", *Power Apparatus and Systems, IEEE Transactions* on, vol.PAS-91, no.4, pp.1624-1636, July 1972.

[19] Edwards L, Gregor, J. D, Osborn, D.L, Doudna J. H, Pasternack, B.M, Thompson W.G, "Turbine fast valving to aid system stability: benefits and other considerations", *Power Systems, IEEE Transactions on*, vol.1, no.1, pp.143-153, Feb 1986.

[20] "IEEE Guide for identification, testing, and evaluation of the dynamic performance of excitation control systems", ANSI/IEEE Std 421A-1978, vol.no, pp.0_1, 1978.

[21] McGowan D.J, Morrow D.J, Fox B, "Integrated governor control for a diesel-generating set", *Energy Conversion, IEEE Transactions on* , vol.21, no.2, pp. 476- 483, Jun 2006.

[22] Doan R.E, Natarajan.K, "Modeling and control design for governing hydroelectric turbines with leaky wicket gates", *Energy Conversion, IEEE Transactions on*, vol.19, no.2, pp. 449- 455, Jun 2004.

[23] Ramakrishna G, "*Beyond Gain-Type Scheduling Controllers" New Tools of Identification and Control for Adaptive PSS*", Ph.D. Dissertation, University of Calgary, May 2000.

[24] Larsen E.V, Swann D.A, "Applying power system stabilizers Part III: practical considerations," *Power Apparatus and Systems, IEEE Transactions on*, vol.PAS-100, no.6, pp.3034-3046, Jun 1981.

[25] Lawrenson P.J, Miller T.J.E, Stephenson J.M, Ula A.H.M.S, "Damping and screening in the synchronous superconducting generator", *Electrical Engineers, Proceedings of the Institution of*, vol.123, no.8, pp.787-794, Aug 1976.

[26] Takao.T, Tsukamoto.O, Hirao.T, Morita.M, Ikeda.B, "Quench characteristics of rotor winding of superconducting generator in static and rotating conditions", *Magnetics, IEEE Transactions* on, vol.32, no.4, pp.2365-2368, Jul 1996.

[27] Mbaruku A, "*Electromechanical and fatigue properties of as manufactured and quench damaged YBCO coated conductor*", Ph.D. thesis, Florida State University – 2006.

[28] Nitta T, Shirai Y, Okada T, Imai Y, Kobayashi Y, "High response excitation control of superconducting generator for stability of superconducting field winding", A*pplied Superconductivity, IEEE Transactions on*, vol.10, no.1, pp.935-938, Mar 2000.

[29] Shirato.H, Guohong Wu, Oikawa.S, Sisido.H, "Investigation of power system stability enhancement by superconducting generator with high response excitation considering its detailed excitation system", *POWERCON, 2010 International Conference*, pp.1-6, 24-28, Oct 2010.

[30] Paul N. Barnes, Michael D. Sumption, Gregory L. Rhoads, "Review of high power density superconducting generators: present state and prospects for incorporating YBCO windings", *Cryogenics vol. 45, Issues 10–11,* pp.670–686, Oct–Nov 2005.

[31] Kirtley J.L, "Armature motion damping of superconducting generators", *Power Apparatus and Systems, IEEE Transactions on*, vol.PAS-100, no.6, pp.2870-2879, Jun 1981.

[32] Kirtley J.L, Jr. Furuyama M, "A design concept for large superconducting alternators resonance problems with turbine-generator components", *IEEE Power Engineering Review*, vol.PER-1, Issue 6, pp.50 – 51, 1981.

[33] Einstein T.H, "System performance characteristics of superconducting alternators for electric utility power generation", *Power Apparatus and Systems, IEEE Transactions on*, vol.94, no.2, pp.310- 319, Mar 1975.

[34] Alyan, M.A.A.S, Rahim Y.H, "The role of governor control in transient stability of super-conducting turbo-generators", IEEE Transactions on Energy Conversion, vol.EC-2, Issue 1, pp.38 – 46, 1987.

[35] Morsy G.A, Kinawy A. Osheba, S.M, "Frequency domain analysis of a superconducting generator", *Electric Power Systems Research*, vol.30, Issue 2, pp.107 – 113, 1994.

[36] Saleh, R.A.F, Bolton H.R, "Genetic algorithm-aided design of a fuzzy logic stabilizer for a superconducting generator", *Power Systems, IEEE Transactions on*, vol.15, no.4, pp.1329-1335, Nov 2000.

[37] Osheba S.M, Alyan M.A.A.S, Rahim Y.H.A, "Comparison of transient performance of superconducting and conventional generators in a multimachine system", *Generation, Transmission and Distribution, IEE Proceedings*, vol.135, no.5, pp.389-395, Sep 1988.

[38] Alyan, M.A.A.S, Rahim, Y.H, "A discrete state-space controller for superconducting turbo generators", *Energy Conversion, IEEE Transactions on*, vol.3, no.2, pp.300-304, Jun 1988.

[39] Pahalawatha N.C, Hope G.S, Malik O.P, Wong K, "Real time implementation of a MIMO adaptive power system stabiliser", *Generation, Transmission and Distribution, IEE Proceedings*, vol.137, no.3, pp.186-194, May 1990.

[40] Bin Wu, *Multi-input multi-output APSS for rotor angle stability 2008*, Ph.D. Dissertation, University of Calgary, May 2000.

[41] Ibrahim A.S, Hogg B.W, Sharaf M.M, "Self-tuning controllers for turbo generator excitation and governing systems", *Control Theory and Applications, IEE Proceedings* D , vol.136, no.5, pp. 238- 251, Sep 1989.

[42] Malik O.P, Hope G.S, Huber D.W, "Design and test results of a software based digital AVR", *Power Apparatus and Systems, IEEE Transactions on*, vol.95, no.2, pp. 634- 642, Mar 1976.

[43] R.A.F. Saleh, H.R. Bolton, "Comparison of an adaptive stabilizer and a fuzzy logic stabilizer for superconducting generator governor control", *Electric Power Systems Research*, vol.57, pp.65–71, Mar 2001.

[44] Astrom K.J, Watson W, "On self-tuning regulators", *Automatica*, vol. 9, pp.185-199, 1973.

[45] Astrom K.J, Wittenmark B, " *Adaptive Control*", Addison Wesley Publishing Company, Reading, MA, 1995.

[46] Landau I.D, "A survey of model reference adaptive techniques: theory and application", *Automatica*, vol. 10, 1974, pp. 353-379.

[47] Dr. Malik O.P, "Tutorial on enhancement of power system stability using adaptive and artificial intelligent control", *16th national power conference India*, Dec 2010.

[48] Astrom K.J, Borisson U, Ljung L, Wittenmark B, "Theory and application of self-tuning regulators", *Automatica*, vol. 13, pp.457-476, 1977.

[49] Mitsukura, Yamamoto T, Kaneda M, "A design of self-tuning PID controllers using a genetic algorithm", *American Control Conference*, vol.2 pp.1361-1365, Jun 1999

[50] Wellstead P.E, Edmunds J.M, Prager D, Zanka P, "Self-tuning pole/zero assignment regulators", *Intl. J. of Control*, vol. 30, pp. 1-26, 1979.

[51] Wellstead P.E, Prager D, Zanka P, "Pole-assignment self-tuning regulator", *Proceedings IEEE*, vol. 126, pp.781-787, 1979.

[52] Robert Schrieffer J," *Theory of Superconductivity*", Perseus Books; Revised edition, January 1, 1999.

[53] Peter J. Lee, *"Engineering Superconductivity*", Wiley-Interscience, 2001.

[54] Charles P.Poole, Charles K. Poole, Horacio A. Farach, "*Handbook of Superconductivity*", Academic Press; 1 edition, October 1999.

[55] Jeffrey W Lynn, Philip B.Allen, "*High Temperature Superconductivity*", Springer, 1990.

[56] Rainer W, "*High Temperature Superconductors: materials, properties, and applications*", Kluwer Academic Publishers, 1998.

[57] Oberhauser CJ, Kinner HR, "Some considerations in the design of a superconducting alternator", *Adv Cryogenic Eng*, pp.13:161-7, 1968.

[58] Air force applications of lightweight superconducting machinery", *Magnetics, IEEE Transactions on*, vol.13, no.1, pp.260- 268, Jan 1977.

[59] Power systems, generation, and storage in power applications of superconductivity in Japan and Germany, WTEC Panel Report, 1977, http://www.wtec.org/pdf/scpa.pdf, Accessed on March, 2012.

[60] Maki N, Yamaguchi K, Takahashi M, Shiobara R, "Development of superconducting AC generator", *Magnetics, IEEE Transactions on*, vol.24, no.2, pp.792- 795, Mar 1988.

[61] Lebov I, Shaktarin V, "High efficiency and low consumption material electrical generators", *Magnetics, IEEE Transactions on*, vol.19, no.3, pp.541- 544, May 1983.

[62] ``Corporate_Brochure_2010 from Converter team, a part of General Electric Company", http://www.converteam.com/majic/dl/4/doc/Corporate_brochure_2010/CONVERTEAM_BROCHURE_CORPORATE_2010_2.pdf, Accessed on Apr 2012.

[63] Lambrecht.D, "Status of development of superconducting AC generators", *Magnetics, IEEE Transactions on*, vol.17, no.5, pp. 1551- 1559, Sep 1981.

[64] Kumagai M, Tanaka, Watanabe Y, Sato, K, Gocho Y, "Development of Superconducting AC Generator", *Energy Conversion, IEEE Transactions on* , vol.EC-1, no.4, pp.122-129, Dec 1986.

[65] Lorch H.O, "Feasibility of turbo generator with superconducting rotor and conventional stator", *Electrical Engineers, Proceedings of the Institution of*, vol.120, no.2, pp.221-227, Feb 1973.

[66] Yamaguchi K, Maki N, Shiobara R, "Rotor design of a 1000 MW superconducting generator", *Energy Conversion, IEEE Transactions on*, vol.4, no.2, pp.244-249, Jun 1989.

[67] Ragey Saleh, *Control and Stability of Superconducting Generator*, VDM Publishing, 2010.

[68] Suryanarayana T, Bhattacharya J.L, Raju K.S.N, Durga Prasad K.A, "Development and performance testing of a 200 kVA damperless superconducting generator," *Energy Conversion, IEEE Transactions on*, vol.12, no.4, pp.330-336, Dec 1997.

[69] Dynamic Models for steam and hydro turbines in power system studies, *Power Apparatus and Systems, IEEE Transactions on*, vol.PAS-92, no.6, pp.1904-1915, Nov. 1973.

[70] Ljung L, Soderstrom T, "*Theory and Practice of Recursive Identification*", the MIT Press Cambridge, Massachusetts London, England, 1983.

[71] Bruce P. Gibbs, *Advanced Kalman Filtering, Least-squares and Modeling: A Practical Handbook*, John-Wiley, 2011.

[72] Soderstrom T,.Ljung L, Gustavsson, "A theoretical Analysis of recursive identification method", *Automatica*, Vol.14, pp.231-244, 1978.

[73] Anas Albakkar, *ADALINE network based adaptive controller for STATCOM*, M.Sc thesis, The University of Calgary, 2006.

[74] Genshiro Kitagawa, *Introduction to Time Series Modeling*, CRC Press, Apr 22, 2010.

[75] Ales Prochazka, Kingsbury, P.J.W. Payner, J.Uhlir, *Signal Analysis and Prediction*, Birkhauser, 1998.

[76] Toresten Soerstorm, "*System Identification*", Prentice hall international, 1989.

[77] Lezano R, "Independent tracking and regulation adaptive control with forgetting factor", *Automatica*, vol.18, pp.455-459, 1982.

[78] Wellstead P.E, Sanoff S.P, "Extended self-tuning algorithm", *Int. J. Control*, vol.34, No. 3, pp.433-456, 1981.

[79] Cheetham R.G, "A Turbo-Generator self-tuning voltage regulator", *Int. J. Control*, vol. 36, pp.127-142, 1982.

[80] Latawiec K., Chyra M., "On Low frequency and long-run effects in self tuning control", *Automatica*, vol.19, pp.419-424, 1983.

[81] Shi-Jie Cheng, "*A Self-Tuning Power System Stabilizer*", Ph.D. Thesis, Department of Electrical Engineering, The University of Calgary, Canada, 1986.

[82] Kalman R. E., "New approach to linear filtering and prediction problems", *Transaction of the ASME-Journal of Basic Engineering*, 82 (Series D), pp.35-45, 1960.

[83] Dasgupta K.S, "*Transmission line impedance protection using an optimal Kalman filters*", Ph.D. Dissertation, The University of Calgary, Calgary, Canada, 1984.

[84] Peterka V, "Predictor based self-tuning control system", *in proceedings of 6th IFAC Symposium on Identification and System Parameter Estimation*, Washington DC, USA, Jun 1982.

[85] Cheng, Shi-jie, Chow Y.S, Malik O.P, Hope G.S, "An Adaptive synchronous machine stabilizer," *Power Systems, IEEE Transactions on*, vol.1, no.3, pp.101-107, Aug 1986.

[86] Wael Hussaien, "*Studies on duplicate Adaptive PSS*", Department of Electrical and Computer Engineering, The University of Calgary, M.Sc Dissertation, Aug 2002

APPENDIX

A.1 Excitation system of SCG

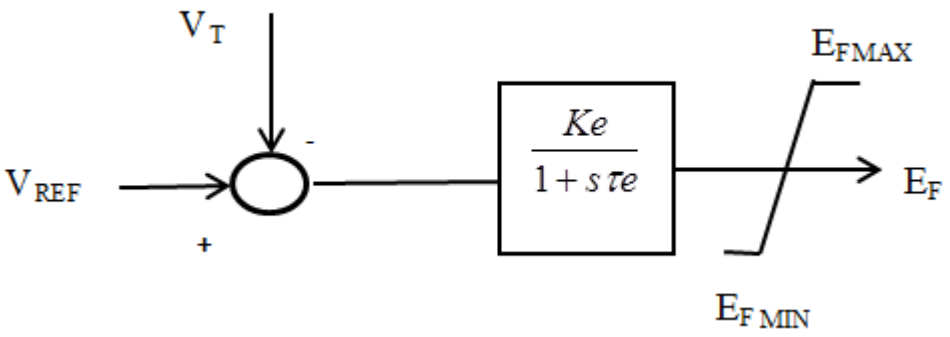

Fig.A.1 Excitation system for SCG

A.2 The conventional power systems stabilizer or the phase advance network of SCG

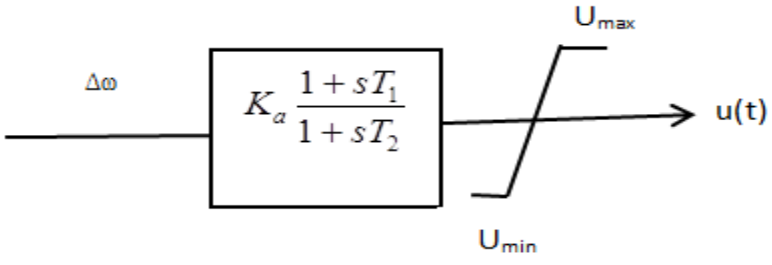

Fig.A.2 CPSS for SCG

A3. Parameters for SCG

All resistances and reactances are in p.u and time constants in seconds (s)

Superconducting Generator

$L_f = 0.541$, $L_d = L_q = 0.5435$, $L_{D1} = L_{Q1} = 0.2567$,

$L_{D2} = L_{Q2} = 0.4225$, $L_{fd} = L_{fD1} = L_{dD1} = L_{dD2} = L_{D1D2} = 0.237$,

$L_{fD2} = 0.3898$,

$L_{qQ1} = L_{qQ2} = L_{Q1Q2} = 0.237$, $\tau f = 750$, $R_d = R_q = 0.003$,

$R_{D1} = R_{Q1} = 0.01008$, $R_{D2} = R_{Q2} = 0.00134$, $H = 3$ kW s/kVA

$R_a = 0.003$

Turbine and governor of SCG

$\tau_{GM} = \tau_{GI} = 0.1$,

$\tau_{HP} = 0.1$, $\tau_{RH} = 10$, $\tau_{IP} = \tau_{LP} = 0.3$, $P_o = 1.2$ p.u,

$F_{HP} = 0.26$, $F_{IP} = 0.42$, $F_{LP} = 0.32$

Governor valve movements and constraints

$0 \leq (G_M, G_I) \leq 1$ $\quad\quad$ $-6.7 \leq (\rho_{max}, \rho_{min}) \leq 6.7$

Transmission line

$X_L = 0.2$, $R_L = 0.08$

Exciter and AVR of SCG

$K_e = 200, \quad \tau_e = 0.01\ s$

$E_{f\,max} = +5, E_{f\,min} = -5$

CPSS for SCG

$T_1 = 0.5, T_2 = 0.01, K_a = 0.1$

A.4 Excitation system of CSG

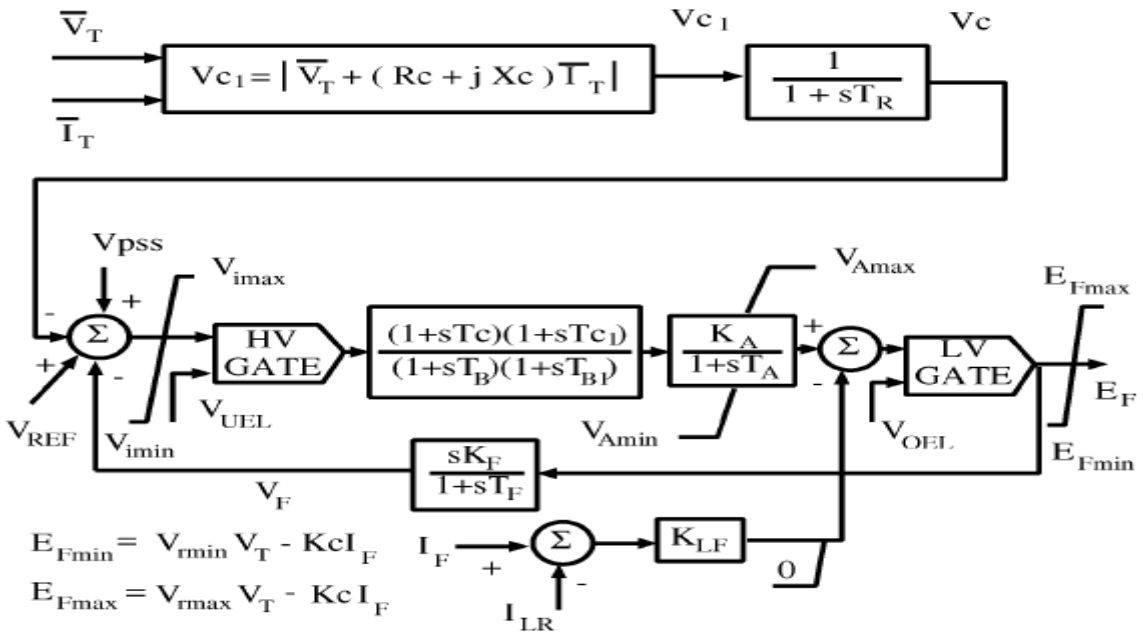

Fig. A4 Excitation system of CSG

A.5 CPSS for CSG

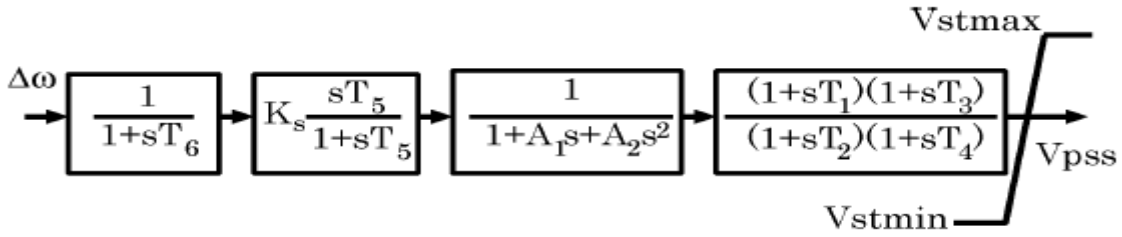

Figure A.5 CPSS model for CSG

A.6 Parameters for conventional synchronous generator

All resistances and reactances are in p.u and time constants in seconds (s)

X_f = 1.33, X_d = 1.24, X_q = 0.743, X_{kd} = 1.15,

X_{kq} = 0.652, X_{mq} = 0.626, X_{md} = 1.126,

H = 3.46 kW s/kVA

r_a = 0.007, r_f = 0.00089, r_{kd} = 0.023, r_{kq} = 0.023, K_d = -0.0027

Exciter cum AVR, and Governor of CSG

R_c = 0.0, X_e = 0.65, R_c = 0.0, X_c = 0.0 , T_R = 0.04 K_A = 190,

K_c = 0.08, K_f = 0.0 K_{LF} = 0.0, I_{LR} = 0 , T_B = 10.0, T_C = 1.00, T_A = 0.01 T_F = 0.0,

T_{B1} = 0.0 T_{C1} =0.0, V_{OEL} = 999, V_{UEL} = -999, V_{IMAX} = 999, V_{IMIN} = -999, V_{AMAX} = 999,

V_{AMIN} = -999, V_{RMAX} = 7.8, V_{RMIN} = -6.7

a = -0.001328, b = -0.17, Tg = 0.25

CPSS for CSG

T_1 = 0.2, T_2 = 0.045, T_3= 0.2, T_4 = 0.045, T_5 = 2.65, T_6 = 0.009, K_s = 11.31, A_1 = 0.0,

A_2 = 0.0